

# **Design of Antigen-Specific Immunotherapies Through Modulation of Peripheral Tolerance Pathways**

By

Matthew A. Christopher

Submitted to the graduate degree program in Pharmaceutical Chemistry and the Graduate Faculty of the University of Kansas in partial fulfillment of the requirements for the degree of Doctor of Philosophy.

---

Chairperson Dr. Cory Berkland

---

Dr. Teruna Siahaan

---

Dr. Laird Forrest

---

Dr. David Volkin

---

Dr. Arghya Paul

Date Approved: July 2, 2019

The Dissertation Committee for Matthew Christopher

certifies that this is the approved version of the following dissertation:

**Design of Antigen-Specific Immunotherapies Through  
Modulation of Peripheral Tolerance Pathways**

---

Chairperson Dr. Cory Berkland

Date Approved: July 2, 2019

## Abstract

Current therapies for autoimmune diseases lack specificity for the offending immune cell population resulting in a wide range of side effects and weakening of the immune system. This presents a clear need for antigen-specific immunotherapies (ASITs) capable of selectively modulating autoreactive immune cells while maintaining the patient's ability to respond to foreign pathogens. Lymphocyte activation is dependent on receiving two signals in tandem: interaction with the antigen of interest and co-stimulatory signals. Disruption of this two-signal model for lymphocyte activation in the context of the autoantigen is key to developing successful ASITs. Antigen-drug conjugates represent a novel class of therapeutics for the induction of immune tolerance designed to direct the effects of small molecule immunosuppressants through conjugation to the autoantigen of interest (Chapter 2). This strategy has proven successful in ameliorating paralytic symptoms in a murine model of multiple sclerosis (MS) known as experimental autoimmune encephalomyelitis (EAE). This was achieved through conjugation of the corticosteroid dexamethasone (DEX) to the peptide autoantigen proteolipid protein (PLP<sub>139-151</sub>). Further studies into the disruption of co-stimulatory signals in EAE revealed a protective role for the programmed cell death 1 (PD-1) pathway, and antagonism of natural receptor engagement resulted in cellular exhaustion, alleviating inflammatory markers (Chapter 3). Ultimately, antigen-only ASITs represent possibly the safest form of immune modulation in autoimmune diseases and may be achieved through multivalent displays of autoantigen. For example, a tetravalent display of PLP<sub>139-151</sub> (4-arm PLP<sub>139-151</sub>) completely ameliorated EAE symptoms through depletion of PLP-responsive B cells and induction of a tolerogenic shift in co-stimulatory markers (Chapter 4). These results support the advancement of multiple avenues of approach in the development of ASIT for treating autoimmunity.

## Acknowledgements

For the work performed in Chapter 2, I would like to acknowledge many of our previous and current lab members for their contributions. Chad Pickens contributed greatly to this project with his knowledge of synthetic strategies and analytical characterization. Additional work in these areas was contributed by Martin Leon, Stephanie Johnson, and Melissa Pressnall. Both Bradley Sullivan and Sharadvi Thati contributed excellent scientific input in designing biological assays and influenced the overall direction of the project. We gratefully acknowledge support from the National Institutes of Health Graduate Training Program in Dynamic Aspects of Chemical Biology Grant (T32 GM008545) from the National Institutes of General Medical Sciences (C.J.P., M.A.L., and S.N.J.), and the Howard Rytting pre-doctoral fellowship from the Department of Pharmaceutical Chemistry at the University of Kansas (C.J.P.). Additionally, we would like to acknowledge support from the National Institutes of Health Biotechnology Training Grant (NIH0073415) (M.A.C.). We would also like to thank the KU NMR facility and the KU Macromolecule and Vaccine Stabilization Center (MVSC) for collaboration and instrument use. As well as, support for the NMR instrumentation was provided by NIH Shared Instrumentation Grant # S10RR024664 and NSF Major Research Instrumentation Award # 1625923. We also thank Tom Prisinzano for the useful discussions on synthetic strategy.

For the work performed in Chapter 3, I would like to acknowledge support from Leidos Inc. for providing both funding and peptide materials for testing in addition to scientific input regarding the PD-1 pathway.

For Chapter 4, I would like to acknowledge Stephanie Johnson for her instrumental role in the synthesis and characterization of 4-arm PLP<sub>139-151</sub>. Additionally, Jonathan Daniel Griffin guided the design and analysis of the PLP-specific ELISA. We gratefully acknowledge support

from the National Institutes of Health Graduate Training Program in Dynamic Aspects of Chemical Biology Grant (T32 GM008545) from the National Institutes of General Medical Sciences (S.N.J.), and the National Institutes of Health Biotechnology Training Grant (NIH0073415) (M.A.C.).

## Table of Contents

### Chapter 1: Autoimmune Diseases and Antigen-Specific Immunotherapies

1. Designing Autoimmune Therapies
2. Introduction to Autoimmune Diseases
  - 2.1. Immunology of Autoimmunity
  - 2.2. Self-Recognition and Immune Tolerance
3. Current Therapeutics for Autoimmunity
  - 3.1. Immunosuppressants
  - 3.2. Immune Cell Depletion Therapies
  - 3.3. Modifying Immune Cell Transport
  - 3.4. Antigen-Specific Immunotherapies
    - 3.4.1. Antigen-Only Therapies
    - 3.4.2. Altered Peptide Ligands and Antigen Mimicry
4. Modulating the Immunological Synapse
  - 4.1. Altering Co-Stimulation
    - 4.1.1. Small Molecule Immunosuppressants
    - 4.1.2. Co-stimulation Antagonists
  - 4.2. Modifying Antigen Interactions to Induce Anergy
    - 4.2.1. Multivalent Antigen Display
5. Conclusions

### Chapter 2: Antigen-Drug Conjugates as a Novel Therapeutic Class for the Treatment of Antigen-Specific Autoimmune Disorders

1. Introduction
2. Materials and Methods
  - 2.1. Synthesis of azide-functionalized DEX (DEX-N<sub>3</sub>)
  - 2.2. Synthesis of PLP<sub>139-151</sub>-DEX
  - 2.3. Analytical characterization
  - 2.4. Drug release and stability studies
  - 2.5. Induction of EAE
  - 2.6. *In vivo* Efficacy in EAE Mice
  - 2.7. Splenocyte Isolation
  - 2.8. Cell Metabolic Assay
  - 2.9. Cytokine Response
3. Results
  - 3.1. Analytical Characterization of Chemical Entities
  - 3.2. Conjugate Stability and Release Kinetics
  - 3.3. IC<sub>50</sub> Determination of Conjugates and Payload
  - 3.4. *In Vivo* Screening of Conjugates

4. Discussion
5. Conclusions

## **Chapter 3: Modulation of Regulatory Pathways through Co-administration of Cognate Antigen and PD-1 Antagonists**

1. Introduction
2. Materials and Methods
  - 2.1. Induction of EAE
  - 2.2. Splenocyte Isolation
  - 2.3. Cytokine Response
  - 2.4. Cell Phenotyping via Flow Cytometry
  - 2.5. LD01 Titration
3. Results
  - 3.1. PD-1 Peptides Reduce Cytokine Secretion in the Presence of Cognate Antigen
  - 3.2. PD-1 peptides reduce proportion of major T-cell populations
  - 3.3. Titration of LD01 reveals dose dependency of PD-1 expression
4. Discussion
5. Conclusions

## **Chapter 4: Silencing Autoreactive B Cell Populations Through Tetravalent Antigen Presentation**

1. Introduction
2. Experimental Section
  - 2.1. Materials
  - 2.2. Synthesis of 4-arm PLP<sub>139-151</sub>
  - 2.3. Analytical Characterization of 4-arm PLP<sub>139-151</sub>
  - 2.4. Induction of EAE
  - 2.5. Competitive PLP<sub>139-151</sub> ELISA
  - 2.6. *In Vivo* Efficacy
  - 2.7. Splenocyte Isolation
  - 2.8. Cell Staining for Flow Cytometry
  - 2.9. Cytokine Measurement
3. Results
  - 3.1. Synthesis and Analytical Characterization of 4-arm PLP<sub>139-151</sub>
  - 3.2. Competitive ELISA Demonstrating PLP<sub>139-151</sub> Specificity
  - 3.3. *In Vivo* Efficacy of 4-arm PLP<sub>139-151</sub>
  - 3.4. Analysis of Key Immune Cell Populations
  - 3.5. Cytokine Expression

4. Discussion
5. Conclusions

## **Chapter 5: Conclusions and Future Directions**

1. Conclusions
2. Future Directions
  - 2.1. AgDC Development
    - 2.1.1. Alternate Disease Targets
    - 2.1.2. Modifying Release Kinetics
  - 2.2. Forms of Co-delivery for PD-1 Peptides
    - 2.2.1. Further Elucidate Conditions Necessary for Exhaustion
  - 2.3. Further Development of 4-arm PLP
    - 2.3.1. Altered Valency
    - 2.3.2. Fluorescent Tracking
    - 2.3.3. Application to T1D

# **Chapter 1: Introduction**

## **1. Designing Autoimmune Therapies**

Autoimmune diseases impact countless lives worldwide, representing a major burden in modern healthcare and severely impacting patient quality of life. Our ability to maintain patient health following diagnosis with an autoimmune disease has greatly improved over the past few decades but correcting the underlying condition and reversing damage has been an elusive target. Current treatments generally consist of long-term immunosuppression, a strategy which may alleviate symptoms and slow damage to affected tissue but fails to tolerize the immune system toward self-antigens. Typical immune suppression may be achieved through small molecule drugs such as corticosteroids or numerous biologics capable of inhibiting a variety of co-stimulatory pathways, preventing activation of auto-reactive lymphocytes. Unfortunately, these treatment regimens are indefinite, requiring regular administration throughout the patient's lifetime in an attempt to retain any remaining tissue function. Furthermore, immunosuppressive strategies often result in a wide range of off-target effects and may leave patients open to severe opportunistic infections. Although our ability to manage autoimmune diseases may have improved, there is a clear unmet need for therapies capable of antigen-specific correction of autoimmune responses.

This dissertation outlines research surrounding the development of more effective antigen-specific immunotherapies (ASITs) for the treatment of autoimmune diseases. This chapter shall serve as an introduction to the currently approved disease modifying treatments, the cellular mechanisms associated with autoimmunity, and how these mechanisms may be exploited to reintroduce immunological tolerance toward autoantigens. Ultimately, the goal of these works is to facilitate the development of ASITs which may be capable of treating or curing autoimmune

diseases in a specific manner, reducing off target immunosuppressive effects and maintaining a healthy immune system following treatment.

## **2. Introduction to Autoimmune Diseases**

Although many autoimmune conditions are considered to be rare diseases, the NIH recognizes more than 80 diseases classified by autoimmunity and, collectively, these diseases affect millions of Americans.<sup>1</sup> Some of the more common autoimmune diseases include rheumatoid arthritis (RA), type 1 diabetes (T1D), multiple sclerosis (MS), celiac disease, and inflammatory bowel disease. Furthermore, the prevalence of some of these diseases such as T1D and celiac disease are increasing, resulting in a greater impact on human life and healthcare.<sup>1</sup> These trends in disease development demand a greater understanding of autoimmune pathogenesis as well as the discovery of more effective treatments. ASIT represents a key area of research designed to induce immune tolerance toward a designated antigen while maintaining the patient's immune responsiveness toward pathogens. In order to implement ASIT in the treatment of autoimmunity, however, it is necessary to first identify the disease-causing autoantigens. In tissue-restricted autoimmune diseases such as T1D, RA, and MS many potential antigens responsible for disease have been identified, but for systemic autoimmune diseases such as systemic lupus erythematosus (SLE) there may be multiple antigens responsible for disease, complicating the design of ASITs for systemic indications.

Research into disease-causing autoantigens responsible for T1D have focused primarily on glutamic acid decarboxylase (GAD65) as well as various forms of insulin.<sup>2</sup> Disease progression is believed to be a direct result of an inflammatory response against insulin-producing pancreatic  $\beta$  cells resulting in the inability to regulate blood glucose levels.<sup>3</sup> Current therapies revolve around maintaining the remainder of the patient's ability to secrete insulin and supplementing

this low baseline secretion with exogenous insulin. This results in a clear long-term financial and physical burden on the patient and may not be sufficient to prevent a number of disease-associated complications.<sup>2</sup> Fortunately, in recent years the research into tolerance induction against  $\beta$  cell antigens has grown and mouse models such as the non-obese diabetic (NOD) model have facilitated a greater understanding for disease pathology.<sup>4</sup>

Another autoimmune disease of keen interest to researchers is RA due to its high prevalence and the severe disability associated with late stage disease. Disease onset is typically characterized by T-cell infiltration of synovial tissue resulting in inflammation and damage to cartilage, bones, and further systemic consequences.<sup>5</sup> Current therapies focus on aggressive immunosuppressant therapy to limit disease progression, but patient response to treatment is highly variable. Two major RA patient subsets have been identified based on the presence or absence of antibodies specific for anti-citrullinated proteins (ACPA) indicating a currently incomplete understanding of disease pathology and the need for further identification of disease-causing autoantigens.<sup>6-7</sup>

MS disease progression is characterized by central nervous system (CNS) inflammation resulting in degradation of neuron myelin and progressive disability.<sup>8</sup> MS manifests in several disease forms, but the most common is relapsing-remitting MS (RRMS) which is defined by symptomatic relapses in which patient symptoms rapidly increase in severity followed by remission in which symptom severity is reduced.<sup>8</sup> The pathological differences between the various forms of MS are poorly understood, however treatment strategies are typically similar and involve global immune suppression to limit relapses and slow progression.<sup>9</sup> A few potential CNS autoantigens responsible for disease have been identified including proteolipid protein (PLP), myelin oligodendrocyte glycoprotein (MOG), and myelin basic protein (MBP).<sup>10</sup>

Furthermore, researchers have developed a well-established model of MS in mice known as experimental autoimmune encephalomyelitis (EAE) capable of emulating the various MS pathologies witnessed in humans, aiding in the discovery of potential new therapeutic strategies.<sup>11</sup>

## **2.1. Immunology of Autoimmunity**

Many mechanisms of peripheral and central tolerance exist which may limit aberrant immune cell activation, however, self-reactive T-cells and B cells may still overcome these checkpoints and mount an inflammatory response against native proteins of the human body. Development of these autoimmune responses is poorly understood but is believed to be a result of both genetic and environmental factors.<sup>12</sup> Namely, environmental factors such as infections have long been associated with loss of tolerance toward native antigens due to phenomena such as epitope spreading and bystander activation. Nevertheless, the exact mechanisms involved in the onset of autoimmune responses are poorly understood as these phenomena are difficult to replicate in animal models and even more difficult to observe in patients.<sup>12</sup> To further our understanding of how to reintroduce immunological tolerance and correct autoimmunity, it is first important to review the mechanisms by which the body naturally maintains self-tolerance.

## **2.2. Self-Recognition and Immune Tolerance**

The function of the adaptive immune system is based on the recognition of antigenic targets associated with foreign pathogens. This distinction between foreign antigens and self-antigens represents a major hurdle, one which the immune system overcomes through functional non-responsiveness to native antigens known as self-tolerance. Self-tolerance is maintained through a series of checkpoints which can be classified as either central tolerance or peripheral tolerance. Simply put, central tolerance involves the deletion of autoreactive T-cells and B cells in the

thymus and bone marrow, respectively, prior to their release into systemic circulation. This is accomplished through a process known as negative selection, in which naïve lymphocytes are subjected to a plethora of self-antigens and those cells which bind strongly to these antigens are signaled for apoptosis.<sup>13</sup> Nevertheless, self-reactive lymphocytes do escape the mechanisms of central tolerance and reach systemic circulation, however, further checkpoints to lymphocyte activation limit their responsiveness.

There are many checkpoint mechanisms associated with peripheral tolerance of escaped self-reactive lymphocytes, the simplest of which is physical separation of the self-reactive cells and their cognate antigen. Typically, naïve T-cells which have yet to encounter cognate antigen are limited to systemic circulation, secondary lymphoid organs, and the lymphatic system.<sup>14</sup> As such, naïve, self-reactive T-cells are unlikely to encounter high concentrations of MHC-bound native antigen as these antigens are tissue-restricted under non-inflammatory conditions.<sup>15</sup>

A second mechanism of maintaining peripheral tolerance is dependent on the development of regulatory T-cell (Treg) populations, capable of secreting anti-inflammatory cytokines and altering the function of professional antigen-presenting cells (pAPCs).<sup>16</sup> The development of Treg cells is not fully understood, however it has been demonstrated that these cells act in an antigen-specific manner, similar to conventional T-cells.<sup>17-18</sup> Regulatory T-cells function through multiple mechanisms including contact-independent and contact-dependent pathways. The primary mechanism for contact-independent Treg suppression is through cytokine production. Tregs have been found to generate IL-10 and TGF- $\beta$ , which can suppress immune responses, however, the role of the cytokines in Treg function is not fully understood.<sup>16, 19-20</sup> The contact-dependent mechanisms include expression of co-inhibitory markers such as CTLA-4 capable of altering pAPC function following antigen-MHC recognition.<sup>16</sup> This may be

accomplished through the downregulation of T-cell activation markers on pAPCs following interactions with Tregs, limiting the pAPC's effectiveness in activating T-cells and mounting an inflammatory response.<sup>21</sup> Additionally, it has been found that Tregs can alter dendritic cell (DC) metabolism through upregulation of indoleamine 2,3-dioxygenase (IDO).<sup>22</sup> This results in the catabolism of tryptophan into metabolites, which suppress T-cells in the local environment.

Finally, peripheral tolerance to native antigens is also maintained through a two-signal model of T-cell activation. This model states that T-cells require two signals simultaneously to mount an effective immune response. The first signal is antigen-MHC complex ligation with the T-cell receptor (TCR) as has been discussed thus far. The second signal consists of binding of co-stimulatory ligands expressed on pAPCs to their respective co-stimulatory receptors on the T-cell surface. This interaction is known as the immunological synapse, in which binding between MHC-antigen and TCR (signal 1) and binding of co-stimulatory markers (signal 2) occur simultaneously to activate T-cells. The B7 pathway is one such co-stimulatory system, in which CD28 on T-cells interacts with ligands CD80/CD86 on pAPCs such as DCs and B cells. Importantly, antigen-receptor engagement in the absence of secondary co-stimulatory signals will induce an immunological state of unresponsiveness known as anergy, in which the cell may no longer mount an effective inflammatory response against cognate antigen. This two-signal model acts as a key barrier in T-cell-mediated immunity, helping to mitigate activation of self-reactive T-cells in the absence of additional inflammatory signals. Additionally, T-cells express co-inhibitory receptors such as cytotoxic T-lymphocyte-associated antigen 4 (CTLA-4) and programmed cell death protein 1 (PD-1), both of which negatively regulate T-cell inflammation through the induction of anergy.

### **3. Current Therapeutics for Autoimmunity**

Numerous therapeutic strategies for managing autoimmune diseases have been developed, however, most of the currently approved strategies focus on increasing patient quality of life through symptom suppression and prevention of further autoimmune progression without addressing the underlying causes of the symptoms (Table 1). This is typically achieved through some form of immunosuppression, in which the patient's immune system is globally altered to reduce inflammation (Figure 1).<sup>23</sup> Although this treatment strategy may suppress autoimmune symptoms, it imparts new concerns for the patient's wellbeing as their immune system is often less capable of responding to foreign pathogens.

### **3.1. Immunosuppressants**

Corticosteroids have been used to manage severe inflammatory diseases such as MS, RA, and SLE for many years.<sup>23</sup> This class of synthetic, small molecule drugs is designed to mimic natural human steroids through binding to the nuclear receptor known as the glucocorticoid receptor (GR).<sup>24-25</sup> Due to the natural abundance of GR in nearly all cell types, corticosteroid treatment alters gene transcription in many ways, including the suppression of inflammatory immune responses. This suppression is achieved through both repression of inflammatory gene expression as well as induction of anti-inflammatory pathways.<sup>24-25</sup> Most importantly, due to the widespread effects of corticosteroids on gene expression, this class of drugs is capable of inhibiting both the innate and adaptive immune responses, leading to their use in many autoimmune and inflammatory disease indications. Namely, corticosteroid treatment leads to immune suppressive effects on macrophages, T-cells, and B cells through blocking key inflammatory transcription factors such as NF- $\kappa$ B.<sup>26</sup> The result is an overall reduction of stimulatory cytokines responsible for immune cell proliferation and survival, including granulocyte-macrophage colony-stimulating factor (GM-CSF), interleukin-2 (IL-2), and tumor

necrosis factor alpha (TNF- $\alpha$ ).<sup>24</sup> Clinically, the result of these mechanisms is the widespread suppression of the patient's immune system which is necessary in cases of severe relapses in RRMS and severe indications of SLE. Nevertheless, the expression of GR on nearly all cells in the human body leads to a long list of potential side effects, and the lack of specificity for over-reactive lymphocytes results in global immune suppression and the risk for opportunistic infection.<sup>27-28</sup>

Another small molecule immunosuppressant, dimethyl fumarate (DMF), has recently been approved for use in MS patients in 2013.<sup>29-31</sup> The mechanism of DMF on suppressing inflammatory responses is not completely understood, however, it has been shown to bind heme oxygenase-1, an antioxidant.<sup>31</sup> As a result, DMF treatment reduces the expression of inflammatory cytokines such as IL-12, TNF- $\alpha$ , and IL-6 while stimulating Tregs.<sup>31</sup> Interestingly, DMF treatment appears to decrease lymphocyte counts with a bias toward reducing T-helper Th1 and Th17 subsets, with less of an impact on Th2 subsets.<sup>32</sup> This is a key consideration when treating MS, in which increased Th2 subsets are associated with positive disease outcomes.<sup>33</sup> Despite the benefits of DMF treatment, it does not correct the underlying autoimmune condition and has been associated with the onset of a rare and deadly CNS infection known as progressive multifocal leukoencephalopathy (PML).<sup>34</sup>

Immune suppression in autoimmune diseases has also been achieved using cytokine modifying treatments which act to disrupt cellular interactions with soluble stimulatory factors such as interferon gamma (IFN- $\gamma$ ), IL-6, and TNF- $\alpha$ . Perhaps the most common disease modifying treatment in MS is interferon- $\beta$  (IFN- $\beta$ ). Subcutaneous injection of IFN- $\beta$  can reduce relapse rates in RRMS patients by approximately one third over a 2-3-year period and represents possibly the most well tolerated treatment option for MS patients.<sup>35</sup> Nevertheless, the effects of

IFN- $\beta$  treatments act globally on the immune system with the potential for some adverse events.<sup>35</sup>

Tocilizumab, a humanized monoclonal antibody directed against the IL-6 receptor (IL-6R), has been approved for use in rheumatoid arthritis. Early attempts at IL-6 blockade treatments resulted in increased half-life of the cytokine, however, focus has shifted toward designing antibodies directed against the IL-6R in both the soluble form and transmembrane form.<sup>36</sup> IL-6R blockade with tocilizumab results in fast and effective reduction in joint pain when given as a monotherapy or in combination with other drugs and has been proven to reduce symptoms in RA patients who are non-responsive to other frontline treatment options.<sup>36</sup> One such frontline treatment often employed in both RA and psoriasis is etanercept, designed to block the action of the inflammatory cytokine TNF- $\alpha$ .<sup>37</sup> Etanercept is a dimeric fusion protein comprised of the TNF- $\alpha$  receptor fused with human IgG, allowing for effective binding to TNF- $\alpha$  preventing interaction with cellular receptors. This treatment option has proven effective in moderate and severe cases of RA, modifying disease progression both short-term and long-term.<sup>37</sup>

Despite the successes of these cytokine modifying treatments in RA, methotrexate, a chemotherapeutic agent, remains one of the most widely used drugs for limiting the progression of RA. The efficacy associated with methotrexate treatments in RA is tied to the numerous anti-inflammatory effects of the drug stemming from its ability to inhibit cell proliferation and induce apoptosis in immune cells.<sup>38</sup> Furthermore, methotrexate treatment results in a reduction of proinflammatory cytokines in the synovial membrane of RA patients.<sup>39</sup> Not all RA patients respond to low dose methotrexate, however, and the potent effects of this drug may result in some severe adverse events.<sup>40</sup>

### **3.2. Immune Cell Depletion Therapies**

More recently, the development of new forms of immunosuppression for autoimmunity has shifted toward immune cell depletion therapies.<sup>41-42</sup> These treatment options focus on the deletion of specific immune cell populations, namely B cells, in order to prevent inflammation. Overall, B cell depletion is a very effective strategy for eliminating autoimmune responses, however, it severely limits the patient's ability to maintain a functioning immune system capable of responding to infections.<sup>43</sup> Treatment with monoclonal antibodies capable of depleting B cells is often reserved for the most severe and unresponsive autoimmune cases. Rituximab, an anti-CD20 monoclonal antibody, has been approved in the U.S. for severe cases of RA in which the patient does not respond to anti-TNF- $\alpha$  therapies.<sup>44</sup> Additionally, rituximab has been used in some off-label applications for other autoimmune diseases such as MS, SLE, vasculitis, and others.<sup>45</sup> Without properly controlled clinical studies the overall tolerability and efficacy of rituximab in these applications is poorly understood, but recently the FDA approved another anti-CD20 monoclonal antibody, known as ocrelizumab, for application in MS.<sup>42, 46</sup> This class of antibodies is believed to inhibit inflammatory responses through the elimination of antigen-presentation associated with B cells as well as antibody mediated responses. Notably, the deletion of mature B cells which may act as antigen-presenting cells also imparts a downstream immunosuppressive effect on T-cell populations, limiting the overall activation of peripheral T-cells.<sup>47</sup> As mentioned previously, CD20 B cell depletion is an effective strategy for treating autoimmunity however the lack of specificity for antigens of interest limits their application following careful risk/benefit analysis per patient.

### **3.3. Modifying Immune Cell Transport**

Immune cell transport inhibitors have also been explored in the treatment of autoimmune diseases, particularly in MS. Natalizumab, a monoclonal antibody against  $\alpha$ 4-integrin, limits

immune cell trafficking across the blood-brain barrier, preventing autoreactive T-cells and B cells from reaching the CNS.<sup>48</sup> This represents a selective treatment option for MS, exploiting the physical barriers between the CNS and systemic circulation to maintain tolerance against myelin antigens. Natalizumab has proven efficacious in improving annual relapse rates in RRMS patients, however, its use in association with IFN- $\beta$  has resulted in a rise in the number of PML cases in RRMS patients.<sup>48-49</sup> Nevertheless, FDA approval of natalizumab for indications in treating RRMS has been maintained under the stipulation that it should be administered as a mono-therapy in IFN- $\beta$  non-responders.

Similarly, efalizumab is a monoclonal antibody designed to limit lymphocyte trafficking through blood vessels into peripheral tissue. This antibody is directed against lymphocyte function-associated antigen 1 (LFA-1) and inhibits T-cell adhesion to endothelium.<sup>50</sup> For a short time efalizumab was approved for the treatment of psoriasis, but the drug was removed from the market in 2009 due to the high risk for PML associated fatalities.<sup>49</sup> Ultimately, the risks for PML observed across numerous immunosuppressant therapies have led to the development of PML risk-management plans by regulatory agencies in both the U.S. and Europe.

Alternatively, a small molecule drug known as fingolimod has been developed to sequester lymphocytes in lymph nodes, rather than limit immune cells to systemic circulation. Fingolimod binds to sphingosine-1-phosphate receptor and prevents the migration of T-cells and B cells to the site of inflammation.<sup>51</sup> Interestingly, the effects of fingolimod favor the sequestration of naïve and central memory T-cells and B cells, but with less influence on effector memory T-cells.<sup>52</sup> Furthermore, patient serum levels of IL-17, a potent inflammatory cytokine associated with MS, are reduced when on fingolimod, likely contributing to patient relapse rate improvement.<sup>53</sup> Treatment of severe RRMS patients with fingolimod has resulted in reduction of

relapses by approximately one-half over a 2-year period, and has assisted patients who have proven less responsive to frontline treatments such as IFN- $\beta$ .<sup>51</sup> Due to the globally immunosuppressive effects of fingolimod the risk for opportunistic infection is increased, with some severe cases in patients following drug approval.<sup>51</sup>

### **3.4. Antigen-Specific Immunotherapies**

The development of therapies capable of modulating immune responses in an antigen-specific manner has long been of keen interest to researchers. Perhaps the most successful example of antigen-specific immunotherapies (ASITs) in the clinic is that of vaccines, designed to induce protective immunity against foreign pathogens through administration of key antigen targets associated with the disease. Alternatively, ASITs have also been applied toward inducing tolerance of antigenic targets in the form of hyposensitization therapy. Commonly referred to as “allergy shots”, hyposensitization therapies have proven successful in the clinic at tolerizing a patient against allergens without hampering their immune system.

#### **3.4.1. Antigen-Only Therapies**

Hyposensitization therapy was discovered in the early 1900s when Noon and Freeman inoculated patients subcutaneously with grass pollen resulting in improved hay fever symptoms.<sup>54-55</sup> The dosing regimen implemented by both Noon and Freeman involved short-term up-dosing followed by long-term maintenance doses, establishing a therapeutic strategy for allergen desensitization that is still in use today. Nevertheless, numerous studies over the years have established greater control in formulation of allergens as well as exploration of various routes of administration including sublingual.<sup>56</sup> Overall, adverse events associated with hyposensitization therapies are reduced when administered via the sublingual route, however, the greatest limitation to allergen desensitization remains: the multi-year duration of dosing.

In recent years, investigations into the success of hyposensitization have revealed a key role of regulatory T-cells (Tregs) in positive clinical outcomes, resulting in widespread suppression of allergen responsive immune cells.<sup>57</sup> Similar to hyposensitization therapies, initial developments of antigen-specific immunotherapies for the treatment of autoimmunity focused on administration of the autoantigen in various forms including whole antigen, peptide antigen, or altered peptide ligands (APLs).<sup>58</sup> Unfortunately, adapting antigen-only therapies for the induction of tolerance in autoimmune diseases has generally been met with limited success. Multiple studies have attempted to administer insulin via various routes to induce tolerance toward pancreatic  $\beta$  cells with no clear change in disease progression.<sup>59-62</sup> Additionally, other T1D antigens such as GAD65 have produced mixed results in inducing tolerance when administered with adjuvant via subcutaneous injection in children.<sup>63-64</sup> In MS patients, the oral administration of MBP for tolerance induction yielded little to no improvement in relapses.<sup>65</sup> These trials indicate that simple administration of antigen in its native form is insufficient to tolerize the immune system in cases of autoimmunity, leading to the design of APLs and antigen mimics.

### **3.4.2. Altered Peptide Ligands and Antigen Mimicry**

Typically, APLs are designed through key substitutions of amino acids in disease-causing antigen with the intent to disrupt T-cell activation through TCR-MHC interactions. Attempts at inducing tolerance through APLs have shown promise in animal models of autoimmunity, however translation to human disease has been met with limited success.<sup>66-67</sup> Numerous clinical studies on the administration of altered peptide ligands (APLs) of disease associated autoantigens in multiple sclerosis (MS), rheumatoid arthritis (RA), and type 1 diabetes (T1D) have shown limited efficacy and the potential for symptom exacerbation.<sup>68-70</sup> Studies into the intranasal

administration of an MBP derived APL in a murine model of MS have indicated that this molecular mechanism of TCR-MHC disruption may be capable of inducing bystander suppression of autoreactive lymphocytes through the generation of IL-10 secreting Tregs.<sup>71</sup> Alternatively, enhancements to MHC binding through the introduction of a thiol-disulfide oxidoreductase motif (CXXS) has been shown to induce cytolytic T-cell activity directed against pAPCs and subsequent protection from diabetes onset in mice.<sup>72-73</sup> Unfortunately, attempts at implementing APLs in treating human disease have resulted in hypersensitivity and exacerbation of symptoms. Although APL treatments have not successfully translated to humans, these studies provide valuable insight into the association between MHC-antigen-TCR binding strength and tolerance induction.

Despite the limited success of many antigen-only therapies outlined above, the strategy of antigen mimics has demonstrated some success in treating autoimmune diseases. The first, possibly most successful, example of antigen mimicry is that of glatiramer acetate (GA) for the treatment of RRMS. Comprising of a heterogeneous mixture of copolymers designed to mimic MBP, GA can reduce relapse rates by approximately 30%.<sup>74</sup> GA copolymer mixtures are synthesized with four amino acids in the approximate molar ratios in which they occur in MBP with a molecular weight ranging from 2,500 to 20,000 Da.<sup>75</sup> The discovery of GA's ability to modulate immune responses in MS patients was serendipitous, and as such the mechanisms behind its efficacy are still poorly understood.<sup>76</sup> Various studies have indicated that GA is capable of binding to MHC class II on pAPCs and inhibit proper presentation of myelin antigens.<sup>77</sup> Alternatively, others have demonstrated that GA treatment is associated with a shift to a Th2 T-cell response which is considered anti-inflammatory in MS pathology, however, how this is achieved has not been fully elucidated.<sup>78</sup> Finally, it is possible that this copolymer mixture

is retained at the injection site acting as an immunogenic decoy, a theory which is supported by common injection site reactions and very limited systemic bioavailability.<sup>75</sup> Further understanding of the underlying mechanisms responsible for GA's efficacy could guide future ASIT design for autoimmune indications.

#### **4. Modulating the Immunological Synapse**

The underlying mechanisms behind many of the currently approved autoimmune therapeutics stem from disruption of signal 2 of the immunological synapse, altering the expression of co-stimulatory signals necessary for activation of lymphocytes. Furthermore, the results of APL research in a pre-clinical setting demonstrate the potential tolerizing effects which can be achieved through modulation of signal 1 of the immunological synapse by altering TCR-MHC binding to antigen. As such, future ASIT designs have two primary avenues of inducing long lasting tolerance toward native antigens.

##### **4.1. Altering Co-Stimulation**

The first avenue of approach for the design of ASIT involves directing the action of current therapeutic options against autoreactive lymphocytes to selectively modulate co-stimulation in those which recognize self-antigens. The advantages of this strategy are the high potency of many current immunosuppressants and their ability to induce bystander suppression, reducing inflammation in response to other autoantigens not directly addressed by the ASIT. Bystander suppression is necessary to correct autoimmune inflammation in cases where more than one native antigen may be recognized by the immune system, but this bystander suppression must be confined to the tissue space in which inflammation is occurring (e.g. the CNS in MS or pancreas in T1D).

#### **4.1.1. Small Molecule Immunosuppressants**

As discussed previously, corticosteroids are capable of effectively promoting anti-inflammatory responses while suppressing inflammation with high potency. This class of drugs has been used in severe cases of autoimmune inflammation for many years but the prevalence of GRs on nearly all human cell types results in numerous off-target effects, and the global immune suppression following corticosteroid treatment impacts patient health and quality of life. Previous research into co-administration of OVA peptide and a corticosteroid, dexamethasone (DEX), in OVA-sensitive mice by Kang et al. demonstrates that the immunosuppressant action of DEX may be directed against an antigen of interest in murine models of inflammation.<sup>79</sup> Taking these works one step further, Peine et al. used acetalated dextran particles to co-deliver DEX and MOG in EAE mice, maintaining the spatial and temporal delivery of the drug alongside autoantigen.<sup>80</sup> Ultimately, co-delivery of DEX and MOG was more effective at reducing clinical scores and lowering inflammatory cytokines than simple co-administration of these components.<sup>80</sup> In chapter 2, we will focus on designing a novel class of compounds known as antigen-drug conjugates (AgDCs) to simply and effectively co-deliver potent immunosuppressants, such as DEX, to autoreactive lymphocytes in EAE mice. AgDCs are inspired by the recent interest in the development of antibody-drug conjugates (ADCs) for cancer therapies and seek to utilize the same antibody-antigen interactions to increase the tolerability for highly potent small molecule drugs.

#### **4.1.2. Co-stimulation Antagonists**

Further attempts at modulating co-stimulatory signals in autoimmune disease have resulted in the development of antagonists against co-stimulatory ligands. Fusion proteins such as abatacept consist of the Fc region of IgG1 fused with the extracellular domain of CTLA-4, a co-

inhibitory receptor.<sup>81</sup> The goal of this biologic is to bind to the co-stimulatory ligands CD80/CD86 expressed on pAPCs and prevent ligation to CD28 on T-cells.<sup>81</sup> As a result, T-cells will bind MHC class II presenting cognate antigen (signal 1) but will not receive co-stimulation (signal 2) and will become anergic. The success of abatacept in treating patients with severe RA suggests that biologics capable of antagonizing co-stimulatory pathways are an effective means to induce tolerance, however, these effects are not directed against autoreactive lymphocytes exclusively. In chapter 3, we explore the role of a co-inhibitory pathway in the progression of EAE through the use of peptide antagonists. These studies are designed to elucidate the protective mechanisms of the programmed cell death 1 (PD-1) pathway in autoimmunity and justify the future design of peptide agonists/antagonists for co-delivery alongside disease causing autoantigen.

#### **4.2. Modifying Antigen Interactions to Induce Anergy**

The second avenue of approach for ASIT development is that of antigen-only therapies, such as APLs or multivalent antigen arrays. The design of APLs offers the distinct advantage of targeting only a specific lineage of lymphocytes, as the only lymphocytes capable of responding to treatment are those that recognize the antigen from which the APL is derived. Unfortunately, the mechanisms behind tolerance induction through APL administration are not well understood and they lack potency in humans. As we gain a greater understanding for modulating signal 1 of the immunological synapse, we unlock the potential to reverse autoimmunity in a highly specified manner. One strategy that has emerged with regards to antigen-only therapies is that of multivalent antigen arrays. Typically, these compounds are comprised of a polymer backbone or particle which multivalently displays antigen with highly controlled characteristics including molecular weight and valency.

### **4.2.1. Multivalent Antigen Display**

The potential for multivalent arrays of autoantigen to induce tolerance has been known for years. Early work by Dintzis and colleagues demonstrate tolerance induction through administration of soluble, low molecular weight multivalent antigen arrays.<sup>82</sup> They postulated that these antigen arrays gathered within germinal centers of the animals and suppressed antigen-specific antibody secretion through interactions with antigen-specific B cells.<sup>82</sup> Further studies regarding these low molecular weight antigen arrays indicated their ability to irreversibly suppress high-affinity antigen-specific B cells regardless of the presence of T-cell stimulatory signals.<sup>83</sup> Following these promising results, our lab has previously devised a strategy for displaying multivalent antigen in association with peptide antagonists against cellular adhesion molecules to elucidate the role of cell-cell interactions in multivalent antigen array tolerization. These soluble antigen arrays (SAgAs) have been shown to cluster B cell receptors and reduce symptom severity in EAE mice.<sup>84-85</sup> Furthermore, SAgAs designed for applications in T1D have been shown to induce an anergic state in insulin-reactive B cells.<sup>86</sup> In chapter 4, we will discuss the design a new soluble multivalent antigen array of low molecular weight comprised of only the autoantigen of interest, PLP<sub>139-151</sub>, on a tetravalent polyethylene glycol (PEG) backbone. These well-defined tetravalent antigen arrays have been tested in the EAE model of MS with promising results in tolerizing autoreactive B cell populations.

## **5. Conclusions**

Current therapies for treating autoimmunity have proven effective at managing symptoms and offer some improvement to patient quality of life, but they have yet to correct the underlying condition. Many approved therapeutics lack specificity for the lymphocytes of interest, resulting in widespread off-target effects and global immune suppression. ASITs offer the potential to

correct autoimmunity in a targeted manner, however, commonly employed ASIT techniques such as allergy shots have failed to translate into the treatment of autoimmunity. Outlined here are a few potential strategies by which ASIT may be developed for the treatment of autoimmune diseases, but current knowledge of immune tolerance induction is lacking. Future work for ASIT development should focus on selectively modulating the immunological synapse of autoreactive lymphocytes. Currently, highly potent small molecule corticosteroids alter the expression of co-stimulatory molecules but lack the specificity for disease causing autoantigen. Introducing a targeted mechanism for administration of these compounds to offending, autoreactive lymphocytes represents a key first step in improving autoimmune therapies. Ultimately, exploiting peripheral tolerance mechanisms through antigen-only therapies has enormous potential for curing the underlying autoimmune condition while eliminating off-target effects, but these strategies will require a greater understanding for immune cell-antigen interactions before reaching the clinic.

**Table 1.** Numerous approved therapeutics for autoimmune indications.

Category	Drug	Autoimmune Applications:			
		MS	T1D	RA	SLE
Immunosuppressants	Dexamethasone	✓		✓	✓
	Dimethyl Fumarate	✓			
	Interferon Beta	✓			
	Etanercept			✓	
	Tocilizumab			✓	
	Methotrexate			✓	✓
B-cell Depletion	Rituximab			✓	✓
	Ocrelizumab	✓			
Immune Cell Transport Inhibitors	Natalizumab	✓			
	Efalizumab				
	Fingolimod	✓			
Antigen Mimic	Glatiramer Acetate	✓			
Co-Stimulation Antagonists	Abatacept			✓	
	Belatacept				

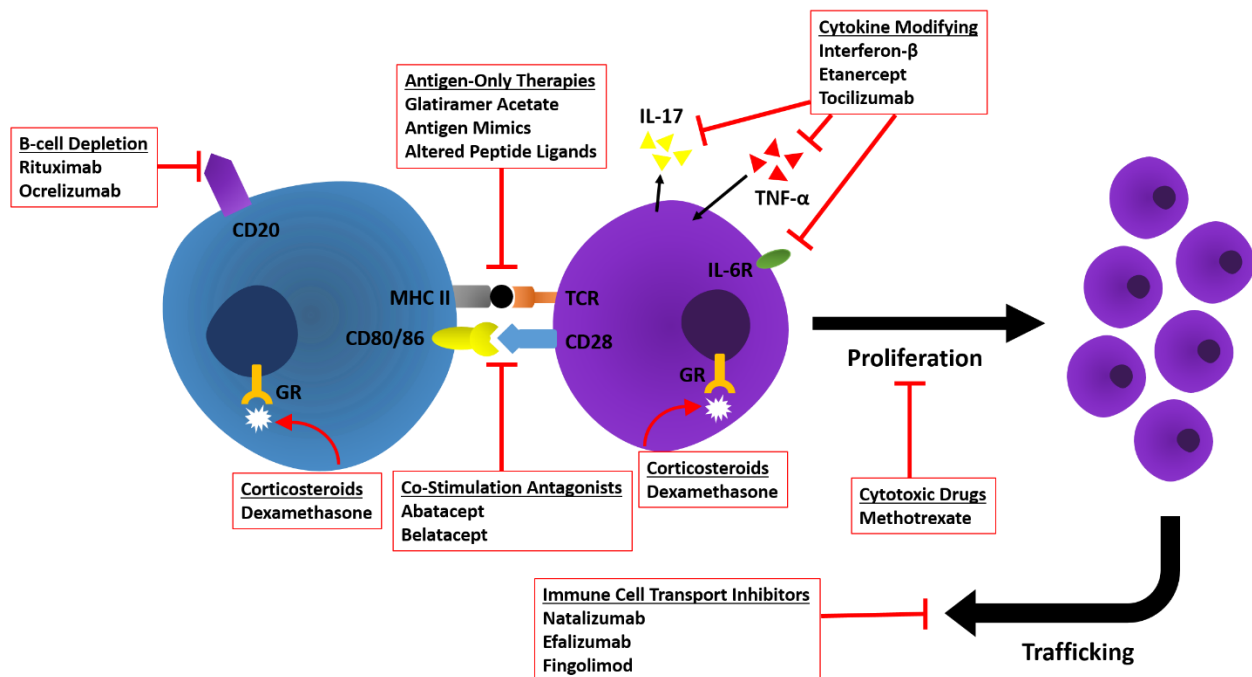


**Figure 1.** Depiction of the various stages of immune cell activation, proliferation, and trafficking and numerous therapeutics targeting these pathways.

## References

1. NIH Biennial Report 2008-2009 Autoimmune Diseases; National Institute of Health: 2009.
2. Atkinson, M. A.; Eisenbarth, G. S.; Michels, A. W., Type 1 diabetes. *Lancet (London, England)* **2014**, *383* (9911), 69-82.
3. Bluestone, J. A.; Herold, K.; Eisenbarth, G., Genetics, pathogenesis and clinical interventions in type 1 diabetes. *Nature* **2010**, *464*, 1293.
4. Anderson, M. S.; Bluestone, J. A., THE NOD MOUSE: A Model of Immune Dysregulation. *Annual Review of Immunology* **2005**, *23* (1), 447-485.
5. McInnes, I. B.; Schett, G., The Pathogenesis of Rheumatoid Arthritis. *New England Journal of Medicine* **2011**, *365* (23), 2205-2219.
6. Daha, N. A.; Toes, R. E., Rheumatoid arthritis: Are ACPA-positive and ACPA-negative RA the same disease? *Nature reviews. Rheumatology* **2011**, *7* (4), 202-3.
7. Trouw, L. A.; Huizinga, T. W. J.; Toes, R. E. M., Autoimmunity in rheumatoid arthritis: different antigens—common principles. *Annals of the Rheumatic Diseases* **2013**, *72* (suppl 2), ii132-ii136.
8. Dendrou, C. A.; Fugger, L.; Friese, M. A., Immunopathology of multiple sclerosis. *Nature Reviews Immunology* **2015**, *15*, 545.
9. Haghikia, A.; Hohlfeld, R.; Gold, R.; Fugger, L., Therapies for multiple sclerosis: translational achievements and outstanding needs. *Trends in Molecular Medicine* **2013**, *19* (5), 309-319.
10. Hellings, N.; Barée, M.; Verhoeven, C.; D'Hooghe, M. B.; Medaer, R.; Bernard, C. C. A.; Raus, J.; Stinissen, P., T-cell reactivity to multiple myelin antigens in multiple sclerosis patients and healthy controls. *Journal of Neuroscience Research* **2001**, *63* (3), 290-302.
11. Constantinescu, C. S.; Farooqi, N.; O'Brien, K.; Gran, B., Experimental autoimmune encephalomyelitis (EAE) as a model for multiple sclerosis (MS). *Br J Pharmacol* **2011**, *164* (4), 1079-1106.
12. Rosenblum, M. D.; Remedios, K. A.; Abbas, A. K., Mechanisms of human autoimmunity. *The Journal of clinical investigation* **2015**, *125* (6), 2228-2233.
13. Hogquist, K. A.; Baldwin, T. A.; Jameson, S. C., Central tolerance: learning self-control in the thymus. *Nature Reviews Immunology* **2005**, *5* (10), 772-782.
14. Lämmermann, T.; Sixt, M., The microanatomy of T-cell responses. *Immunological Reviews* **2008**, *221* (1), 26-43.
15. Mueller, D. L., Mechanisms maintaining peripheral tolerance. *Nature Immunology* **2009**, *11*, 21.
16. Vignali, D. A. A.; Collison, L. W.; Workman, C. J., How regulatory T-cells work. *Nature reviews. Immunology* **2008**, *8* (7), 523-532.
17. Hori, S.; Haurly, M.; Coutinho, A.; Demengeot, J., Specificity requirements for selection and effector functions of CD25+4+ regulatory T-cells in anti-myelin basic protein T-cell receptor transgenic mice. *Proceedings of the National Academy of Sciences of the United States of America* **2002**, *99* (12), 8213-8218.
18. Yamazaki, S.; Iyoda, T.; Tarbell, K.; Olson, K.; Velinzon, K.; Inaba, K.; Steinman, R. M., Direct expansion of functional CD25+ CD4+ regulatory T-cells by antigen-processing dendritic cells. *The Journal of experimental medicine* **2003**, *198* (2), 235-247.
19. Hawrylowicz, C. M.; O'Garra, A., Potential role of interleukin-10-secreting regulatory T-cells in allergy and asthma. *Nature Reviews Immunology* **2005**, *5* (4), 271-283.

20. Nakamura, K.; Kitani, A.; Strober, W., Cell Contact–Dependent Immunosuppression by Cd4<sup>+</sup>Cd25<sup>+</sup>Regulatory T-cells Is Mediated by Cell Surface–Bound Transforming Growth Factor  $\beta$ . *The Journal of Experimental Medicine* **2001**, *194* (5), 629-644.
21. Oderup, C.; Cederbom, L.; Makowska, A.; Cilio, C. M.; Ivars, F., Cytotoxic T lymphocyte antigen-4-dependent down-modulation of costimulatory molecules on dendritic cells in CD4<sup>+</sup> CD25<sup>+</sup> regulatory T-cell-mediated suppression. *Immunology* **2006**, *118* (2), 240-9.
22. Fallarino, F.; Grohmann, U.; Hwang, K. W.; Orabona, C.; Vacca, C.; Bianchi, R.; Belladonna, M. L.; Fioretti, M. C.; Alegre, M. L.; Puccetti, P., Modulation of tryptophan catabolism by regulatory T-cells. *Nat Immunol* **2003**, *4* (12), 1206-12.
23. Wiseman, A. C., Immunosuppressive Medications. *Clin J Am Soc Nephrol* **2016**, *11* (2), 332-343.
24. Newton, R., Molecular mechanisms of glucocorticoid action: what is important? *Thorax* **2000**, *55* (7), 603-613.
25. Rhen, T.; Cidlowski, J. A., Antiinflammatory Action of Glucocorticoids — New Mechanisms for Old Drugs. *New England Journal of Medicine* **2005**, *353* (16), 1711-1723.
26. De Bosscher, K.; Vanden Berghe, W.; Haegeman, G., The Interplay between the Glucocorticoid Receptor and Nuclear Factor- $\kappa$ B or Activator Protein-1: Molecular Mechanisms for Gene Repression. *Endocrine Reviews* **2003**, *24* (4), 488-522.
27. Youssef, J.; Novosad, S. A.; Winthrop, K. L., Infection Risk and Safety of Corticosteroid Use. *Rheum Dis Clin North Am* **2016**, *42* (1), 157-x.
28. Liu, D.; Ahmet, A.; Ward, L.; Krishnamoorthy, P.; Mandelcorn, E. D.; Leigh, R.; Brown, J. P.; Cohen, A.; Kim, H., A practical guide to the monitoring and management of the complications of systemic corticosteroid therapy. *Allergy Asthma Clin Immunol* **2013**, *9* (1), 30-30.
29. Gold, R.; Kappos, L.; Arnold, D. L.; Bar-Or, A.; Giovannoni, G.; Selmaj, K.; Tornatore, C.; Sweetser, M. T.; Yang, M.; Sheikh, S. I.; Dawson, K. T., Placebo-controlled phase 3 study of oral BG-12 for relapsing multiple sclerosis. *The New England journal of medicine* **2012**, *367* (12), 1098-107.
30. Fox, R. J.; Miller, D. H.; Phillips, J. T.; Hutchinson, M.; Havrdova, E.; Kita, M.; Yang, M.; Raghupathi, K.; Novas, M.; Sweetser, M. T.; Vigiuetta, V.; Dawson, K. T., Placebo-controlled phase 3 study of oral BG-12 or glatiramer in multiple sclerosis. *The New England journal of medicine* **2012**, *367* (12), 1087-97.
31. Mills, E. A.; Ogrodnik, M. A.; Plave, A.; Mao-Draayer, Y., Emerging Understanding of the Mechanism of Action for Dimethyl Fumarate in the Treatment of Multiple Sclerosis. *Front Neurol* **2018**, *9*, 5-5.
32. Gross, C. C.; Schulte-Mecklenbeck, A.; Klinsing, S.; Posevitz-Fejfar, A.; Wiendl, H.; Klotz, L., Dimethyl fumarate treatment alters circulating T helper cell subsets in multiple sclerosis. *Neurology(R) neuroimmunology & neuroinflammation* **2016**, *3* (1), e183.
33. Oreja-Guevara, C.; Ramos-Cejudo, J.; Aroeira, L. S.; Chamorro, B.; Diez-Tejedor, E., TH1/TH2 Cytokine profile in relapsing-remitting multiple sclerosis patients treated with Glatiramer acetate or Natalizumab. *BMC Neurol* **2012**, *12*, 95-95.
34. Gieselbach, R.-J.; Muller-Hansma, A. H.; Wijburg, M. T.; de Bruin-Weller, M. S.; van Oosten, B. W.; Nieuwkamp, D. J.; Coenjaerts, F. E.; Wattjes, M. P.; Murk, J.-L., Progressive multifocal leukoencephalopathy in patients treated with fumaric acid esters: a review of 19 cases. *Journal of Neurology* **2017**, *264* (6), 1155-1164.

35. Torkildsen, Ø.; Myhr, K.-M.; Bø, L., Disease-modifying treatments for multiple sclerosis – a review of approved medications. *European Journal of Neurology* **2016**, *23* (S1), 18-27.
36. Oldfield, V.; Dhillon, S.; Plosker, G. L., Tocilizumab. *Drugs* **2009**, *69* (5), 609-632.
37. Scott, L. J., Etanercept: A Review of Its Use in Autoimmune Inflammatory Diseases. *Drugs* **2014**, *74* (12), 1379-1410.
38. Genestier, L.; Paillot, R.; Fournel, S.; Ferraro, C.; Miossec, P.; Revillard, J. P., Immunosuppressive properties of methotrexate: apoptosis and clonal deletion of activated peripheral T-cells. *The Journal of Clinical Investigation* **1998**, *102* (2), 322-328.
39. CUTOLO, M.; SULLI, A.; PIZZORNI, C.; SERIOLO, B.; STRAUB, R. H., Anti-inflammatory mechanisms of methotrexate in rheumatoid arthritis. *Annals of the Rheumatic Diseases* **2001**, *60* (8), 729-735.
40. Gilani, S. T.; Khan, D. A.; Khan, F. A.; Ahmed, M., Adverse effects of low dose methotrexate in rheumatoid arthritis patients. *Journal of the College of Physicians and Surgeons-Pakistan : JCPSP* **2012**, *22* (2), 101-4.
41. Emery, P.; Deodhar, A.; Rigby, W. F.; Isaacs, J. D.; Combe, B.; Racewicz, A. J.; Latinis, K.; Abud-Mendoza, C.; Szczepański, L. J.; Roschmann, R. A.; Chen, A.; Armstrong, G. K.; Douglass, W.; Tyrrell, H., Efficacy and safety of different doses and retreatment of rituximab: a randomised, placebo-controlled trial in patients who are biological naïve with active rheumatoid arthritis and an inadequate response to methotrexate (Study Evaluating Rituximab's Efficacy in MTX iNadequate rEsponders (SERENE)). *Annals of the Rheumatic Diseases* **2010**, *69* (9), 1629-1635.
42. Hauser, S. L.; Bar-Or, A.; Comi, G.; Giovannoni, G.; Hartung, H.-P.; Hemmer, B.; Lublin, F.; Montalban, X.; Rammohan, K. W.; Selmaj, K.; Traboulsee, A.; Wolinsky, J. S.; Arnold, D. L.; Klingelschmitt, G.; Masterman, D.; Fontoura, P.; Belachew, S.; Chin, P.; Mairon, N.; Garren, H.; Kappos, L., Ocrelizumab versus Interferon Beta-1a in Relapsing Multiple Sclerosis. *New England Journal of Medicine* **2017**, *376* (3), 221-234.
43. Gottenberg, J. E.; Ravaut, P.; Bardin, T.; Cacoub, P.; Cantagrel, A.; Combe, B.; Dougados, M.; Flipo, R. M.; Godeau, B.; Guillevin, L.; Le Loet, X.; Hachulla, E.; Schaeffer, T.; Sibilia, J.; Baron, G.; Mariette, X., Risk factors for severe infections in patients with rheumatoid arthritis treated with rituximab in the autoimmunity and rituximab registry. *Arthritis and rheumatism* **2010**, *62* (9), 2625-32.
44. Dörner, T.; Isenberg, D.; Jayne, D.; Wiendl, H.; Zillikens, D.; Burmester, G., Current status on B-cell depletion therapy in autoimmune diseases other than rheumatoid arthritis. *Autoimmunity Reviews* **2009**, *9* (2), 82-89.
45. Sailler, L., Rituximab Off Label Use for Difficult-To-Treat Auto-Immune Diseases: Reappraisal of Benefits and Risks. *Clinical Reviews in Allergy & Immunology* **2008**, *34* (1), 103-110.
46. Mulero, P.; Midaglia, L.; Montalban, X., Ocrelizumab: a new milestone in multiple sclerosis therapy. *Ther Adv Neurol Disord* **2018**, *11*, 1756286418773025.
47. Liossis, S.-N. C.; Sfrikakis, P. P., Rituximab-induced B cell depletion in autoimmune diseases: Potential effects on T-cells. *Clinical Immunology* **2008**, *127* (3), 280-285.
48. McCormack, P. L., Natalizumab: A Review of Its Use in the Management of Relapsing-Remitting Multiple Sclerosis. *Drugs* **2013**, *73* (13), 1463-1481.
49. Carson, K. R.; Focosi, D.; Major, E. O.; Petrini, M.; Richey, E. A.; West, D. P.; Bennett, C. L., Monoclonal antibody-associated progressive multifocal leucoencephalopathy in patients

- treated with rituximab, natalizumab, and efalizumab: a Review from the Research on Adverse Drug Events and Reports (RADAR) Project. *The Lancet Oncology* **2009**, *10* (8), 816-824.
50. Leonardi, C. L., Efalizumab: an overview. *Journal of the American Academy of Dermatology* **2003**, *49* (2, Supplement), 98-104.
  51. Sanford, M., Fingolimod: A Review of Its Use in Relapsing-Remitting Multiple Sclerosis. *Drugs* **2014**, *74* (12), 1411-1433.
  52. Mehling, M.; Brinkmann, V.; Antel, J.; Bar-Or, A.; Goebels, N.; Vedrine, C.; Kristofic, C.; Kuhle, J.; Lindberg, R. L. P.; Kappos, L., FTY720 therapy exerts differential effects on T-cell subsets in multiple sclerosis. *Neurology* **2008**, *71* (16), 1261-1267.
  53. Mehling, M.; Lindberg, R.; Raulf, F.; Kuhle, J.; Hess, C.; Kappos, L.; Brinkmann, V., Th17 central memory T-cells are reduced by FTY720 in patients with multiple sclerosis. *Neurology* **2010**, *75* (5), 403-410.
  54. Freeman, J., FURTHER OBSERVATIONS ON THE TREATMENT OF HAY FEVER BY HYPODERMIC INOCULATIONS OF POLLEN VACCINE. *The Lancet* **1911**, *178* (4594), 814-817.
  55. Noon, L., PROPHYLACTIC INOCULATION AGAINST HAY FEVER. *The Lancet* **1911**, *177* (4580), 1572-1573.
  56. Krishna, M. T.; Huissoon, A. P., Clinical immunology review series: an approach to desensitization. *Clinical & Experimental Immunology* **2011**, *163* (2), 131-146.
  57. Akdis, C. A.; Akdis, M., Mechanisms of allergen-specific immunotherapy and immune tolerance to allergens. *The World Allergy Organization journal* **2015**, *8* (1), 17-17.
  58. Peakman, M.; Dayan, C. M., Antigen-specific immunotherapy for autoimmune disease: fighting fire with fire? *Immunology* **2001**, *104* (4), 361-366.
  59. Pozzilli, P.; Pitocco, D.; Visalli, N.; Cavallo, M. G.; Buzzetti, R.; Crino, A.; Spera, S.; Suraci, C.; Multari, G.; Cervoni, M.; Manca Bitti, M. L.; Matteoli, M. C.; Marietti, G.; Ferrazzoli, F.; Cassone Faldetta, M. R.; Giordano, C.; Sbriglia, M.; Sarugeri, E.; Ghirlanda, G., No effect of oral insulin on residual beta-cell function in recent-onset type I diabetes (the IMDIAB VII). IMDIAB Group. *Diabetologia* **2000**, *43* (8), 1000-4.
  60. Nanto-Salonen, K.; Kupila, A.; Simell, S.; Siljander, H.; Salonsaari, T.; Hekkala, A.; Korhonen, S.; Erkkola, R.; Sipila, J. I.; Haavisto, L.; Siltala, M.; Tuominen, J.; Hakalax, J.; Hyoty, H.; Ilonen, J.; Veijola, R.; Simell, T.; Knip, M.; Simell, O., Nasal insulin to prevent type 1 diabetes in children with HLA genotypes and autoantibodies conferring increased risk of disease: a double-blind, randomised controlled trial. *Lancet* **2008**, *372* (9651), 1746-55.
  61. Harrison, L. C.; Honeyman, M. C.; Steele, C. E.; Stone, N. L.; Sarugeri, E.; Bonifacio, E.; Couper, J. J.; Colman, P. G., Pancreatic beta-cell function and immune responses to insulin after administration of intranasal insulin to humans at risk for type 1 diabetes. *Diabetes Care* **2004**, *27* (10), 2348-55.
  62. Chaillous, L.; Lefevre, H.; Thivolet, C.; Boitard, C.; Lahlou, N.; Atlan-Gepner, C.; Bouhanick, B.; Mogenet, A.; Nicolino, M.; Carel, J. C.; Lecomte, P.; Marechaud, R.; Bougneres, P.; Charbonnel, B.; Sai, P., Oral insulin administration and residual beta-cell function in recent-onset type 1 diabetes: a multicentre randomised controlled trial. Diabete Insuline Orale group. *Lancet* **2000**, *356* (9229), 545-9.
  63. Ludvigsson, J.; Cheramy, M.; Axelsson, S.; Pihl, M.; Akerman, L.; Casas, R., GAD-treatment of children and adolescents with recent-onset type 1 diabetes preserves residual insulin secretion after 30 months. *Diabetes/metabolism research and reviews* **2014**, *30* (5), 405-14.

64. Ludvigsson, J.; Faresjo, M.; Hjorth, M.; Axelsson, S.; Cheramy, M.; Pihl, M.; Vaarala, O.; Forsander, G.; Ivarsson, S.; Johansson, C.; Lindh, A.; Nilsson, N. O.; Aman, J.; Ortqvist, E.; Zerhouni, P.; Casas, R., GAD treatment and insulin secretion in recent-onset type 1 diabetes. *The New England journal of medicine* **2008**, *359* (18), 1909-20.
65. Weiner, H. L.; Mackin, G. A.; Matsui, M.; Orav, E. J.; Khoury, S. J.; Dawson, D. M.; Hafler, D. A., Double-blind pilot trial of oral tolerization with myelin antigens in multiple sclerosis. *Science (New York, N.Y.)* **1993**, *259* (5099), 1321-4.
66. Serra, P.; Santamaria, P., Antigen-specific therapeutic approaches for autoimmunity. *Nature Biotechnology* **2019**, *37* (3), 238-251.
67. Feldmann, M.; Steinman, L., Design of effective immunotherapy for human autoimmunity. *Nature* **2005**, *435* (7042), 612-619.
68. Bielekova, B.; Goodwin, B.; Richert, N.; Cortese, I.; Kondo, T.; Afshar, G.; Gran, B.; Eaton, J.; Antel, J.; Frank, J. A.; McFarland, H. F.; Martin, R., Encephalitogenic potential of the myelin basic protein peptide (amino acids 83-99) in multiple sclerosis: results of a phase II clinical trial with an altered peptide ligand. *Nature medicine* **2000**, *6* (10), 1167-75.
69. Kappos, L.; Comi, G.; Panitch, H.; Oger, J.; Antel, J.; Conlon, P.; Steinman, L., Induction of a non-encephalitogenic type 2 T helper-cell autoimmune response in multiple sclerosis after administration of an altered peptide ligand in a placebo-controlled, randomized phase II trial. The Altered Peptide Ligand in Relapsing MS Study Group. *Nature medicine* **2000**, *6* (10), 1176-82.
70. Walter, M.; Philotheou, A.; Bonnici, F.; Ziegler, A.-G.; Jimenez, R.; Group, N. B. I. S., No effect of the altered peptide ligand NBI-6024 on beta-cell residual function and insulin needs in new-onset type 1 diabetes. *Diabetes care* **2009**, *32* (11), 2036-2040.
71. Burkhart, C.; Liu, G. Y.; Anderton, S. M.; Metzler, B.; Wraith, D. C., Peptide-induced T-cell regulation of experimental autoimmune encephalomyelitis: a role for IL-10. *International Immunology* **1999**, *11* (10), 1625-1634.
72. Carlier, V. A.; VanderElst, L.; Janssens, W.; Jacquemin, M. G.; Saint-Remy, J. M., Increased synapse formation obtained by T-cell epitopes containing a CxxC motif in flanking residues convert CD4+ T-cells into cytolytic effectors. *PLoS one* **2012**, *7* (10), e45366.
73. Malek Abrahamians, E.; Vander Elst, L.; Carlier, V. A.; Saint-Remy, J. M., Thioreductase-Containing Epitopes Inhibit the Development of Type 1 Diabetes in the NOD Mouse Model. *Frontiers in immunology* **2016**, *7*, 67.
74. Caporro, M.; Disanto, G.; Gobbi, C.; Zecca, C., Two decades of subcutaneous glatiramer acetate injection: current role of the standard dose, and new high-dose low-frequency glatiramer acetate in relapsing-remitting multiple sclerosis treatment. *Patient Preference Adherence* **2014**, *8*, 1123-1134.
75. Song, J. Y.; Larson, N. R.; Thati, S.; Torres-Vazquez, I.; Martinez-Rivera, N.; Subelzu, N. J.; Leon, M. A.; Rosa-Molinar, E.; Schöneich, C.; Forrest, M. L.; Middaugh, C. R.; Berkland, C. J., Glatiramer acetate persists at the injection site and draining lymph nodes via electrostatically-induced aggregation. *Journal of Controlled Release* **2019**, *293*, 36-47.
76. Aharoni, R., Immunomodulation neuroprotection and remyelination – The fundamental therapeutic effects of glatiramer acetate: A critical review. *Journal of autoimmunity* **2014**, *54*, 81-92.
77. Fridkis-Hareli, M.; Teitelbaum, D.; Gurevich, E.; Pecht, I.; Brautbar, C.; Kwon, O. J.; Brenner, T.; Arnon, R.; Sela, M., Direct binding of myelin basic protein and synthetic copolymer 1 to class II major histocompatibility complex molecules on living antigen-presenting cells--

- specificity and promiscuity. *Proceedings of the National Academy of Sciences* **1994**, *91* (11), 4872-4876.
78. Duda, P. W.; Schmied, M. C.; Cook, S. L.; Krieger, J. I.; Hafler, D. A., Glatiramer acetate (Copaxone) induces degenerate, Th2-polarized immune responses in patients with multiple sclerosis. *J Clin Invest* **2000**, *105* (7), 967-76.
79. Kang, Y.; Xu, L.; Wang, B.; Chen, A.; Zheng, G., Cutting edge: Immunosuppressant as adjuvant for tolerogenic immunization. *J Immunol* **2008**, *180* (8), 5172-5176.
80. Peine, K. J.; Guerau-de-Arellano, M.; Lee, P.; Kanthamneni, N.; Severin, M.; Probst, G. D.; Peng, H.; Yang, Y.; Vangundy, Z.; Papenfuss, T. L.; Lovett-Racke, A. E.; Bachelder, E. M.; Ainslie, K. M., Treatment of Experimental Autoimmune Encephalomyelitis by Codelivery of Disease Associated Peptide and Dexamethasone in Acetalated Dextran Microparticles. *Molecular Pharmaceutics* **2014**, *11* (3), 828-835.
81. Keating, G. M., Abatacept: A Review of its Use in the Management of Rheumatoid Arthritis. *Drugs* **2013**, *73* (10), 1095-1119.
82. Symer, D. E.; Reim, J.; Dintzis, R. Z.; Voss, E. W.; Dintzis, H. M., Durable elimination of high affinity, T-cell-dependent antibodies by low molecular weight antigen arrays in vivo. *The Journal of Immunology* **1995**, *155* (12), 5608-5616.
83. Leonardi, C. L., Efalizumab: an overview. *J Am Acad Dermatol* **2003**, *49* (2 Suppl), S98-104.
84. Hartwell, B. L.; Pickens, C. J.; Leon, M.; Northrup, L.; Christopher, M. A.; Griffin, J. D.; Martinez-Becerra, F.; Berkland, C., Soluble antigen arrays disarm antigen-specific B cells to promote lasting immune tolerance in experimental autoimmune encephalomyelitis. *Journal of autoimmunity* **2018**, *93*, 76-88.
85. Hartwell, B. L.; Pickens, C. J.; Leon, M.; Berkland, C., Multivalent Soluble Antigen Arrays Exhibit High Avidity Binding and Modulation of B Cell Receptor-Mediated Signaling to Drive Efficacy against Experimental Autoimmune Encephalomyelitis. *Biomacromolecules* **2017**, *18* (6), 1893-1907.
86. Leon, M. A.; Wemlinger, S. M.; Larson, N. R.; Ruffalo, J. K.; Sestak, J. O.; Middaugh, C. R.; Cambier, J. C.; Berkland, C., Soluble Antigen Arrays for Selective Desensitization of Insulin-Reactive B Cells. *Mol Pharm* **2019**, *16* (4), 1563-1572.

**Chapter 2: Antigen-Drug Conjugates as a Novel Therapeutic Class for the Treatment of Antigen-Specific Autoimmune Disorders**

## 1. Introduction

The adaptive immune response is dependent on recognition of target antigens, and autoimmune diseases occur when the body fails to maintain tolerance toward self-antigens.<sup>1</sup> These self-antigens can be present in a number of host tissues in various organs, leading to many types of autoimmune diseases including multiple sclerosis (MS).<sup>2</sup> MS is the most common cause of neurological disability in young adults, affecting approximately 2.5 million patients worldwide<sup>3</sup>, and symptoms of the disease are highly variable<sup>4</sup>. While the mechanisms of disease induction have not been fully elucidated, a prevailing hypothesis is that loss of immune tolerance towards proteins composing the myelin sheath, such as proteolipid protein (PLP) and myelin basic protein (MBP), triggers recruitment of offending myelin-specific CD4<sup>+</sup> T-cells, resulting in demyelination within the central nervous system.<sup>5</sup> Current therapies include monoclonal antibodies and corticosteroids, however, the treatment landscape for MS is expanding as our understanding of disease pathogenesis continues to evolve.<sup>6</sup> Corticosteroids have been a cornerstone for MS therapy, but the lack of specificity results in a wide range of side effects. Attempts have been made to develop antigen-specific immune therapies (ASITs) to reduce side effects and selectively re-tolerize the immune system to myelin sheath proteins. Despite being relatively safe, ASITs have yet to reduce the severity of MS.<sup>7-9</sup> Here, we present antigen-drug conjugates (AgDCs) as a combination of these approaches with the potential to boost the efficacy of ASIT while mitigating the detrimental side effects of current immunosuppressant therapies.

AgDCs merge two general approaches to combat autoimmunity: immunomodulatory agents and ASIT. ASIT provides the specificity necessary to reverse an immune response toward a particular antigen. ASIT has been effective for inducing tolerance towards allergens, but has yet to emerge as an effective autoimmune therapy.<sup>7-9</sup> Immunomodulatory agents can

effectively treat autoimmune diseases, but suffer from systemic exposure and subsequent global immunosuppression, which can be problematic in immunocompromised patient populations by increasing vulnerability to opportunistic infections. By chemically conjugating the antigen and immunomodulator, the antigen may target the immunomodulator to diseased cell populations, potentially limiting off-target side effects. The concept of AgDCs is similar to antibody-drug conjugates (ADCs), however AgDCs likely achieve high affinity specificity by targeting endogenous autoantibodies or cognate B cell receptors, thus essentially flipping the mechanism of ADCs.

The design of AgDCs requires selection of an appropriate antigen or epitope, an immune modulator, and a linking scheme. With this in mind, a murine experimental autoimmune encephalomyelitis (EAE) model exhibiting clinical and histopathological similarities to relapsing-remitting multiple sclerosis (RRMS) in humans<sup>2</sup> was selected to probe the proposed AgDC concept. The model is induced by administering an adjuvanted ‘vaccine’ containing the antigenic epitope PLP<sub>139-151</sub>. This particular EAE model is CD4<sup>+</sup> T-cell-mediated disease with B cell involvement, leading to primary demyelination of the axonal tracks in the CNS and subsequent progressive paralysis of the hind-limbs.<sup>10-11</sup> Most importantly, this particular EAE model provided a simplified system for testing the efficacy of AgDCs wherein the disease may be induced with a specific peptide, PLP<sub>139-151</sub>, and subsequently treated with an AgDC utilizing the same PLP<sub>139-151</sub> epitope.

Dexamethasone (DEX) was selected as the immune modulator for testing the AgDC concept. Our lab previously screened multiple immune modulators in combination with PLP<sub>139-151</sub> by using splenocytes derived from EAE mice.<sup>12</sup> DEX emerged as one of the most potent suppressors of proinflammatory cytokines when rechallenging EAE splenocytes with PLP<sub>139-151</sub>

and also showed evidence of inducing markers of immune tolerance (e.g. upregulation of IL-10). DEX possesses the necessary potency required (pMol-nMol range)<sup>13-14</sup>, since the dose typically used for antigen-specific immunotherapy is on the order of milligrams of antigen per injection.<sup>15</sup> Finally, we rationalized DEX must be released in order to escape the typical binding and internalization pathway associated with antigen recognition and processing. Thus, we designed an ester linker capable of releasing DEX from PLP<sub>139-151</sub> via hydrolysis with accelerated release under acidic conditions.

In this article, we outline the synthetic strategy, characterization, and biological screening of an AgDC containing PLP<sub>139-151</sub> and DEX. These two components were conjugated utilizing copper-catalyzed azide-alkyne cycloaddition (CuAAC) chemistry and this linkage was characterized by HPLC and mass spectrometry. Additionally, AgDC linker stability was monitored over a short time frame to confirm the desired release of DEX. Finally, the efficacy of this AgDC was demonstrated first *in vitro* through the use of EAE splenocytes induced against PLP<sub>139-151</sub> and subsequently *in vivo* through subcutaneous administration to EAE mice.

## 2. Materials and Methods

DEX, tris(3-hydroxypropyltriazolylmethyl)amine (THPTA), and sodium ascorbate (NaAsc) were purchased from Sigma-Aldrich (St. Louis, MO). Copper(II) sulfate pentahydrate (CuSO<sub>4</sub> • 5H<sub>2</sub>O) was purchased from Acros Organics (Geel, Belgium). 2,5-dioxopyrrolidin-1-yl 2-azidoacetate, DBCO-PEG<sub>4</sub>-Maleimide, DBCO-NH<sub>2</sub>, and MMAE-DBCO were purchased from Click Chemistry Tools, LLC (Scottsdale, AZ). Doxorubicin hydrochloride was purchased from LC Laboratories (Woburn, MA). Mertansine (DM1) was purchased from Carbosynth Limited (Berkshire, UK). All other chemicals and reagents were analytical grade and were used as received without further purification.

The peptides PLP<sub>139-151</sub>-Alk (*N*-terminal 4-pentynoic acid PLP<sub>139-151</sub>) and PLP<sub>139-151</sub>-N<sub>3</sub> (*N*-terminal 3-(2-(2-(2-azidoethoxy)ethoxy)ethoxy)propanoic acid PLP<sub>139-151</sub>) have been synthesized in our laboratory via solid phase peptide synthesis on a Wang resin, but larger quantities of each peptide were obtained from Biomatik Corporation (Wilmington, DE). In each case, the linker 3-(2-(2-(2-azidoethoxy)ethoxy)ethoxy)propanoic acid was purchased from PurePEG, LLC (San Diego, CA) and 4-pentynoic acid was purchased from Sigma-Aldrich (St. Louis, MO).

### 2.1. Synthesis of azide-functionalized DEX (DEX-N<sub>3</sub>)

DEX (842  $\mu$ mol) was added to a flame dried 250 mL round bottom flask with a stir bar and septa. Anhydrous MeCN (100 mL) was added under nitrogen, followed by DIPEA (919  $\mu$ mol, 1.09 eq.) via glass syringe. The flask was stirred for 10 min before azidoacetic acid NHS ester (908  $\mu$ mol, 1.08 eq.) was added as a powder. The reaction mixture was stirred overnight at room temperature before being analyzed by HPLC. Additional equimolar aliquots of azidoacetic acid NHS ester were added, followed by stirring for 2 hours at room temperature and analyzing by HPLC, until no additional benefit was observed. The crude reaction mixture was evaporated under reduced pressure, then dissolved in 4:6 MeCN:H<sub>2</sub>O and purified by prep HPLC. The resulting column fractions were evaporated under reduced pressure to yield the final product as a white powder. <sup>1</sup>H NMR (500 MHz, DMSO-d<sub>6</sub>)  $\delta$  7.30 (d, *J* = 10.2 Hz, 1H), 6.23 (dd, *J* = 10.1, 1.9 Hz, 1H), 6.01 (t, *J* = 1.7 Hz, 1H), 5.45 (dd, *J* = 5.0, 1.4 Hz, 1H), 5.23 (s, 1H), 5.17 (d, *J* = 17.5 Hz, 1H), 4.90 (d, *J* = 17.6 Hz, 1H), 4.32 – 4.19 (m, 2H), 4.19 – 4.11 (m, 1H), 2.88 (dq, *J* = 11.5, 7.2, 4.1 Hz, 1H), 2.62 (tdd, *J* = 13.6, 6.0, 1.7 Hz, 1H), 2.44 – 2.32 (m, 1H), 2.35 – 2.28 (m, 1H), 2.22 – 2.05 (m, 3H), 1.77 (dt, *J* = 11.2, 5.2 Hz, 1H), 1.70 – 1.58 (m, 1H), 1.56 (dd, *J* = 13.8, 2.0 Hz, 1H), 1.49 (s, 3H), 1.35 (qd, *J* = 12.9, 5.0 Hz, 1H), 1.08 (ddd, *J* = 12.1, 8.2, 4.1 Hz, 1H),

0.89 (s, 3H), 0.80 (d, J = 7.2 Hz, 3H). <sup>13</sup>C NMR (126 MHz, DMSO) δ 204.36, 185.30, 168.28, 167.10, 152.77, 129.03, 124.12, 102.00, 100.61, 90.52, 70.63, 70.34, 69.00, 49.34, 48.09, 48.05, 47.87, 43.33, 35.69, 35.53, 33.67, 33.51, 31.92, 30.28, 27.32, 23.03, 22.98, 16.31, 15.15, 1.19. Expected [M+H]<sup>+</sup> = 476.2191 Da, Observed [M+H]<sup>+</sup> = 476.2067 Da.

## 2.2. Synthesis of PLP<sub>139-151</sub>-DEX

To a solution of PLP<sub>139-151</sub>-Alk (93.6 μmol) in 120 mL deionized H<sub>2</sub>O was added DEX-N<sub>3</sub> (189.4 μmol, 2.02 eq.) in 12 mL EtOH. 5.7 mL of a premixed solution of CuSO<sub>4</sub>•5H<sub>2</sub>O (38.1 μmol) and THPTA (189.8 μmol) in deionized H<sub>2</sub>O was added to the reaction mixture, followed by 7.2 mL of NaAsc (726.9 μmol) in deionized H<sub>2</sub>O. The reaction was allowed to stir at room temperature for 1 hour before an aliquot was removed for analytical HPLC to monitor reaction progress. After 3 hours, the reaction mixture was concentrated under reduced pressure, and purified by preparative HPLC on a Waters XBridge BEH C<sub>18</sub>, 5 μm, 130 Å, 19x250 mm column using a gradient of MeCN in H<sub>2</sub>O (constant 0.05% TFA). The isolated fractions were evaporated under reduced pressure to remove residual MeCN, then frozen at -20°C and lyophilized to yield a white powder. Expected [M+2H]<sup>2+</sup> = 1039.5224 Da, [M+3H]<sup>3+</sup> = 693.3507 Da; Observed [M+2H]<sup>2+</sup> = 1039.5145 Da, [M+3H]<sup>3+</sup> = 693.3478 Da.

## 2.3. Analytical characterization

All HPLC chromatographic analysis was conducted on a Waters Alliance HPLC system equipped with either a diode array detector or dual wavelength UV/Vis detector. For RP-HPLC, general chromatographic conditions employed a linear elution gradient from 5-95% acetonitrile in water (constant 0.05% trifluoroacetic acid) over 50 min, on a Waters XBridge BEH C<sub>18</sub>, 3.5 μm, 130 Å stationary phase (4.6 x 150 mm), with a 1.0 mL/min flow rate and a 35°C column temperature. For semi-preparative HPLC, a linear elution gradient of acetonitrile in water

(constant 0.05% trifluoroacetic acid) over 20 min, on a Waters XBridge BEH C<sub>18</sub>, 5 μm, 130 Å stationary phase (19 x 250 mm), with a 14.0 mL/min flow rate was utilized. Gradients were optimized for each run using the identical stationary phase in a 4.6 x 250 mm configuration.

LC/MS sample analysis was completed on a Waters Xevo G2, employing linear elution gradients of 15-100% acetonitrile in water (constant 0.1% formic acid) over 45 min, on a Waters XBridge BEH C<sub>18</sub>, 1.7 μm, 130 Å stationary phase (0.075 x 250 mm), with a 0.5 μL/min flow rate and 50°C column temperature. Electrospray ionization, operating in the positive mode (ESI+), was used as the ionization source with a QTOF mass analyzer used for detection.

NMR spectra were collected on a Bruker Avance AVIII 500 MHz spectrometer equipped with a dual carbon/proton cryoprobe, and all samples were dissolved in 650 μL of D<sub>2</sub>O or DMSO-*d*<sub>6</sub>. Data processing was completed using MestReNova 11.0 (Santiago de Compostela, Spain).

#### **2.4. Drug release and stability studies**

Release and stability studies were conducted via HPLC with UV detection by dissolving the compound of interest in various buffers (typically pH 7.0 phosphate, pH 5.5 acetate, deionized H<sub>2</sub>O, etc.) and evaluating the release at temperatures and times relevant to the particular study. Peak integration is used for quantification, accounting for initial purity of the PLP<sub>139-151</sub>-DEX at T = 0.

#### **2.5. Induction of EAE**

*In vitro* and *in vivo* studies were performed through the use of 4-6 week old SJL/J (H-2) female mice purchased from Envigo Laboratories (Indianapolis, IN). All experiments were approved through the University's Institutional Animal Care and Use Committee with animal

housing in pathogen-free conditions. An emulsion containing 200 µg PLP<sub>139-151</sub> in Complete Freund's Adjuvant (CFA) was prepared by combining IFA and heat-killed *M. Tuberculosis* strain H37RA at a final concentration of 4 mg/mL with subsequent emulsification between CFA and PBS containing 200 µg PLP<sub>139-151</sub>. This PLP<sub>139-151</sub> in CFA emulsion was administered to mice on day 0 by four subcutaneous injections of 50 µL each located above each shoulder and hind flank for a total of 0.2 mL. Additionally, intraperitoneal injections of pertussis toxin (100 ng in 100 µL PBS) were administered on day 0 and day 2. Disease severity was recorded using the following clinical scoring system: 0, no clinical disease symptoms; 1, weakness or limpness of the tail; 2, weakness or partial paralysis of one or two hind limbs (paraparesis); 3, full paralysis of both hind limbs (paraplegia); 4, paraplegia plus weakness or paralysis of forelimbs; 5, moribund (euthanasia necessary). Mouse body weight was also recorded daily throughout the duration of the studies.

## **2.6. In Vivo Efficacy in EAE Mice**

*In vivo* studies were performed with 9 mice per treatment group. Five mice were euthanized on day 14 (peak-of-disease) while the remaining mice were euthanized on day 25. Treatments were administered to mice through subcutaneous injection of 100 µL at the base of the neck on the back of the mouse on days 4, 7, and 10 following EAE induction. All treatments were dosed at a 200 nmol DEX basis in 40 mg/mL mannitol as vehicle. Mice were weighed daily from day 0 and scored daily from day 7 until the end of the study at day 25.

## **2.7. Splenocyte Isolation**

Spleens were harvested from EAE and healthy control mice on peak-of-disease or day 25 for *in vitro* and *in vivo* studies, respectively. Spleens were placed in 5 mL of RPMI 1640 containing L-glutamine and 1% Penicillin-Streptomycin and placed on ice for transportation.

The spleens were pressed through sterile wire mesh with the use of a rubber 1 mL syringe plunger and the cellular extract was collected and centrifuged at 1100 xg for 5 minutes. In order to lyse red blood cells, the cell pellet was resuspended in 5 mL of Gey's lysis solution for 5 minutes on ice. Quenching of the lysis solution was performed by adding 10 mL of RPMI 1640 supplemented with L-glutamine, 1% Penicillin-Streptomycin, and 10% fetal bovine serum (FBS) (complete RPMI, cRPMI). Cells were centrifuged at 1100 xg for 5 minutes and resuspended in cRPMI prior to counting in 0.04% trypan blue. Cultures with *in vitro* treatments or PLP<sub>139-151</sub> rechallenge were kept at 37°C and 5% CO<sub>2</sub>.

## **2.8. Cell Metabolic Assay**

Cellular metabolism was determined through the use of resazurin. Splenocytes were incubated with 75 µmol/L resazurin for 3 hours. Change in fluorescence (ex 560/em 590) provides a measurement of metabolic reductive capacity. Results for *in vitro* treated samples were normalized against untreated controls and background fluorescence was subtracted from all samples through fluorescence measurements on cRPMI containing resazurin. These readings were performed using a Spectramax M5 (Molecular Devices) plate reader.

## **2.9. Cytokine Response**

Following the day 14 and day 25 splenocyte harvests from *in vivo* studies, *in vitro* splenocyte supernatants were collected after 96 hours incubation with PLP<sub>139-151</sub>. Incubation was performed at 1x10<sup>6</sup> cells/well in 96 well plates in the presence or absence of 25 µM PLP<sub>139-151</sub>. The secretion of GM-CSF, IFN-γ, TNF-α, IL-2, IL-6, IL-10, IL-15, IL-17, IL-21, and IL-23 was measured using a U-Plex kit following manufacturer instructions (Meso Scale Discovery).

## **Statistical Analysis**

Statistical analysis of data was performed using two-way analysis of variance (ANOVA) and Tukey multiple comparison tests. IC<sub>50</sub> studies were analyzed using a 4PL-sigmoidal function. Criteria for significance are as follows: \* p<0.05, \*\* p<0.01, \*\*\* p<0.001, \*\*\*\* p<0.0001. For Figure 7 and Figure 9 significant differences between the PLP<sub>139-151</sub> and DEX mixture and mannitol vehicle control are denoted by # p<0.05. All statistical analysis was performed using GraphPad Software (GraphPad Software Inc.).

### 3. Results

#### 3.1. Analytical characterization of chemical entities

The constituent and conjugate molecules can be characterized by traditional chemical methods, including NMR, HPLC, LC/MS, and other spectroscopic means to confirm the structure of the entity. HPLC analysis of PLP<sub>139-151</sub>-DEX with UV/Vis detection provides typical purity values in excess of 93% following preparative HPLC purification (Figure 2). A similar analysis by LC-MS corroborates these results, showing a mass shift in the final conjugate indicative of attachment of DEX to PLP<sub>139-151</sub> (Figure 3). From an NMR perspective, an added benefit to installing the alkyne linker on PLP<sub>139-151</sub> is the presence of a distinct resonance in <sup>1</sup>H/<sup>13</sup>C heteronuclear single quantum coherence (HSQC) experiment, corresponding to the terminal alkyne correlation ( $\delta(^1\text{H}) \approx 2.3\text{ppm}$ ,  $\delta(^{13}\text{C}) \approx 70\text{ ppm}$ ) which is present in a unique chemical environment and well separated from other signals (Figures 4 and S1). After conjugation, this resonance undergoes a significant downfield shift ( $\delta(^1\text{H}) \approx 7.8\text{ppm}$ ) as it is incorporated as part of the conjugated triazole ring system (Figure 4). One additional advantage of conjugating hydrophobic drug molecules to hydrophilic peptides is the impact on aqueous solubility. The PLP<sub>139-151</sub> peptide is soluble in excess of 60 mg/mL, providing a significant enhancement in drug solubility in the resulting amphiphilic conjugates.

### **3.2. Conjugate stability and drug release kinetics**

PLP<sub>139-151</sub>-DEX contains an acid-labile ester linkage capable of releasing the unadulterated parent drug in acidic microenvironments present inside cells. A study of the release kinetics (Figure 5) indicated DEX is released over greater than 100 hours in unbuffered solutions and is released completely over approximately 50 hours when in acidic conditions (pH 5.5). Interestingly, complete hydrolysis of the linker occurs in a few hours when in phosphate buffered solutions, indicating that phosphate anions catalyze the release of DEX from PLP<sub>139-151</sub>, likely through nucleophilic attack on the ester bond. Due to this finding, *in vivo* administration of PLP<sub>139-151</sub>-DEX was carried out in 40 mg/mL mannitol to prevent hydrolysis prior to injection.

### **3.3. IC<sub>50</sub> determination of conjugates and payload**

In order to determine the impact of the CuAAC chemical linkage on the activity of esterified DEX, EAE splenocytes harvested at peak of disease (Day 12) were isolated and treated with DEX or PLP<sub>139-151</sub>-DEX over a range of concentrations. After 120 hours, a resazurin assay was performed to assess cellular metabolism and these data were normalized to untreated EAE splenocytes (Figure 6). These data provide calculated IC<sub>50</sub>s for DEX and PLP<sub>139-151</sub>-DEX of 6.84 +/- 4.18 nM and 7.55 +/- 2.80 nM, respectively. This result indicates that DEX maintains activity after release from the AgDC and demonstrates the rapid release of DEX from the acid-labile ester linkage in an *in vitro* setting, as evidenced by the similar IC<sub>50</sub> values obtained for the free drug and the AgDC.

### **3.4. *In vivo* screening of conjugates**

*In vivo* efficacy of PLP<sub>139-151</sub>-DEX in the treatment of EAE was determined through subcutaneous administration of the conjugate as well as component treatments at a dose

equivalent to 200 nmol DEX. Treatments were administered in 40 mg/mL mannitol on days 4, 7, and 10 with n=9 prior to day 14 and n=4 after day 14. Five mice in each treatment group were chosen at random and euthanized at peak of disease in order to assess splenocyte response to 25  $\mu$ M PLP<sub>139-151</sub> rechallenge. This *in vivo* schedule allows for determination of the effectiveness of AgDCs in ameliorating EAE clinical symptoms as well as mechanistic insight into changes in cellular expression after treatment.

*In vivo* clinical score data indicates the importance of conjugation of DEX to the antigen of interest (Figure 7). EAE mice treated with the AgDC demonstrated no clinical symptoms throughout the 25-day study (Figure 7B). This represents a vast improvement over the free drug, DEX (Figure 7A), which appears to have no clinical effect in the EAE model at a 200 nmol dose. Similar to the AgDC, administration of a combination of the components, PLP<sub>139-151</sub> and DEX, ameliorates symptoms and appears to delay the onset of paralysis in EAE mice (Figure 7B); however, this co-administration is less effective than co-delivery through direct conjugation. Additionally, co-administration of PLP<sub>139-151</sub> and DEX as a mixture resulted in delayed symptom onset in those mice which developed disease (Table 1). Treatment with individual components, PLP<sub>139-151</sub> or DEX, had no significant effect in reducing EAE symptoms (Figure 7A). Similar trends are observed in animal weight data (Figure 9), in which weight gain is associated with a healthy mouse and weight loss correlates to symptom severity. In combination therapies (Figure 9B), continuous weight gain is observed throughout the duration of the study. Conversely, mice treated with individual components as well as mannitol (Figure 9A) displayed significant weight loss leading up to disease remission.

As previously stated, 5 mice were euthanized on day 14 in order to assess cellular differences due to the various *in vivo* treatments (Figures 10 and S2-S8). Of note, at day 14 a

small but significant reduction in GM-CSF (Figure 10A), an inflammatory cytokine, was observed for combination therapies. Additionally, detection of IL-2 (Figure 10B), a cytokine associated with T-cell proliferation, was greatly diminished in combination therapies as well as the PLP<sub>139-151</sub> control. These results demonstrate the early immunosuppressive effects of combination treatments containing DEX. Comparisons of GM-CSF and IL-2 between the mixture of PLP<sub>139-151</sub> and DEX and the AgDC revealed no significant differences between co-administration and co-delivery at this stage of treatment. One notable difference between these treatment groups in cytokine expression was observed in IL-10 (Figure 10C), in which the mixture treatment group experienced a significant reduction in IL-10 expression compared to control. This result was not observed in the conjugate treatment group and may account for the differences in efficacy observed *in vivo* by maintaining an anti-inflammatory effector cell population. Numerous other cytokines were analyzed; however, no significant changes associated with treatment efficacy were observed in the expression of these cytokines (Figures S2-S8).

#### **4. Discussion**

Clinical researchers attempting to treat autoimmune diseases such as MS have historically focused on either administering drugs to suppress and/or modulate the immune response (e.g. classic immunosuppression) or, more recently, ASIT (e.g. long treatment regimens of low doses of antigen or altered antigen analogs).<sup>16</sup> Currently, potent immunomodulatory drugs represent the core treatment options for MS patients, but these drugs act in a non-specific manner and may eliminate or suppress healthy immune cell populations. Conversely, although ASIT is relatively safe, this approach has not yielded sufficient efficacy to suppress autoimmunity.<sup>7-9</sup> Through direct conjugation of potent immunomodulators to self-antigens,

targeted immunosuppression of self-reactive populations may boost the efficacy of ASIT and diminish the side effects associated with immunosuppressants.

The encephalitogenic peptide selected as the targeting moiety is a portion of the intracellular loop<sup>17</sup> of the full-length transmembrane protein, PLP<sub>139-151</sub>. Previous studies have shown the impact of PLP<sub>139-151</sub> sequence variability on TCR binding affinity<sup>18</sup>, highlighting the influence of side chain interactions in the major histocompatibility class 2 binding pocket. Therefore, disrupting interactions through traditional synthetic methods targeting side chain residues of the native sequence were hypothesized to alter conjugate binding and/or uptake. To circumvent these potential deleterious effects, all modifications to the targeting antigen occurred through the *N*-terminal amino acid and were installed via heterobifunctional linkers as the final step of solid-phase peptide synthesis, prior to cleavage from the resin. Linker length, flexibility, and stability were key AgDC design considerations. The overarching strategy utilizing CuAAC enabled rapid and efficient synthesis of PLP<sub>139-151</sub>-DEX (Figure 2) and related conjugates.

Data reported here supports a growing base of literature highlighting the benefits of delivering autoantigen alongside immunomodulators. Although historically categorized as an immunosuppressant, DEX is now known to skew cellular responses towards immune tolerance via multiple mechanisms.<sup>19-22</sup> For example, DEX was shown to enhance CTLA-4 expression during T-cell activation, thus countering the typical B7/CD28 pro-inflammatory co-stimulatory signal.<sup>22</sup> DEX also inhibited IL-12 secretion by dendritic cells and increased FoxP3 expression in naïve T lymphocyte co-cultures.<sup>20</sup> DEX was reported to induce expression of indoleamine 2-3 dioxygenase (IDO), an enzyme implicated in T-cell tolerance<sup>21</sup> that has been used to create ‘tolerogenic dendritic cells’ (defined as high TLR-2, CXCR4, and CCR7 expression levels) from healthy donors.<sup>19</sup>

Because of these pluripotent mechanisms, some have tested DEX as an adjuvant that can be co-administered along with antigen as a means to induce antigen-specific immune tolerance.<sup>20, 23-24</sup>

Previously, Kang and colleagues demonstrated desensitization specific to OVA<sub>323-339</sub> peptide after co-administration of this peptide alongside DEX.<sup>25</sup> Additionally, applying this strategy of co-administration to the NOD autoimmune diabetes model protected nearly all mice from disease induction throughout the study period, suggesting these therapies may be adapted for application to numerous autoimmune diseases with known autoantigens.<sup>25</sup> Further development of this treatment strategy by Peine et al. utilized acetalated dextran particles as a co-delivery vehicle for a myelin oligodendrocyte glycoprotein (MOG) peptide and DEX in EAE, and administration of these microparticles to EAE mice after disease onset resulted in significant reduction in disease severity when both components were present.<sup>26</sup> With such striking differences *in vivo* between combination therapies and free DEX, our findings highlight the advantages associated with delivery of an immunosuppressive drug in the context of the autoantigens of interest.

Furthermore, conjugation of DEX to PLP<sub>139-151</sub> may maximize co-delivery of autoantigen and immunomodulator in larger organisms, enhancing drug potency as demonstrated and potentially limiting off-target effects.

## **5. Conclusions**

Antigen-drug conjugates represent a novel class of therapeutics with broad applicability to a variety of antigen-specific autoimmune disorders. By combining the benefits of two traditional treatment approaches, ASIT and immunomodulatory therapy, AgDCs employ a synergistic approach by conjugating the antigen to the immunomodulatory agent. The enhanced specificity associated with therapeutics of this class may help to minimize global immunosuppression often observed with immunomodulatory small molecule treatments. This publication serves as an

introduction to the modular synthetic design achieved in our lab and demonstrates both efficacy and safety of *in vivo* AgDC treatment in a mouse model of MS in which the autoreactive antigen is identified. The EAE model provides a valuable system for the initial testing of AgDCs as induction and treatment of the disease can be achieved utilizing a single antigen epitope, in this case PLP<sub>139-151</sub>. Subcutaneous treatment with free DEX at a 200 nmol dose appears to have little effect compared to control on modifying the disease course. EAE mice treated *in vivo* with PLP<sub>139-151</sub>-DEX; however, demonstrated no onset of disease over a 25-day period and appeared healthy throughout the study, which demonstrates the efficacy achievable with co-delivery of the antigen and immunomodulator. The modular fashion of this AgDC approach, coupled with the consistency and specificity of the chemistries employed, make AgDCs a potential disease-specific therapeutic class for autoimmune disorders.

## Figures

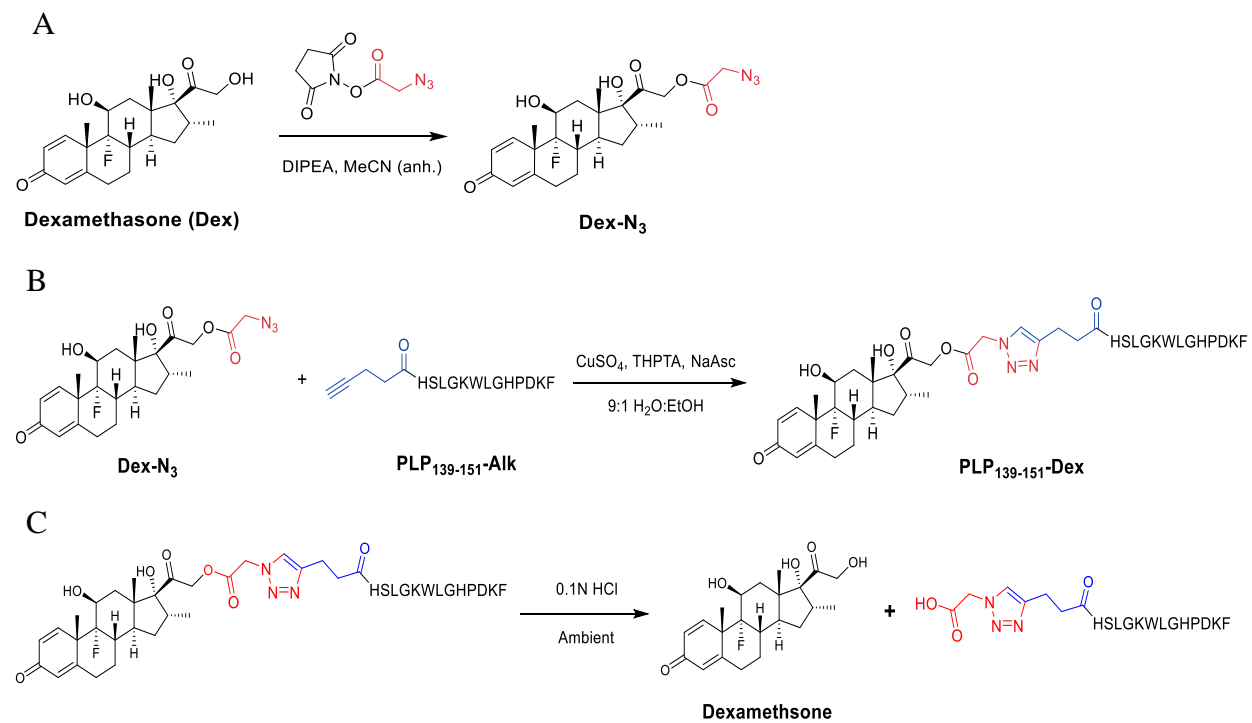


**Figure 1.** (A) Reaction scheme for the synthesis of DEX-N<sub>3</sub>. (B) Reaction scheme for the synthesis of PLP<sub>139-151</sub>-DEX. (C) Degradation of PLP<sub>139-151</sub>-DEX to release parent drug, DEX.

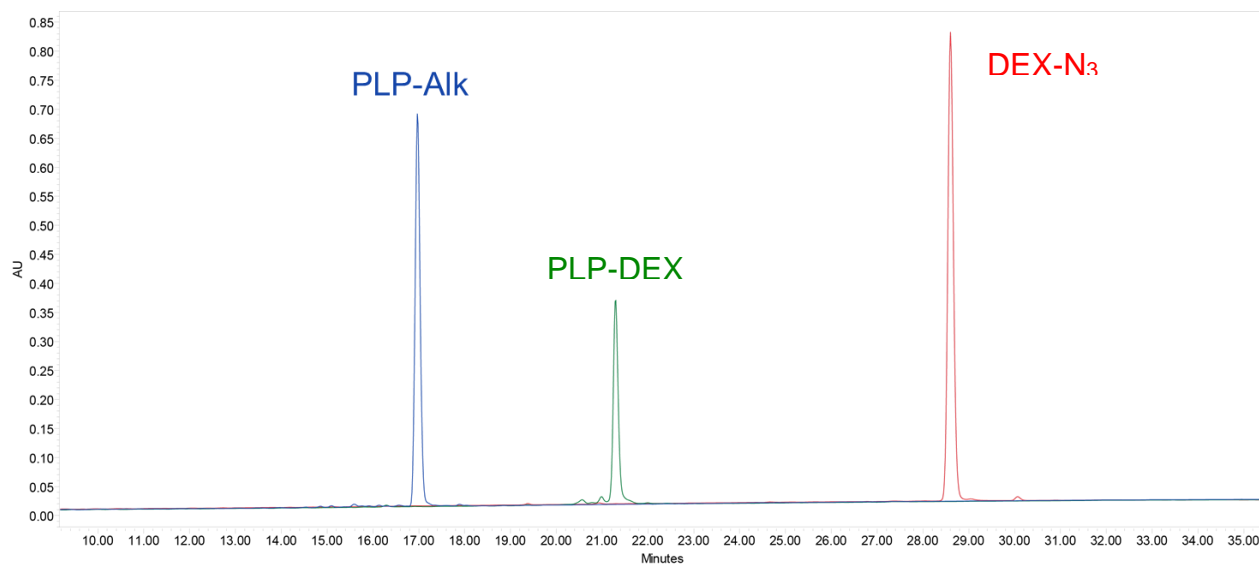


**Figure 2.** Representative analytical HPLC chromatogram showing the starting materials, PLP<sub>139-151</sub>-Alk, and DEX-N<sub>3</sub>, along with the purified reaction product, PLP<sub>139-151</sub>-DEX.

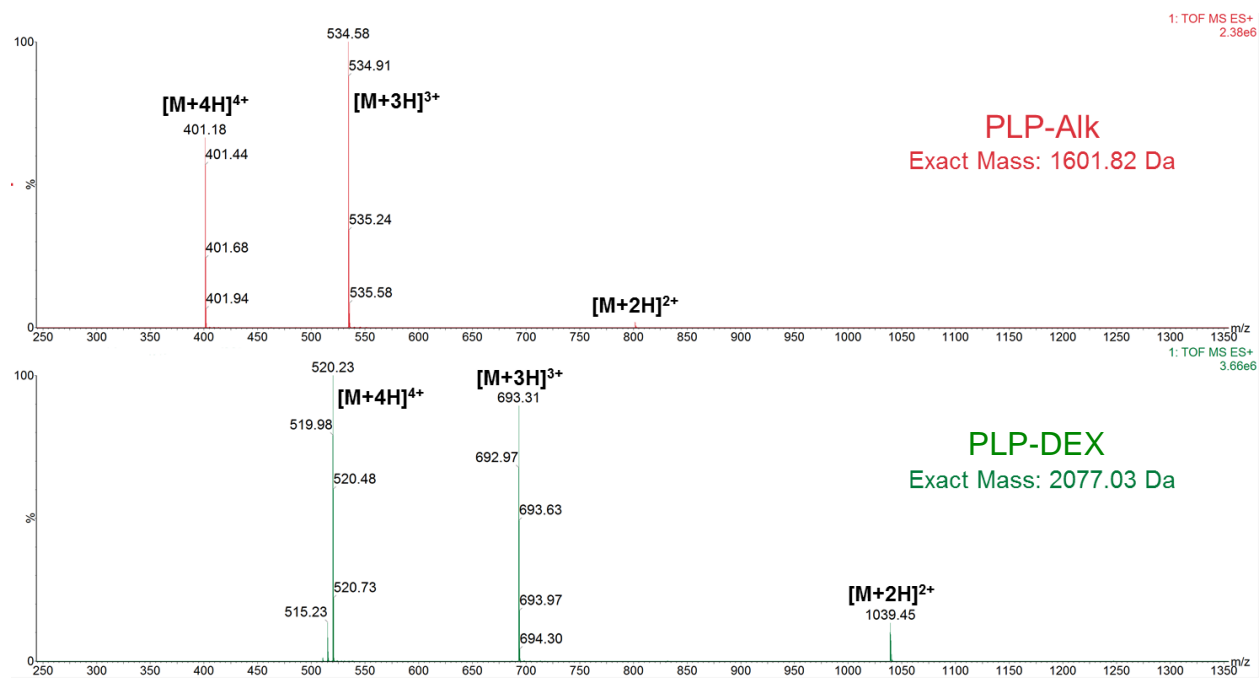


**Figure 3.** Representative mass spectral characterization showing multiple charge states of the starting peptide and the antigen-drug conjugate, PLP<sub>139-151</sub>-DEX.

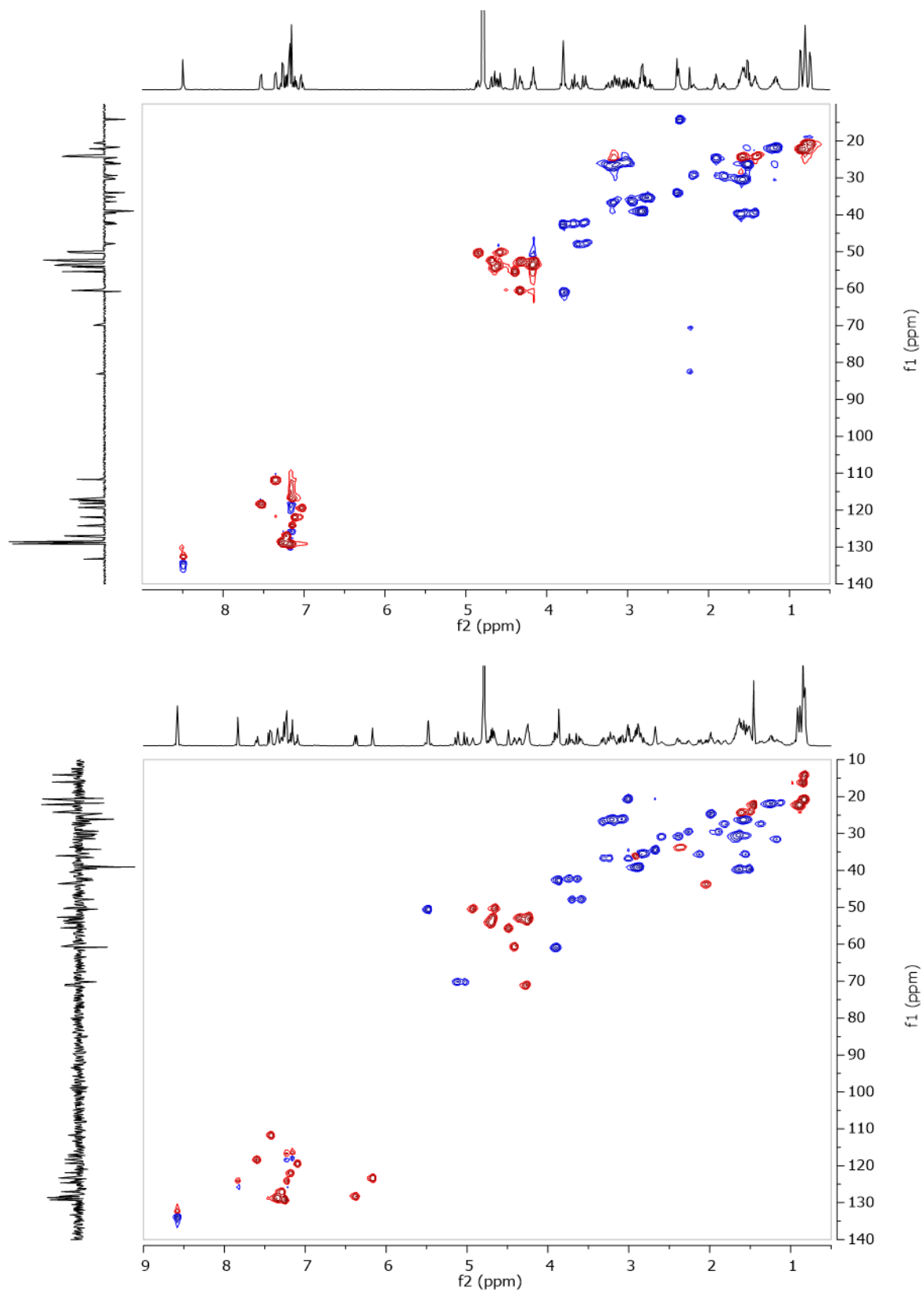


**Figure 4.**  $^1\text{H}/^{13}\text{C}$  HSQC NMR data for PLP<sub>139-151</sub>-Alk (top) and PLP<sub>139-151</sub>-DEX (bottom).

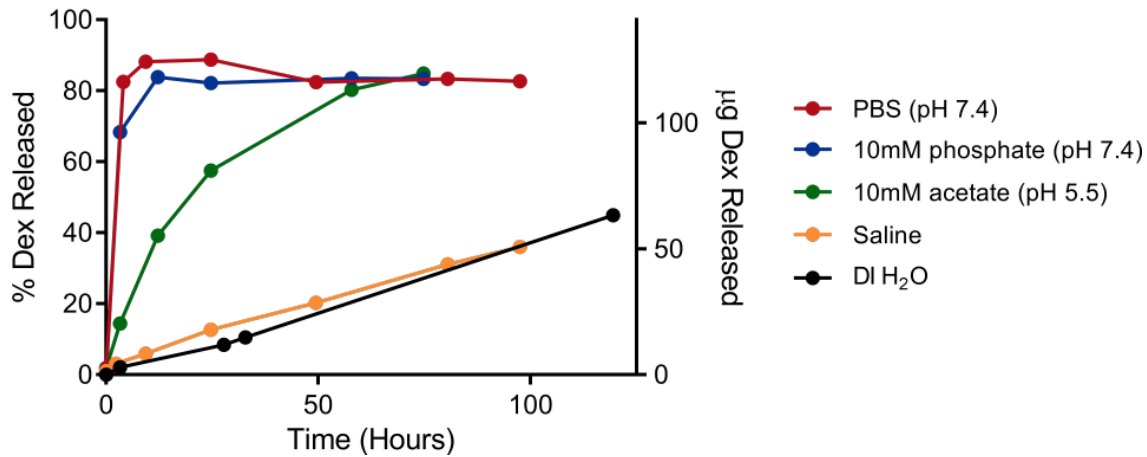


**Figure 5.** Release of DEX from PLP<sub>139-151</sub>-DEX as a function of time and buffer, at 37°C. Starting peptide concentration was 1 mg/mL, corrected for potency, and quantified via linear calibration curve.

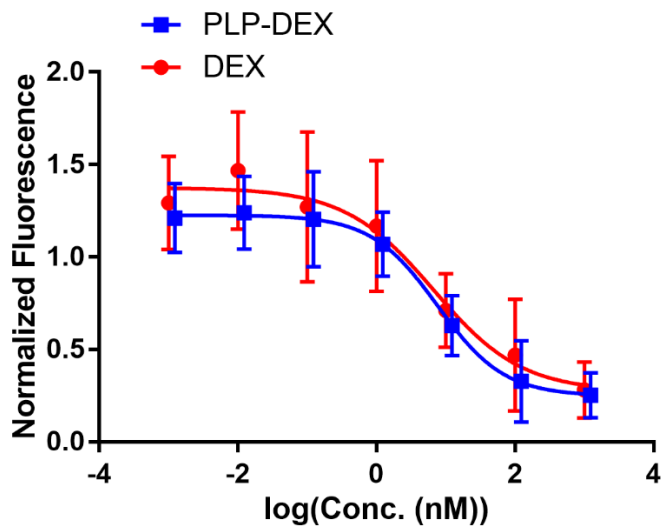


**Figure 6.** Resorufin fluorescence of EAE splenocytes treated with free DEX or PLP<sub>139-151</sub>-DEX for 120 hours (n=6). These data are normalized to untreated EAE splenocytes. Calculated IC<sub>50</sub>s for these treatments are 6.84 ± 4.18 nM and 7.55 ± 2.80 nM for DEX and PLP<sub>139-151</sub>-DEX, respectively. Reported values are with standard error.

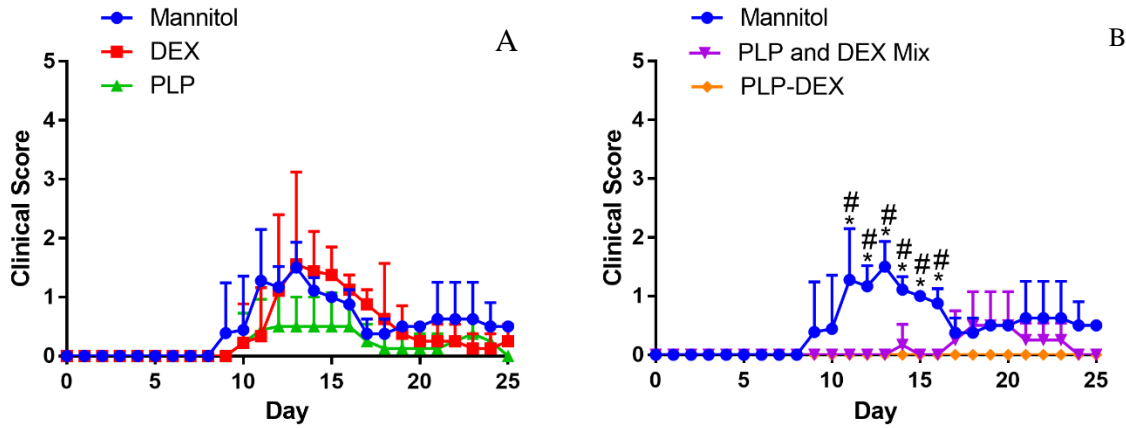


**Figure 7.** Clinical score data for EAE mice treated in vivo with (A) free DEX and free PLP<sub>139-151</sub> as well as (B) a mixture of free DEX and PLP<sub>139-151</sub> and the PLP<sub>139-151</sub>-DEX conjugate. Treatments were administered subcutaneously on days 4, 7, and 10 at doses of 200 nmol DEX basis. N=9 until day 14 and n=4 after day 14. Five mice were chosen at random from each group on day 14 for euthanasia in order to assess splenocyte differences in treatment groups around peak of disease. Data provided is mean ± SD. \*p<0.05 for Mannitol vs PLP<sub>139-151</sub>-DEX and # p<0.05 for Mannitol vs PLP<sub>139-151</sub> and DEX Mix.

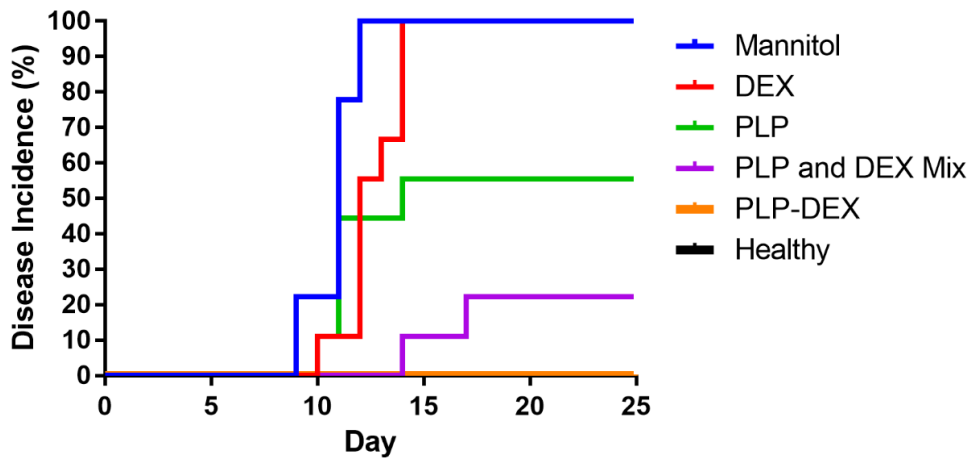


**Figure 8.** Percent disease incidence for all treatment groups where disease onset is characterized by a c.s.  $\geq 1$ . N=9 until day 14 and n=4 after day 14. Five mice were chosen at random from each group on day 14 for euthanasia in order to assess splenocyte differences in treatment groups around peak of disease.

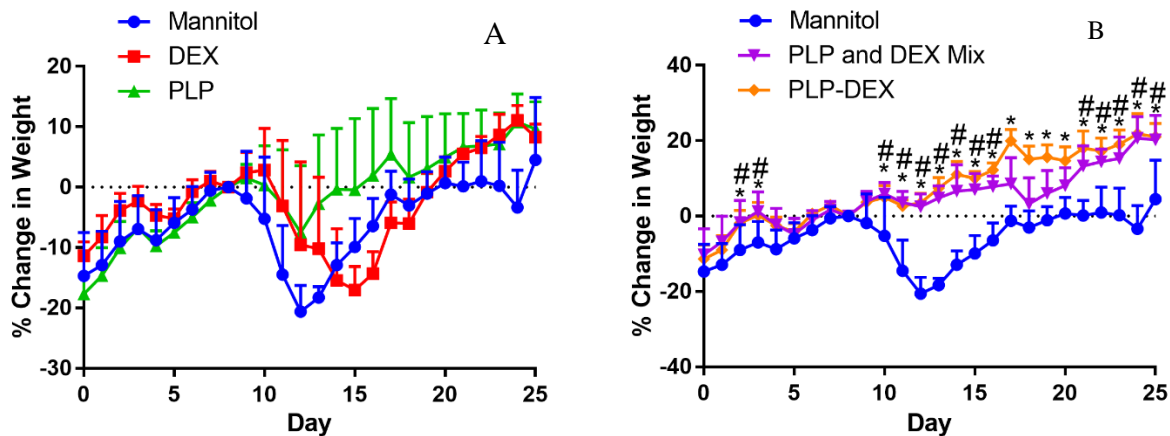
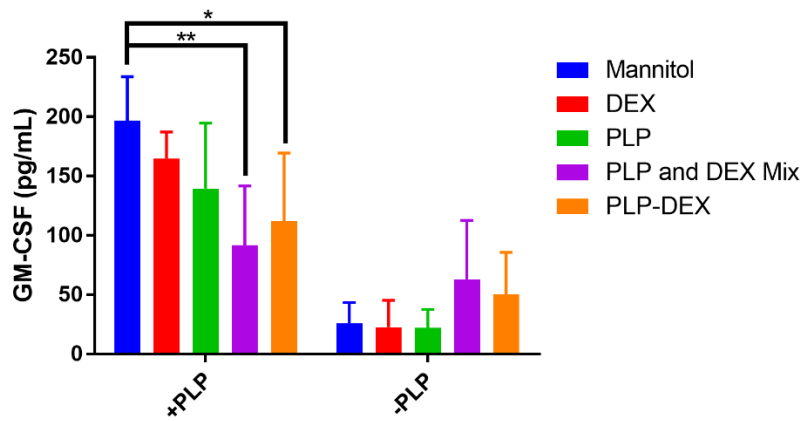


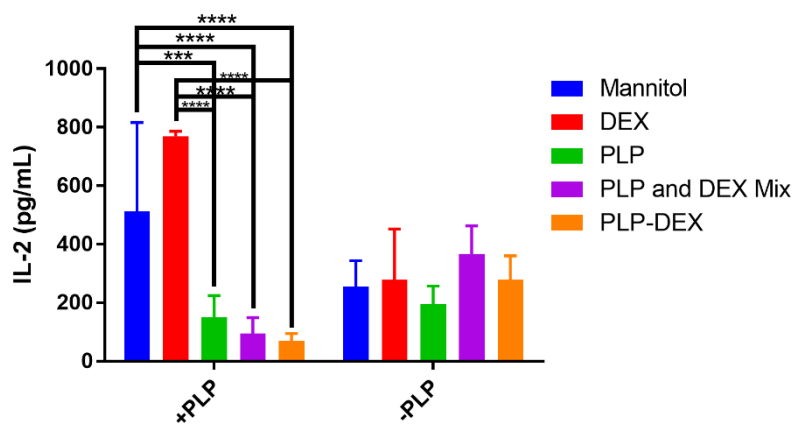
**Figure 9.** Mouse weight data for EAE mice treated in vivo with (A) free DEX and free PLP<sub>139-151</sub> as well as (B) a mixture of free DEX and PLP<sub>139-151</sub> and the PLP<sub>139-151</sub>-DEX conjugate. Data are normalized to the individual mouse weight at day 8 (symptom onset). Treatments were administered subcutaneously on days 4, 7, and 10 at doses of 200 nmol DEX basis. N=9 until day 14 and n=4 after day 14. Five mice were chosen at random from each group on day 14 for euthanasia in order to assess splenocyte differences in treatment groups around peak of disease. \*p<0.05 for Mannitol vs PLP<sub>139-151</sub>-DEX and # p<0.05 for Mannitol vs PLP<sub>139-151</sub> and DEX Mix.

**Table 1.** Disease incidence rate and mean day of disease onset ± SD for each treatment group. Incidence rate is represented as a fraction of total mice per treatment group with clinical score ≥ 1. Mean day of onset is calculated only for symptomatic animals.

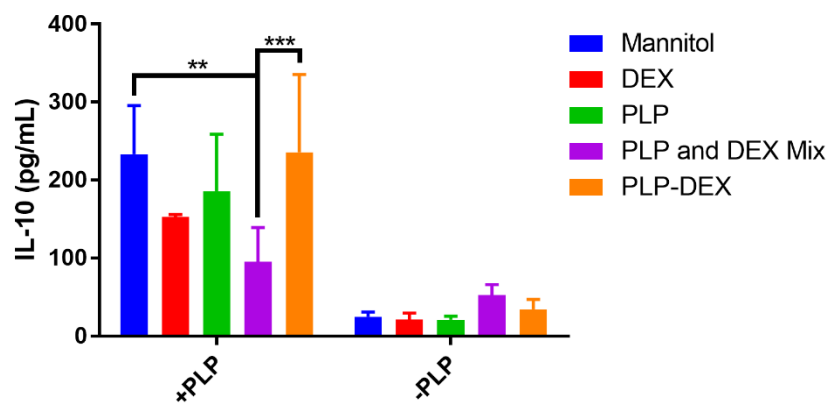
	Mannitol	DEX	PLP <sub>139-151</sub>	PLP <sub>139-151</sub> and DEX mix	PLP <sub>139-151</sub> -Dex
<b>Incidence Rate (Fraction)</b>	9/9	9/9	5/9	2/9	0/9
<b>Mean Day of Onset ± SD</b>	10.8 ± 1.1	12.6 ± 1.3	11.4 ± 1.5	15.5 ± 2.1	-



A



B



C

**Figure 10.** Levels of (A) GM-CSF (B) IL-2 and (C) IL-10 were observed at peak of disease (day 14) after isolated splenocytes from in vivo treated mice were incubated for 96 hours with 25  $\mu$ M PLP<sub>139-151</sub>. N=5, \* p<0.05, \*\* p<0.01, \*\*\* p<0.001, \*\*\*\* p<0.0001.

## References

1. Murphy, K. M., *Janeway's Immunobiology*. 8th ed.; Garland Science: 2012.
2. Perl, A., *Autoimmunity Methods and Protocols*. 2nd ed.; Humana Press: 2012.
3. Compston, A. C., A., Multiple Sclerosis. *Lancet* **2002**, *359*, 1221-1231.
4. Dendrou, C. A.; Fugger, L.; Friese, M. A., Immunopathology of multiple sclerosis. *Nat Rev Immunol* **2015**, *15* (9), 545-58.
5. Podbielska, M.; Banik, N. L.; Kurowska, E.; Hogan, E. L., Myelin recovery in multiple sclerosis: the challenge of remyelination. *Brain Sci* **2013**, *3* (3), 1282-324.
6. Karussis, D., Immunotherapy of multiple sclerosis: the state of the art. *BioDrugs* **2013**, *27* (2), 113-48.
7. Bielekova, B.; Goodwin, B.; Richert, N.; Cortese, I.; Kondo, T.; Afshar, G.; Gran, B.; Eaton, J.; Antel, J.; Frank, J. A.; McFarland, H. F.; Martin, R., Encephalitogenic potential of the myelin basic protein peptide (amino acids 83–99) in multiple sclerosis: Results of a phase II clinical trial with an altered peptide ligand. *Nature medicine* **2000**, *6*, 1167.
8. Kappos, L.; Comi, G.; Panitch, H.; Oger, J.; Antel, J.; Conlon, P.; Steinman, L.; Comi, G.; Kappos, L.; Oger, J.; Panitch, H.; Rae-Grant, A.; Castaldo, J.; Eckert, N.; Guarnaccia, J. B.; Mills, P.; Johnson, G.; Calabresi, P. A.; Pozzilli, C.; Bastianello, S.; Giugni, E.; Witjas, T.; Cozzone, P.; Pelletier, J.; Pöhlau, D.; Przuntek, H.; Hoffmann, V.; Bever Jr, C.; Katz, E.; Clanet, M.; Berry, I.; Brassat, D.; Brunet, I.; Edan, G.; Duquette, P.; Radue, E.-W.; Schött, D.; Lienert, C.; Taksouli, A.; Rodegher, M.; Filippi, M.; Evans, A.; Bourgouin, P.; Zijdenbos, A.; Salem, S.; Ling, N.; Alleva, D.; Johnson, E.; Gaur, A.; Crowe, P.; Liu, X.-J., Induction of a non-encephalitogenic type 2 T helper-cell autoimmune response in multiple sclerosis after administration of an altered peptide ligand in a placebo-controlled, randomized phase II trial. *Nature medicine* **2000**, *6*, 1176.
9. Freedman, M. S.; Bar-Or, A.; Oger, J.; Traboulsee, A.; Patry, D.; Young, C.; Olsson, T.; Li, D.; Hartung, H.-P.; Krantz, M.; Ferenczi, L.; Verco, T., A phase III study evaluating the efficacy and safety of MBP8298 in secondary progressive MS. *Neurology* **2011**, *77* (16), 1551-1560.
10. Miller, S. D.; Karpus, W. J., Experimental autoimmune encephalomyelitis in the mouse. *Curr Protoc Immunol* **2007**, *Chapter 15*, Unit 15 1.
11. Miyagaki, T.; Fujimoto, M.; Sato, S., Regulatory B cells in human inflammatory and autoimmune diseases: from mouse models to clinical research. *International Immunology* **2015**, *27* (10), 495-504.
12. Northrup, L.; Sullivan, B. P.; Hartwell, B. L.; Garza, A.; Berkland, C., Screening Immunomodulators To Skew the Antigen-Specific Autoimmune Response. *Molecular Pharmaceutics* **2017**, *14* (1), 66-80.
13. Brandl, C.; Haas, C.; d'Argouges, S.; Fisch, T.; Kufer, P.; Brischwein, K.; Prang, N.; Bargou, R.; Suzich, J.; Baeuerle, P. A.; Hofmeister, R., The effect of dexamethasone on polyclonal T-cell activation and redirected target T-cell lysis as induced by a CD19/CD3-bispecific single-chain antibody construct. *Cancer immunology, immunotherapy : CII* **2007**, *56* (10), 1551-63.
14. Palma, L.; Sfara, C.; Antonelli, A.; Magnani, M., Dexamethasone restrains ongoing expression of interleukin-23p19 in peripheral blood-derived human macrophages. *BMC pharmacology* **2011**, *11*, 8.
15. Peakman, M.; Dayan, C. M., Antigen-specific immunotherapy for autoimmune disease: fighting fire with fire? *Immunology* **2001**, *104* (4), 361-6.

16. Cox, L.; Compalati, E.; Kundig, T.; Larche, M., New directions in immunotherapy. *Current allergy and asthma reports* **2013**, *13* (2), 178-95.
17. Greer, J. M., Autoimmune T-cell reactivity to myelin proteolipids and glycolipids in multiple sclerosis. *Mult Scler Int* **2013**, *2013*, 151427.
18. V K Kuchroo, J. M. G., D Kaul, G Ishioka, A Franco, A Sette, R A Sobel, M B Lees, A single TCR antagonist peptide inhibits experimental allergic encephalomyelitis mediated by a diverse T-cell repertoire. *J. Immunol.* **1994**, *153*, 3326-3336.
19. Garcia-Gonzalez, P.; Morales, R.; Hoyos, L.; Maggi, J.; Campos, J.; Pesce, B.; Garate, D.; Larrondo, M.; Gonzalez, R.; Soto, L.; Ramos, V.; Tobar, P.; Molina, M. C.; Pino-Lagos, K.; Catalan, D.; Aguillon, J. C., A short protocol using dexamethasone and monophosphoryl lipid A generates tolerogenic dendritic cells that display a potent migratory capacity to lymphoid chemokines. *Journal of translational medicine* **2013**, *11*, 128.
20. Gong, Y. B.; Huang, Y. F.; Li, Y.; Han, G. C.; Li, Y. R.; Wang, D. J.; Du, G. P.; Yu, J. F.; Song, J., Experimental study of the mechanism of tolerance induction in dexamethasone-treated dendritic cells. *Medical science monitor : international medical journal of experimental and clinical research* **2011**, *17* (5), BR125-31.
21. Grohmann, U.; Volpi, C.; Fallarino, F.; Bozza, S.; Bianchi, R.; Vacca, C.; Orabona, C.; Belladonna, M. L.; Ayroldi, E.; Nocentini, G.; Boon, L.; Bistoni, F.; Fioretti, M. C.; Romani, L.; Riccardi, C.; Puccetti, P., Reverse signaling through GITR ligand enables dexamethasone to activate IDO in allergy. *Nature medicine* **2007**, *13* (5), 579-86.
22. Xia, M.; Gasser, J.; Feige, U., Dexamethasone enhances CTLA-4 expression during T-cell activation. *Cellular and molecular life sciences : CMLS* **1999**, *55* (12), 1649-56.
23. Zheng, G.; Zhong, S.; Geng, Y.; Munirathinam, G.; Cha, I.; Reardon, C.; Getz, G. S.; van Rooijen, N.; Kang, Y.; Wang, B.; Chen, A., Dexamethasone promotes tolerance in vivo by enriching CD11clo CD40lo tolerogenic macrophages. *European journal of immunology* **2013**, *43* (1), 219-27.
24. Unger, W. W.; Laban, S.; Kleijwegt, F. S.; van der Slik, A. R.; Roep, B. O., Induction of Treg by monocyte-derived DC modulated by vitamin D3 or dexamethasone: differential role for PD-L1. *European journal of immunology* **2009**, *39* (11), 3147-59.
25. Kang, Y.; Xu, L.; Wang, B.; Chen, A.; Zheng, G., Cutting Edge: Immunosuppressant as Adjuvant for Tolerogenic Immunization. *The Journal of Immunology* **2008**, *180* (8), 5172-5176.
26. Peine, K. J.; Guerau-de-Arellano, M.; Lee, P.; Kanthamneni, N.; Severin, M.; Probst, G. D.; Peng, H.; Yang, Y.; Vangundy, Z.; Papenfuss, T. L.; Lovett-Racke, A. E.; Bachelder, E. M.; Ainslie, K. M., Treatment of Experimental Autoimmune Encephalomyelitis by Codelivery of Disease Associated Peptide and Dexamethasone in Acetalated Dextran Microparticles. *Molecular Pharmaceutics* **2014**, *11* (3), 828-835.

## **Chapter 3: Modulation of Regulatory Pathways through Co-administration of Cognate Antigen and PD-1 Antagonists**

## 1. Introduction

In recent years, interest in modulating immune inhibitory pathways has grown immensely. The development of immune checkpoint inhibitors against targets such as programmed death-1 (PD-1) has highlighted the delicate balance between tolerance and immunity and has helped shed light on the role of this pathway in both autoimmunity and chronic inflammation. The PD-1 pathway is primarily responsible for regulating T-cell responses through inhibitory signaling, which helps maintain immune tolerance and return immune homeostasis. The receptor protein, PD-1, is expressed predominantly on T-cells and B cells and is up-regulated during chronic inflammation<sup>1</sup> Expression of one of the ligands, PD-L1, is quite broad, with the ligand being found on both hematopoietic cells and non-hematopoietic cells.<sup>1</sup> Conversely, PD-L2 is primarily expressed on APCs and may be induced in inflammatory environments.<sup>1</sup> Attempts at modulating the interactions between PD-1 and its ligands have provided new insights into the profound role of inhibitory pathways in maintaining immune homeostasis.

Research into the antagonism of the PD-1 pathway has manifested in the clinic in the form of checkpoint inhibitors, capable of inducing anti-tumor immune responses in specific patient populations. The US Food and Drug Administration has approved numerous monoclonal antibodies for this purpose, including pembrolizumab (anti-PD-1), nivolumab (anti-PD-1), avelumab (anti-PD-L1), durvalumab (anti-PD-L1), and atezolizumab (anti-PD-L1). These antagonistic antibodies can disrupt the inhibitory immune pathways leveraged by cancer cells to evade deletion, thereby re-activating silenced, tumor-specific cytotoxic T-lymphocytes (CTLs). The success of checkpoint inhibitors in oncology highlights the importance of the PD-1 pathway in immune regulation, but many patients have experienced immune-related adverse events (IRAEs) from checkpoint inhibitor therapies.<sup>2</sup> Unsurprisingly, disruption of the PD-1 inhibitory

pathway has been shown to exacerbate disease in animal models of autoimmunity including type 1 diabetes, inflammatory bowel disease, rheumatoid arthritis, and multiple sclerosis.<sup>3</sup> Nevertheless, genetic knockout of the PD-1 pathway in a model of chronic inflammation has also been shown to overstimulate T-cells and induce a terminal state of immune cell exhaustion. Initially, lymphocyte proliferation in the acute phase of infection was enhanced but the lack of PD-1 expression resulted in a failure to mount an effective inflammatory response in later, chronic stages on infection.<sup>4</sup> This would suggest that during chronic inflammation the ligation of PD-1 protects lymphocytes from overstimulation and, ultimately, depletion.

In these works, we explore the effects of PD-1 blockade on EAE splenocytes using PD-1 antagonistic peptides derived from ligands of this pathway. These peptides are believed to block ligation and prevent downstream activation of the PD-1 pathway in a similar manner to anti-PD-1 products on the market. Studies of cellular changes following PD-1 blockade were carried out using splenocytes isolated from EAE mice at peak of disease and cultured *in vitro*. This design allows for in-depth study of the effects of PD-1 blockade in EAE splenocytes in the presence of cognate antigen, providing insight into changes in cell phenotype and cytokine secretion following co-administration of these components.

## **2. Materials and Methods**

### **2.1. Peptide Materials**

Peptides designed to antagonize the PD-1 pathway were provided by Leidos Inc. with confidential sequences. These peptides have been labeled as LD01, LD02, LD10, and LD12 for reference in this publication.

## **2.2. Induction of EAE**

*In vitro* studies were carried out using 4-6-week-old SJL/J (H-2) female mice purchased from Envigo Laboratories (Indianapolis, IN). All experiments were approved through the University's Institutional Animal Care and Use Committee with animal housing in pathogen-free conditions. First, an emulsion containing 200 µg PLP<sub>139-151</sub> in Complete Freund's Adjuvant (CFA) was prepared by combining IFA and heat-killed *M. Tuberculosis* strain H37RA at a final concentration of 4 mg/mL with subsequent emulsification between CFA and PBS containing 200 µg PLP<sub>139-151</sub>. On day 0, this PLP in CFA emulsion was administered to the mice through four subcutaneous injections of 50 µL above each shoulder and hind flank. Additionally, intraperitoneal injections of pertussis toxin (100 ng in 100 µL PBS) were administered on day 0 and day 2. These mice were monitored for disease severity and weight loss leading up to peak of disease at day 12.

## **2.3. Splenocyte Isolation**

Spleens harvested from EAE and healthy control mice at peak-of-disease (day 12) were placed in 5 mL of RPMI 1640 containing L-glutamine and 1% Penicillin-Streptomycin. Using a sterile wire mesh and a 1 mL syringe plunger the spleen tissue was disrupted, and the cellular extract was collected and centrifuged at 1100 xg for 5 minutes. The cell extract was resuspended in 5 mL of Gey's lysis solution for 5 minutes on ice to lyse red blood cells. The red blood cell lysis process was halted by adding 10 mL of RPMI 1640 supplemented with L-glutamine, 1% Penicillin-Streptomycin, and 10% fetal bovine serum (FBS). Cells were centrifuged at 1100 xg for 5 minutes and resuspended in cRPMI prior to counting in 0.04% trypan blue.

Following splenocyte harvest at peak-of-disease, the cells were cultured with 25 µM peptide treatments with groups consisting of: LD01 only, LD02 only, a combination of LD01 and

LD02 each at 25  $\mu$ M, LD10 only, LD12 only, and media controls. Leidos peptides were solubilized using DMSO with a final cell incubation concentration of 0.1% DMSO. These conditions were also met in one of the media control groups to identify any cellular changes due to the inclusion of DMSO. Additionally, these treatment groups were expanded through the inclusion or exclusion of 25  $\mu$ M PLP to assess PD-1 peptide effects on splenocytes in the presence of cognate antigen. These cell cultures were incubated with treatment at 37°C and 5% CO<sub>2</sub> for 72 hours.

#### **2.4. Cytokine Response**

Splenocytes were cultured at 5 x 10<sup>6</sup> cells/mL (1 x 10<sup>6</sup> cells/well) for 72 hours as outlined above and sample supernatants were removed and frozen at -80 °C for storage until the assay could be performed. Cytokine concentrations were determined in cell supernatants using a U-Plex kit following manufacturer instructions (Meso Scale Discovery, Rockville, MD). The following cytokines were assessed in the U-Plex plate: GM-CSF, IFN- $\gamma$ , IL-10, IL-15, IL-17A, IL-2, IL-21, IL-23, IL-6, and TNF- $\alpha$ .

#### **2.5. Cell Phenotyping via Flow Cytometry**

*In vitro* splenocytes were cultured at 5 x 10<sup>6</sup> cells/mL (5 x 10<sup>6</sup> cells/well) with the treatment groups outlined previously for 72 hours prior to cell scraping and collection. These treated splenocytes were washed with RPMI containing 5% FBS and blocked for 15 minutes with TruStain fcX (antimouse CD16/32 antibody, Biolegend) at 10  $\mu$ g/mL in wash buffer. Antibodies used in immunostaining included: BV421 conjugated anti-mouse CD3, AlexaFluor647 conjugated anti-mouse CD4, AlexaFluor488 conjugated anti-mouse CD8, and PE/Dazzle conjugated anti-mouse PD-1 (Biolegend, San Diego, CA). Staining of splenocytes was performed following manufacturer guidelines and splenocytes were washed three times before resuspension in serum-

free RPMI. Following staining, live cell population statistics were assessed by flow cytometry (BD FACSFusion, BD Biosciences, San Jose, CA).

## **2.6. LD01 Titration**

*In vitro* splenocytes were cultured at  $5 \times 10^6$  cells/mL with LD01 treatment at increasing concentrations of 1  $\mu$ M, 5  $\mu$ M, 10  $\mu$ M, and 25  $\mu$ M for 72 hours prior to cell scraping and collection. Treated splenocytes were then washed with RPMI containing 5% FBS and blocked for 15 minutes with TruStain fcX (antimouse CD16/32 antibody, Biolegend) at 10  $\mu$ g/mL. Splenocytes were then stained for PD-1 expression using PE/Dazzle conjugated anti-mouse PD-1 (Biolegend, San Diego) and assessed by flow cytometry (BD FACSFusion, BD Biosciences, San Jose, CA).

## **3. Results**

### **3.1. PD-1 Peptides Reduce Cytokine Secretion in the Presence of Cognate Antigen**

EAE splenocyte responses to treatment with PD-1-derived peptides were studied through the collection of cytokines at two timepoints post-treatment. Treatment groups included each peptide individually at 25  $\mu$ M, as well as a combination group of LD01 and LD02, each with and without PLP re-challenge. Splenocytes were cultured with treatments for 72 hours prior to cytokine analysis.

The treatment groups containing PLP provided the most robust cellular response at 72 hours, with LD01 treatment significantly reducing levels of many pro-inflammatory cytokines including GM-CSF, IFN- $\gamma$ , IL-23, IL-6, and TNF- $\alpha$  (Figure 1). Additionally, a reduction in the levels of IL-10, an anti-inflammatory cytokine, was observed with LD01 treatment (Figure 1C). Similarly, splenocytes treated with LD02 displayed reduced secretion of IFN- $\gamma$ , TNF- $\alpha$ , and IL-10, albeit with lower significance than LD01 treated samples. Combination treatment with both

LD01 and LD02 closely resembled the changes observed in LD01 treatment with a few notable differences. Interestingly, the combination of LD01 and LD02 greatly reduced the levels of IL-17A in EAE splenocytes when treated in the presence of PLP (Figure 1E). This effect was not observed for the individual peptide treatments. Furthermore, the effects of these peptides on IL-10 secretion appear to be additive, with the combination treatment displaying significantly lower levels of IL-10 than either LD01 or LD02 individually (Figure 1C). Treatments with LD10 and LD12 also displayed reduced levels of pro-inflammatory cytokines, albeit with less significance. Notably, LD12 substantially reduced IL-17A secretion in the presence of antigen.

### **3.2. PD-1 peptides reduce proportion of major T-cell populations**

Population changes of T-cells following 72 hours of treatment with PD-1 peptides were observed through flow cytometry (Figures 2-6). Cellular markers for T-cell phenotyping included CD3 for general T-cell populations (Figure 3), CD4 for T-helper cell populations (Figure 4), and CD8 for cytotoxic T-cell populations (Figure 5).

The most notable changes in T-cell populations were observed in splenocytes treated with LD01, LD02, or a combination of these peptides. LD01 reduced the proportion of all T-cells, with this loss being shared across both T-helper cells and cytotoxic T-cells (Figures 4 and 5). Furthermore, this effect of LD01 on T-cell populations persists in the presence of PLP. LD02 also appears to reduce T-cell populations, however this effect is only observed in splenocytes which are not treated with PLP and applies primarily to cytotoxic T-cells (CD8<sup>hi</sup>). Similar to the results seen with the cytokine profiles, the effects of LD02 on cytotoxic T-cell populations may be additive with those of LD01 in combination treatment (Figure 5B). Once again, however, the added effects of LD02 in the combination treatment do not persist in the presence of cognate antigen.

Lastly, general PD-1 expression on all splenocytes was also investigated post-treatment (Figure 6). Of note, LD01 greatly enhanced the expression of PD-1 on EAE splenocytes, both in the presence and absence of PLP. LD02 also increased PD-1 expression on EAE splenocytes, however this effect is only observed in the absence of PLP.

### **3.3. Titration of LD01 reveals dose dependency of PD-1 expression**

To further evaluate the effects of LD01 treatment on splenocyte phenotypic changes, an LD01 titration study was designed with increasing doses of LD01 treatment from 1  $\mu$ M to 25  $\mu$ M. Total splenocyte expression of PD-1 was then evaluated via flow cytometry, revealing a dose dependent expression of PD-1 in response to LD01 when rechallenged with PLP<sub>139-151</sub> (Figure 7). These results may suggest varying levels of cellular exhaustion in response to LD01 treatment in the presence of cognate antigen, however, this study does not reveal saturation of PD-1 expression in these exhausted splenocytes.

## **4. Discussion**

The PD-1 pathway's importance stems from its multifunctional role in lymphocyte inhibition. PD-1 ligation is responsible for resolving inflammation and maintaining immune tolerance and represents one of the last lines of defense against autoreactive cells which have escaped central tolerance. Loss of PD-1 function, whether by knockout or immune checkpoint blockade therapy, results in exacerbated autoimmune symptoms in mouse models of type 1 diabetes and multiple sclerosis.<sup>5-6</sup> These studies highlight the role of PD-1 in maintaining immune tolerance and limiting autoreactive inflammatory responses, but more work must be done to investigate the cellular changes associated with antagonism of the PD-1 pathway in the presence of cognate antigen.

Chronic inflammation due to repeated exposure of T-cells to cognate antigen may result in development of an exhausted phenotype.<sup>7</sup> Exhausted T-cells are characterized by a loss of immune function, and in the most severe cases T-cell exhaustion may result in clonal deletion.<sup>7</sup> This effect has been observed in both CD8<sup>+</sup> T-cells and CD4<sup>+</sup> T-cells and has commonly been observed in numerous viral infections including lymphocytic choriomeningitis virus (LCMV), HIV, and hepatitis C, among other diseases.<sup>7-10</sup> Exhausted T-cells have been observed to upregulate expression of many inhibitory receptors, including PD-1.<sup>7</sup> A study in mice with LCMV infection found that the PD-1 pathway is not required for the induction of an exhausted T-cell phenotype, but rather is a mechanism by which T-cells are protected from reaching a terminal state of exhaustion.<sup>4</sup> In the study, PD-1 knockout mice were infected with LCMV and although T-cell cytotoxic activity increased during the acute phase of infection, the long-term absence of PD-1 resulted in a higher degree of terminally differentiated exhausted T-cells.<sup>4</sup>

In order to explore the relationship between PD-1 and cellular exhaustion in the context of autoimmunity, we cultured EAE splenocytes with peptide antagonists to the PD-1 pathway. Initial studies focused on elucidating effector cell function under these conditions through quantification of cytokines. In the presence of cognate antigen, PLP<sub>139-151</sub>, the splenocytes treated with LD01 demonstrated significantly reduced cytokine expression. Notably, inflammatory cytokines such as GM-CSF, IFN- $\gamma$ , and TNF- $\alpha$  saw substantial reduction when treated with LD01 and in combination treatments containing LD01 and LD02 together in the presence of PLP. Additionally, the combination treatment of LD01 and LD02 saw a reduction in IL-17, a major inflammatory cytokine associated with EAE. These data support loss of effector cell function when treated with antagonistic PD-1 peptides in combination with PLP, despite the normally anti-inflammatory

nature of the PD-1 pathway. Furthermore, the changes observed in IL-17 hint at a cooperative effect between LD01 and LD02, further altering the cellular response when treated in combination.

After observing the reduction of cytokine expression through treatment with antagonistic PD-1 peptides, changes in basic T-cell phenotypes were investigated. This was accomplished by staining for the following surface proteins: CD3, CD4, CD8, and PD-1. After treatment with PD-1 peptides, total T-cell populations (CD3<sup>+</sup>) decreased significantly, a change which was observed in both T-helper cells (CD4<sup>+</sup>) and cytotoxic T-cells (CD8<sup>+</sup>). Interestingly, two populations of CD8<sup>+</sup> T-cells were observed, CD8<sup>hi</sup> and CD8<sup>lo</sup>, and the PD-1 peptides most strongly impacted the CD8<sup>hi</sup> population, regardless of the presence of antigen. These effects in reducing CD8<sup>hi</sup> populations were also enhanced in the combination treatment group of both LD01 and LD02, once again suggesting that these peptides work cooperatively to alter cellular response. Lastly, through treatment with the PD-1 antagonistic peptides, the expression of the receptor PD-1 was greatly enhanced. This result in combination with the reduced expression of IFN- $\gamma$  may suggest that T-cells are exhibiting an exhausted phenotype, incapable of mounting a robust inflammatory response, especially when stimulated with cognate antigen in combination with PD-1 antagonist peptides.

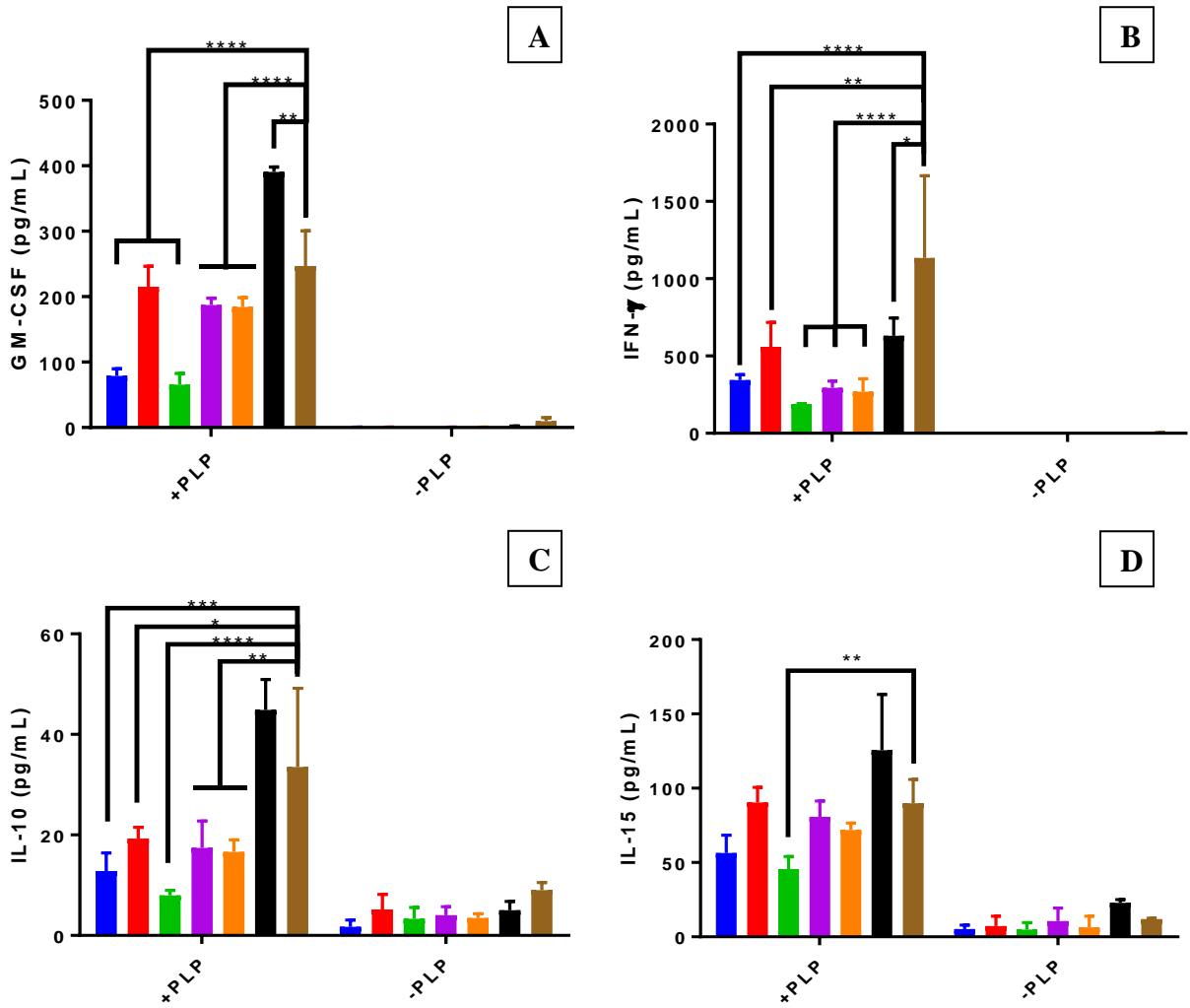
## **6. Conclusions**

Modulation of immune inhibitory pathways such as PD-1 has grown in interest with the advent of immune checkpoint inhibitors, however, the effects of antagonism of the PD-1 pathway have not fully been explored in the presence of cognate antigen. Here, we have demonstrated the efficacy of newly derived PD-1 peptide antagonists resulting in immune cell exhaustion when treated alongside high doses of PLP<sub>139-151</sub> antigen. Overall secretion of inflammatory cytokines, including GM-CSF and IFN- $\gamma$ , was reduced following treatment with LD01 + PLP<sub>139-151</sub> and the

resulting overexpression of PD-1 was shown to be dose dependent on LD01. These results coincide with literature sources to further evidence the protective role of PD-1 in preventing cellular exhaustion, a phenomenon which severely impacts immune responsiveness.

# Figures

- LD01
- LD02
- LD01 + LD02
- LD10
- LD12
- Media Only Control
- Media and DMSO Control



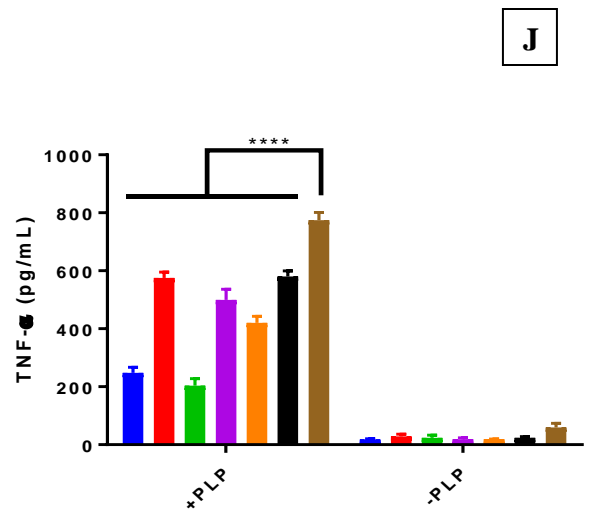
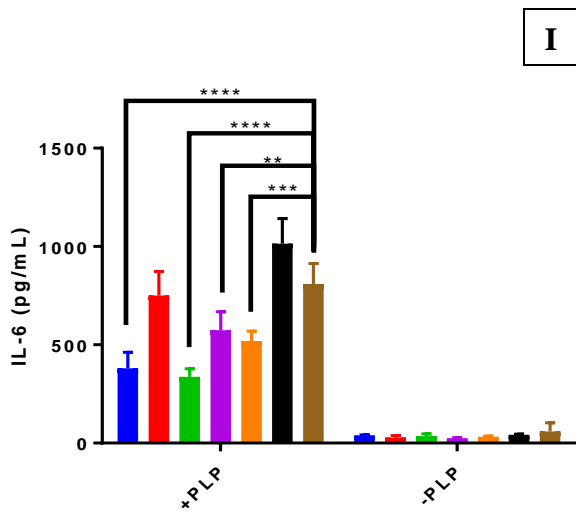
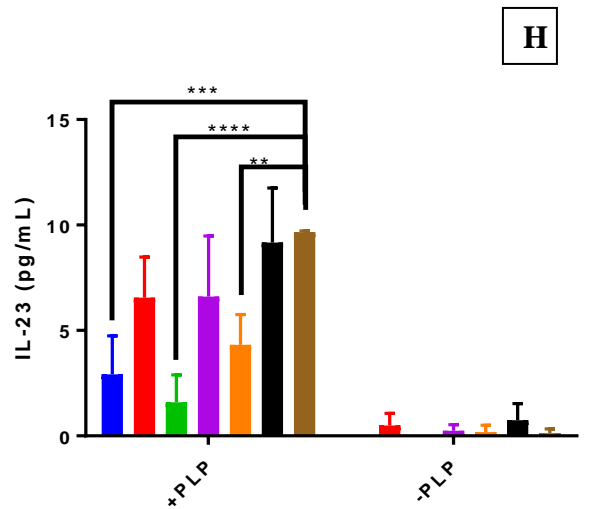
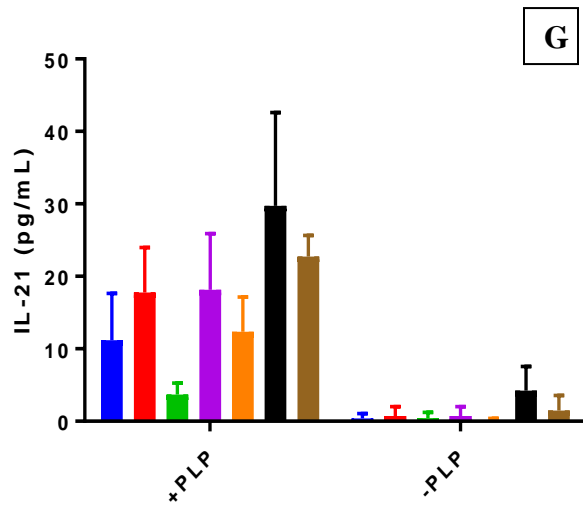
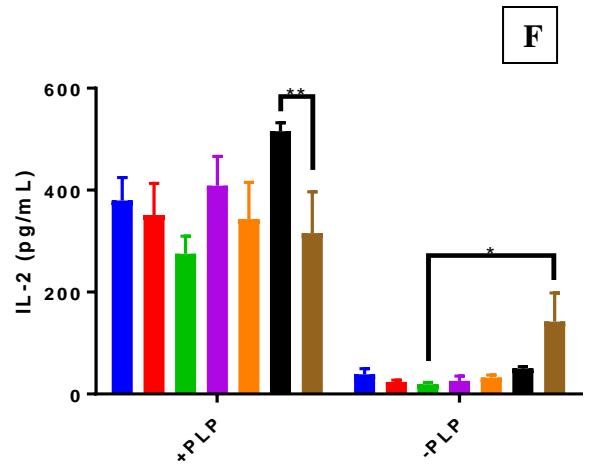
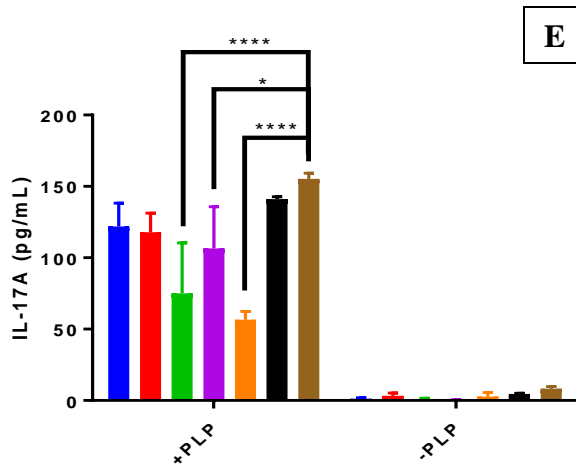


**Figure 1.** Cytokines from EAE splenocytes harvested at peak of disease (day 12) after 72 hours of treatment with Leidos peptides +/- 25  $\mu$ M PLP. Displayed are significances between media + DMSO vehicle control and peptide treatments. \*  $p < 0.05$ , \*\*  $p < 0.01$ , \*\*\*  $p < 0.001$ , \*\*\*\*  $p < 0.0001$

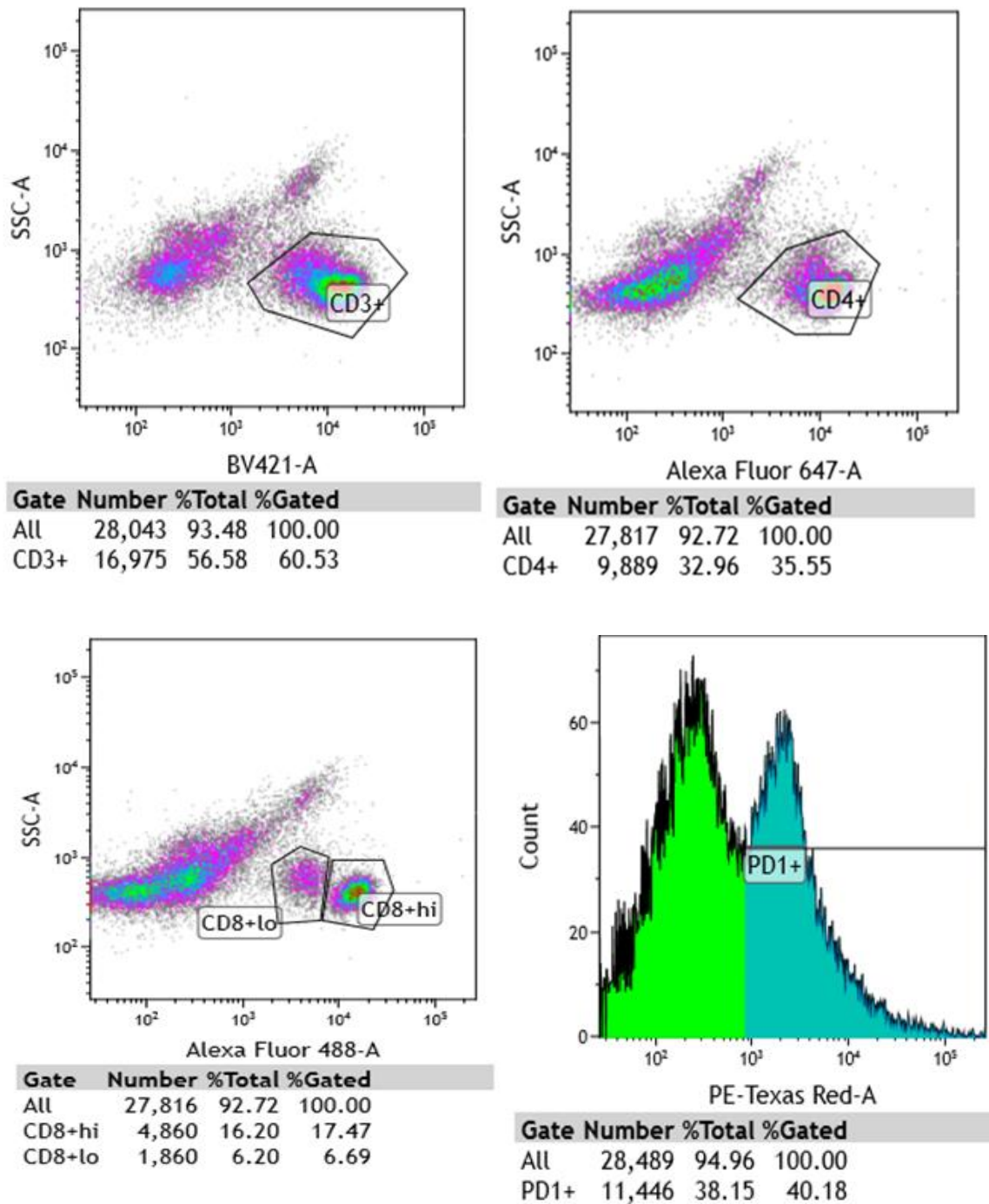


**Figure 2.** Representative flow cytometric plots of the gating schemes used in cell phenotyping. Staining was performed on EAE splenocytes harvested at peak of disease (day 12) following 72 hours peptide treatment *in vitro*. The following antibody stains were used in cell phenotyping: anti-CD3-BV421, anti-CD4-AF647, anti-CD8-AF488, and anti-PD-1-PE-Texas Red.

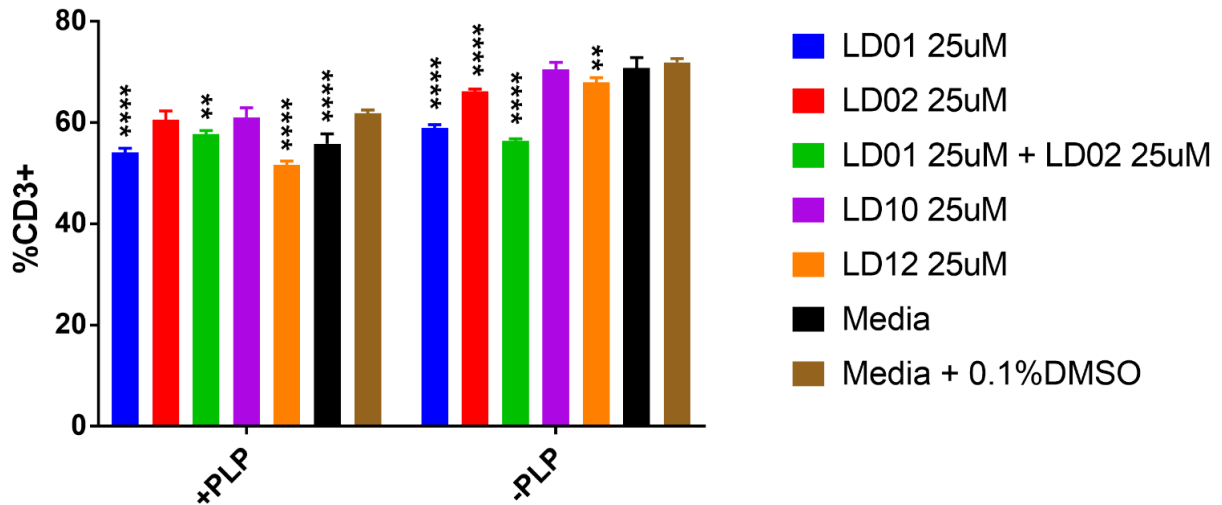


**Figure 3.** Percent CD3<sup>+</sup> T-cell of EAE splenocytes harvested at peak of disease (day 12) following 72 hours treatment with Leidos peptides +/- 25  $\mu$ M PLP. \* represents significant difference from Media + 0.1% DMSO vehicle control. \* p<0.05, \*\* p<0.01, \*\*\* p<0.001, \*\*\*\* p<0.0001

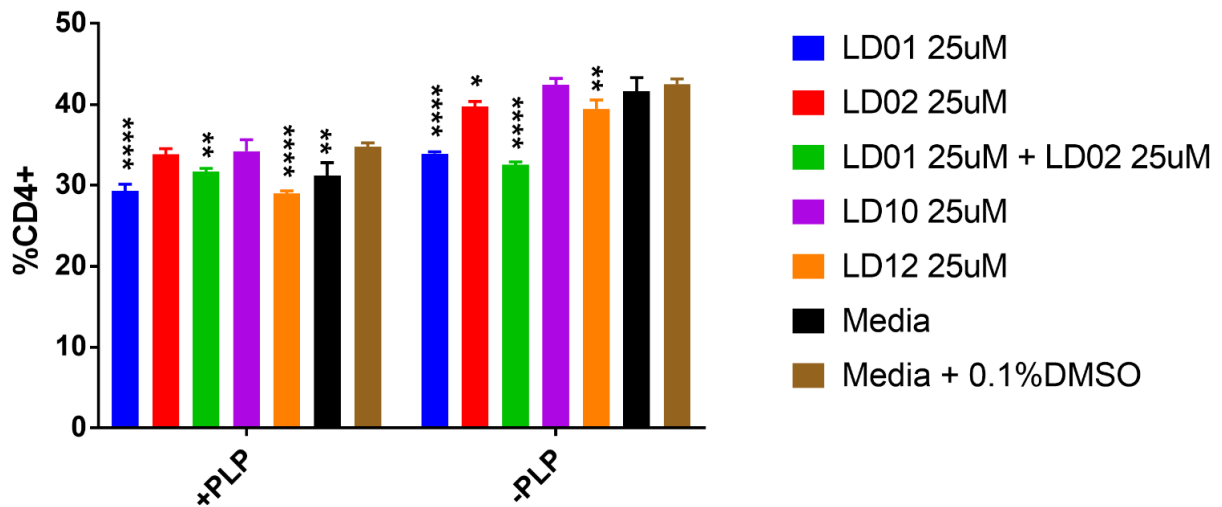


**Figure 4.** Percent CD4<sup>+</sup> T-helper cells of EAE splenocytes harvested at peak of disease (day 12) following 72 hours treatment with Leidos peptides +/- 25  $\mu$ M PLP. \* represents significant difference from Media + 0.1% DMSO vehicle control. \* p<0.05, \*\* p<0.01, \*\*\* p<0.001, \*\*\*\* p<0.0001

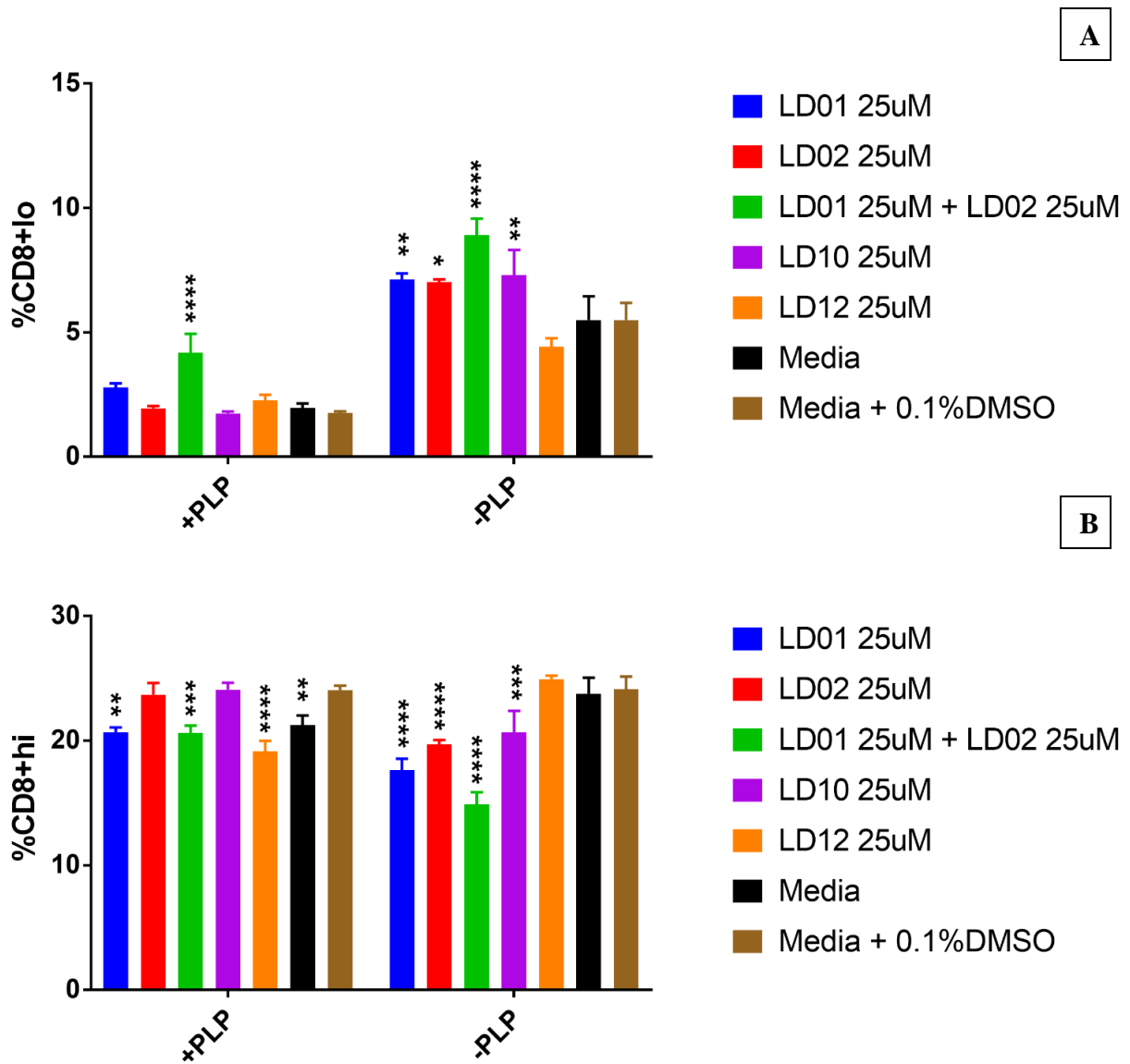


**Figure 5.** Percent CD8<sup>+</sup> cytotoxic T-cells of EAE splenocytes harvested at peak of disease (day 12) following 72 hours treatment with Leidos peptides +/- 25  $\mu$ M PLP. Two populations were observed, (A) CD8<sup>lo</sup> population and (B) CD8<sup>hi</sup> population. \* represents significant difference from Media + 0.1% DMSO vehicle control. \* p<0.05, \*\* p<0.01, \*\*\* p<0.001, \*\*\*\* p<0.0001

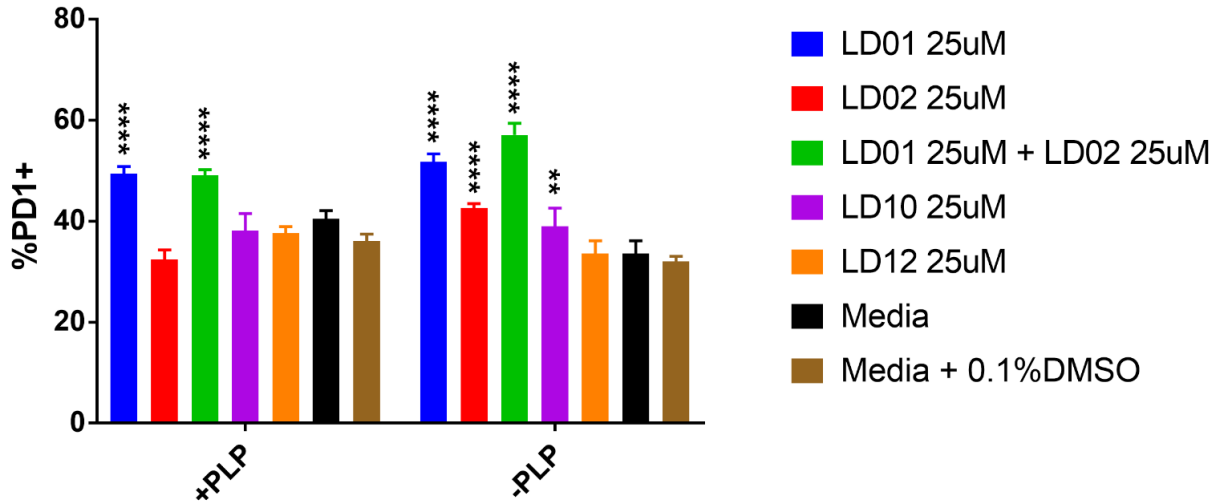


**Figure 6.** Percent PD-1<sup>+</sup> cells of EAE splenocytes harvested at peak of disease (day 12) following 72 hours treatment with Leidos peptides +/- 25  $\mu$ M PLP. \* represents significant difference from Media + 0.1% DMSO vehicle control. \* p<0.05, \*\* p<0.01, \*\*\* p<0.001, \*\*\*\* p<0.0001

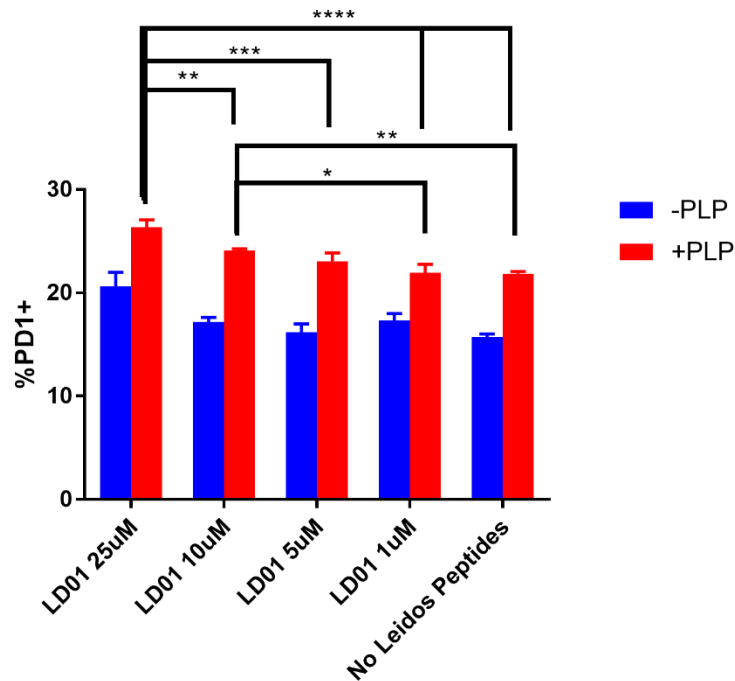


**Figure 7.** Effects of increasing concentration of LD01 on PD-1<sup>+</sup> expression in EAE splenocytes harvested at peak of disease (day 12) following 72 hours treatment with Leidos peptides +/- 25  $\mu$ M PLP. \* p<0.05, \*\* p<0.01, \*\*\* p<0.001, \*\*\*\* p<0.0001

## References

1. Sharpe, A. H.; Pauken, K. E., The diverse functions of the PD1 inhibitory pathway. *Nature Reviews Immunology* **2017**, *18*, 153.
2. Spain, L.; Diem, S.; Larkin, J., Management of toxicities of immune checkpoint inhibitors. *Cancer treatment reviews* **2016**, *44*, 51-60.
3. Francisco, L. M.; Sage, P. T.; Sharpe, A. H., The PD-1 pathway in tolerance and autoimmunity. *Immunological reviews* **2010**, *236*, 219-242.
4. Odorizzi, P. M.; Pauken, K. E.; Paley, M. A.; Sharpe, A.; Wherry, E. J., Genetic absence of PD-1 promotes accumulation of terminally differentiated exhausted CD8<sup>+</sup> T-cells. *The Journal of Experimental Medicine* **2015**, *212* (7), 1125-1137.
5. Ansari, M. J. I.; Salama, A. D.; Chitnis, T.; Smith, R. N.; Yagita, H.; Akiba, H.; Yamazaki, T.; Azuma, M.; Iwai, H.; Khoury, S. J.; Auchincloss, H.; Sayegh, M. H., The Programmed Death-1 (PD-1) Pathway Regulates Autoimmune Diabetes in Nonobese Diabetic (NOD) Mice. *The Journal of Experimental Medicine* **2003**, *198* (1), 63-69.
6. Salama, A. D.; Chitnis, T.; Imitola, J.; Ansari, M. J. I.; Akiba, H.; Tushima, F.; Azuma, M.; Yagita, H.; Sayegh, M. H.; Khoury, S. J., Critical Role of the Programmed Death-1 (PD-1) Pathway in Regulation of Experimental Autoimmune Encephalomyelitis. *The Journal of Experimental Medicine* **2003**, *198* (1), 71-78.
7. Yi, J. S.; Cox, M. A.; Zajac, A. J., T-cell exhaustion: characteristics, causes and conversion. *Immunology* **2010**, *129* (4), 474-481.
8. Gallimore, A.; Glithero, A.; Godkin, A.; Tissot, A. C.; Plückthun, A.; Elliott, T.; Hengartner, H.; Zinkernagel, R., Induction and Exhaustion of Lymphocytic Choriomeningitis Virus-specific Cytotoxic T Lymphocytes Visualized Using Soluble Tetrameric Major Histocompatibility Complex Class I–Peptide Complexes. *The Journal of Experimental Medicine* **1998**, *187* (9), 1383-1393.
9. Day, C. L.; Kaufmann, D. E.; Kiepiela, P.; Brown, J. A.; Moodley, E. S.; Reddy, S.; Mackey, E. W.; Miller, J. D.; Leslie, A. J.; DePierres, C.; Mncube, Z.; Duraiswamy, J.; Zhu, B.; Eichbaum, Q.; Altfeld, M.; Wherry, E. J.; Coovadia, H. M.; Goulder, P. J. R.; Klenerman, P.; Ahmed, R.; Freeman, G. J.; Walker, B. D., PD-1 expression on HIV-specific T-cells is associated with T-cell exhaustion and disease progression. *Nature* **2006**, *443*, 350.
10. Radziewicz, H.; Ibegbu, C. C.; Fernandez, M. L.; Workowski, K. A.; Obideen, K.; Wehbi, M.; Hanson, H. L.; Steinberg, J. P.; Masopust, D.; Wherry, E. J.; Altman, J. D.; Rouse, B. T.; Freeman, G. J.; Ahmed, R.; Grakoui, A., Liver-Infiltrating Lymphocytes in Chronic Human Hepatitis C Virus Infection Display an Exhausted Phenotype with High Levels of PD-1 and Low Levels of CD127 Expression. *Journal of Virology* **2007**, *81* (6), 2545-2553.

## **Chapter 4: Silencing Autoreactive B Cell Populations Through Tetravalent Antigen Presentation**

## 1. Introduction

Autoimmunity is characterized by a loss of immune tolerance toward self-antigens resulting in aberrant inflammatory events. Typical treatments for autoimmune diseases lack specificity for the offending, autoreactive T-cells and B cells, resulting in limited efficacy and a wide range of adverse side effects.<sup>1-2</sup> In addition to these side effects, many autoimmune therapies induce global immune suppression, hindering the immune system's ability to eliminate pathogens.<sup>3</sup> This immune suppression may relieve autoimmune symptoms, but it also leaves the patient open to opportunistic infection. With such severe limitations in existing autoimmune therapies, there is a crucial need for antigen-specific immunotherapies (ASITs) capable of inducing immune tolerance toward an autoantigen without compromising immune function.

In multiple sclerosis (MS), loss of immune tolerance toward myelin sheath autoantigens results in abnormal inflammatory responses in the central nervous system facilitated by both autoreactive T-cells and B cells.<sup>4-5</sup> The result of this inflammation is demyelination and neuronal degradation leading to neurological dysfunction.<sup>6</sup> The role of B cells in MS pathology is still unclear, however, the success of B cell depletion in clinical studies utilizing Rituximab, an anti-CD20 mAb, suggests that autoreactive B cells function beyond autoantibody secretion.<sup>7-10</sup> MS patients who received Rituximab see rapid improvement in disease progression, but they maintain high serum levels of autoantibodies against myelin antigens. These results suggest antibody-independent mechanisms for B cell involvement in MS, including loss of antigen presentation to T-cells and reduced B cell cytokine and chemokine production.<sup>7</sup> Despite their success, B cell depletion therapies result in severe global immune suppression and the demand for safer, more effective antigen-specific strategies remains.

The successes of B cell depletion therapies in MS patients implicate B cells as an excellent target for tolerance reintroduction through ASITs. Due to their antibody-independent roles in MS, autoreactive B cells of interest may be targetable through their high-affinity membrane bound B cell receptor (BCR) specific for MS autoantigens. Prior work by Dintzis demonstrates the potential for low molecular weight antigen arrays to eliminate high affinity B cells specific for the antigen of interest.<sup>11</sup> Tolerance induction through administration of antigen arrays in B cells has been shown to be dependent on a multivalent interaction with antigen-specific B cells.<sup>12</sup> Furthermore, studies in a mouse model of MS known as experimental autoimmune encephalomyelitis (EAE) have demonstrated the potential efficacy of soluble antigen arrays (SAGAs).<sup>13</sup> These SAGAs, defined as a multivalent array of MS autoantigen proteolipid protein (PLP<sub>139-151</sub>) and cell adhesion inhibitor peptide (LABL), were shown to act in an antigen-specific manner and facilitate receptor clustering in B cells.<sup>14</sup> These studies demonstrate the potential efficacy associated with multivalent antigen displays in the treatment of MS.

Herein, we outline the synthesis and characterization of a novel multivalent display of PLP<sub>139-151</sub> for use in the EAE model of MS. This multivalent antigen array, referred to as 4-arm PLP<sub>139-151</sub>, consists of a tetravalent PEG backbone with PLP<sub>139-151</sub> peptide conjugated to each terminus. The efficacy of 4-arm PLP<sub>139-151</sub> was demonstrated *in vivo* through a 25-day EAE study. Additionally, the mechanisms associated with 4-arm PLP<sub>139-151</sub> treatment in splenocytes were explored through cell phenotyping using flow cytometry. Co-stimulatory marker expression was also investigated in these treatment groups, and downstream effector cell responses were gauged by quantification of inflammatory cytokine expression following treatment.

## 2. Experimental Section

### 2.1. Materials

20 kDa 4-arm PEG-azide was purchased from JenKem Technology USA (Beijing, China). Tris(3-hydroxypropyltriazolylmethyl)amine (THPTA) and sodium ascorbate (NaAsc) were purchased from Sigma-Aldrich (St. Louis, MO). Copper (II) sulfate pentahydrate ( $\text{CuSO}_4 \cdot 5 \text{H}_2\text{O}$ ) was purchased from Acros Organics (Geel, Belgium). Alkyne functionalized peptide bearing an *N*-terminal 4-pentynoic acid (homopropargyl, hp) modification, hpPLP<sub>139-151</sub> (hp-HSLGKWLGHDPKF-OH), was obtained from Biomatik, USA, LLC (Wilmington, DE). All reagents were used as received without further purification. For *in vitro* cell assays and *in vivo* studies, female 4-6-week-old SJL/J (H-2) mice were purchased from Envigo Laboratories (Indianapolis, IN). For EAE induction, incomplete Freund's adjuvant (IFA) and heat-killed mycobacterium tuberculosis H37RA were purchased from Difco (Sparks, MD). Additionally, pertussis toxin was purchased from List Biological Laboratories (Campbell, CA). For use in flow cytometry, TruStain fcX (anti-mouse CD16/32), R-phycoerythrin (PE)/Cy7-conjugated anti-mouse CD3, PE-conjugated anti-mouse CD86, FITC-conjugated anti-mouse CD80, AlexaFluor647-conjugated anti-mouse CD19, and BV421-conjugated anti-mouse CD11c were purchased from BioLegend (San Diego, CA).

### 2.2. Synthesis of 4-arm PLP<sub>139-151</sub>

4-arm PLP<sub>139-151</sub> was synthesized by copper-catalyzed azide-alkyne cycloaddition (CuAAC) chemistry, as shown in Scheme 1. First, hpPLP<sub>139-151</sub> (43  $\mu\text{mol}$ ) was added to a 20 mL scintillation vial with a stir bar. The powder was then dissolved in 5 mL of 50 mM phosphate

buffer (pH 7.4) at room temperature. A 10 mM solution of 20 kDa 4-arm PEG-azide (10  $\mu$ mol) in DMSO was then added to the solution, followed by a 120 mM solution of  $\text{CuSO}_4 \cdot 5\text{H}_2\text{O}$  (120  $\mu$ mol) in 50 mM phosphate buffer (pH 7.4). Then, THPTA (600  $\mu$ mol) was added as a 600 mM solution in 50 mM phosphate buffer (pH 7.4). A 100  $\mu$ L aliquot was removed for HPLC analysis before the addition of a 1 M solution of NaAsc (2.4 mmol) in 50 mM phosphate buffer (pH 7.4). The reaction was stirred at room temperature and the extent of conjugation was monitored by HPLC at various times. Upon completion of the reaction at 24 hrs, the solution was purified by semi-preparative HPLC utilizing a linear elution gradient of acetonitrile in water (constant 0.05% trifluoroacetic acid) over 20 min, with a Waters XBridge BEH  $\text{C}_{18}$ , 5 $\mu$ m, 130 Å stationary phase (19  $\times$  250 mm), with a 14.0 mL/min flow rate. The purified fraction was then concentrated under vacuum, transferred to vials, frozen, and lyophilized.

### 2.3. Analytical Characterization of 4-arm PLP<sub>139-151</sub>

RP-HPLC analysis was conducted using a Waters Alliance HPLC system equipped with a dual wavelength UV/vis detector. Chromatographic conditions utilized a linear gradient from 5-95% acetonitrile in water (constant 0.05% trifluoroacetic acid) over 20 min, with a Waters XBridge  $\text{C}_{18}$ , 5 $\mu$ m, 130 Å stationary phase (4.6  $\times$  250 mm) with a 1.0 mL/min flow rate and detection at 214 nm. The followed equation was used to quantitate conjugation of PLP<sub>139-151</sub>

$$N_{\text{con}} = \left[ \left( \frac{n_{\text{PLP}_{139-151}}}{n_{4\text{-arm PEG-azide}}} \right) \left( \frac{V_{\text{pre}} - V_{\text{sam}}}{V_{\text{pre}}} \right) \right] \left( 1 - \frac{\text{PA}_t}{\text{PA}_{\text{start}}} \right)$$

where  $N_{\text{con}}$  = number of conjugated PLP<sub>139-151</sub> molecules per backbone,  $n_{\text{PLP}_{139-151}}$  = moles of PLP<sub>139-151</sub> used in the reaction,  $n_{4\text{-arm PEG-azide}}$  = number of moles of 20 kDa 4-arm PEG-azide used in the reaction,  $V_{\text{pre}}$  = total reaction volume before NaAsc is added,  $V_{\text{sam}}$  = volume of “pre-

NaAsc" aliquot removed from the reaction mixture,  $PA_t$  = the measure peak area of PLP<sub>139-151</sub> at time  $t$ , and  $PA_{start}$  = the measure peak area of PLP<sub>139-151</sub> before NaAsc is added to the reaction.

NMR spectra were collected on a Bruker Avance AVIII 500 MHz spectrometer equipped with a dual carbon/proton cryoprobe, and all samples were dissolved in 600  $\mu$ L D<sub>2</sub>O for analysis. MestReNova 12.0 was used for NMR data analysis.

#### **2.4. Induction of EAE**

*In vivo* efficacy and *in vitro* cell assays were performed through induction of EAE in female 4-6-week-old SJL/J (H-2) mice. All protocols were approved through the University's Institutional Animal Care and Use Committee with animals housed in pathogen-free conditions. Induction of EAE was carried out using an emulsion of 200  $\mu$ g free PLP<sub>139-151</sub> in PBS emulsified with Complete Freund's Adjuvant (CFA) containing 4 mg/mL heat-killed *M. Tuberculosis* strain H37RA. This emulsion was administered subcutaneously to mice on day 0 in 50  $\mu$ L injections above each shoulder and hind flank for a total injection volume of 200  $\mu$ L per mouse. At this time, 100  $\mu$ L intraperitoneal injections of pertussis toxin at 100 ng/mL in PBS were administered to the mice. The administration of pertussis toxin was also repeated on day 2. Beginning on day 7, severity of disease symptoms was recorded daily using the following clinical scoring system: 0, no clinical disease symptoms; 1, weakness or limpness of the tail; 2, weakness or partial paralysis of one or two hind limbs (paraparesis); 3, full paralysis of both hind limbs (paraplegia); 4, paraplegia plus weakness or paralysis of forelimbs; 5, moribund (euthanasia necessary). Mouse body weight was recorded daily throughout the entire study.

#### **2.5. Competitive PLP<sub>139-151</sub> ELISA**

Competitive binding of 4-arm PLP<sub>139-151</sub> to EAE serum antibodies was detected using an indirect ELISA. Initially, 100  $\mu$ L of 1 mg/mL free PLP<sub>139-151</sub> at pH 9.5 (50 mM sodium bicarbonate buffer) was incubated overnight in an Immulon 2HB plate at 4°C. Wash buffer consisting of 1x Phosphate Buffered Saline (PBS) with 0.5% Tween 20 was used to wash the plate 3 times with 300  $\mu$ L/well. Block buffer was prepared using 0.2  $\mu$ m filtered PBS containing 1% Bovine Serum Albumin (BSA). The plate was blocked with 250  $\mu$ L of block buffer incubated at 37°C for 1 hour. Serum samples obtained from EAE mice at peak of disease severity were thawed and pre-incubated with one of the following treatments: 4-arm PLP<sub>139-151</sub>, 20 kDa 4-arm PEG-azide, free PLP<sub>139-151</sub>, or PBS. These treatments were maintained at 25  $\mu$ M PLP<sub>139-151</sub> basis and were incubated with the serum for 1 hour. Once again, the plate was washed 3 times with wash buffer, as described previously. Treated serum samples were added to the plate and serially diluted in reagent diluent consisting of 1% BSA and 0.5% Tween 20 in 1x PBS. Samples were incubated in the plate for 1 hour at 37°C. The plate was washed 3 times with wash buffer, as described previously. Secondary antibody solution was prepared using anti-mouse IgG diluted in reagent diluent. Each well was incubated with 100  $\mu$ L of secondary antibody solution for 1 hour at 37°C. The plate was washed 3 times with wash buffer and 100  $\mu$ L of TMB solution was added to each well. The plate was shaken at 200 rpm for 15 minutes prior to the addition of 100  $\mu$ L/well of 2N sulfuric acid to quench the reaction. Lastly, the absorbance at 450/540 nm was read on a Spectramax M5 (Molecular Devices) plate reader.

## **2.6. *In Vivo* Efficacy**

Treatment efficacy *in vivo* was determined using 6 mice per group. All mice were euthanized after 25 days. Treatments were subcutaneously administered on the back of the neck in 100  $\mu$ L of 40 mg/mL. Each group was dosed on a 200 nmol PLP<sub>139-151</sub> basis, with doses

administered on days 4, 7, and 10 following EAE induction. Mouse weights were recorded daily beginning on day 0 and clinical scores were recorded daily beginning on day 7.

## **2.7. Splenocyte Isolation**

Spleens were isolated from EAE mice at peak of disease for *in vitro* studies. Spleens were placed on ice in 5 mL of RPMI 1640 containing L-glutamine and 1% Penicillin-Streptomycin. Cellular extract was collected by pressing the spleens into a wire mesh using the plunger of a 1 mL syringe. The extract was centrifuged at 1100 xg for 5 minutes and resuspended in red blood cell lysis solution at room temperature for 5 minutes. The lysis solution was quenched through the addition of cold RPMI 1640 supplemented with L-glutamine, 1% Penicillin-Streptomycin, and 10% fetal bovine serum (FBS) (complete RPMI, cRPMI). The cells were then centrifuged at 1100 xg for 5 minutes and resuspended in cRPMI for counting in 0.04% trypan blue. Cells were counted using a Nexcelom Bioscience Cellometer Auto T4. *In vitro* cell incubation was carried out at 37°C and 5% CO<sub>2</sub> for 72 hours following addition of treatment.

## **2.8. Cell Staining for Flow Cytometry**

EAE splenocytes were incubated at 5 x 10<sup>6</sup> cells/well in a 24 well plate at a final volume of 1 mL. Treatments were added on a 25 μM PLP<sub>139-151</sub> basis, and PLP<sub>139-151</sub> rechallenge consisted of the addition of 25 μM free PLP<sub>139-151</sub> to the well. Following 72 hours incubation with treatment, a portion of cell supernatant was removed for future processing and the remaining cells were washed with RPMI + 5% FBS and centrifuged. Cells were resuspended in 50 μL of 20 μg/mL TruStain fcX and placed on ice for 30 minutes. Next, 50 μL of antibody solution was added, according to manufacturer recommendations, and the solution was kept on ice for 1 hour. Antibody stains included: R-phycoerythrin (PE)/Cy7-conjugated anti-mouse

CD3, PE-conjugated anti-mouse CD86, FITC-conjugated anti-mouse CD80, AlexaFluor647-conjugated anti-mouse CD19, and BV421-conjugated anti-mouse CD11c. Sample data was collected using a BD FACSFusion Cytometer with 30,000 events per sample. Sample data was analyzed using Kaluza and GraphPad Prism.

## **2.9. Cytokine Measurement**

Prior to sample processing for flow cytometry, cell supernatant was removed from the samples. This supernatant was frozen at  $-80^{\circ}\text{C}$  until cytokine analysis could be carried out. The secretion of IFN- $\gamma$ , TNF- $\alpha$ , GM-CSF, IL-2, IL-6, IL-10, IL-12p70, IL-15, IL-17A, and IL-23 was detected using a U-Plex kit while following manufacturer instructions (Meso Scale Discovery).

## **Statistical Analysis**

Statistical analysis in all assays was carried out using two-way analysis of variance (ANOVA) and Tukey multiple comparisons tests. Criteria for significance in cytokine analysis are as follows: \*  $p < 0.05$ , \*\*  $p < 0.01$ , \*\*\*  $p < 0.001$ , \*\*\*\*  $p < 0.0001$ . For cytometry samples \* represents significance ( $p < 0.05$  or better) from the 4-arm PLP<sub>139-151</sub> treatment group with  $25\ \mu\text{M}$  PLP<sub>139-151</sub> rechallenge. Additionally, for flow cytometry samples # represents significance ( $p < 0.05$  or better) from the 4-arm PLP<sub>139-151</sub> treatment group with no PLP<sub>139-151</sub> rechallenge. All statistical analysis was performed using GraphPad Prism.

## **3. Results**

### **3.1. Synthesis and Analytical Characterization of 4-arm PLP<sub>139-151</sub>**

The 4-arm PLP<sub>139-151</sub>, with an average of 3.3 PLP<sub>139-151</sub> molecules per backbone, was synthesized by conjugating multiple modified autoantigen (hpPLP<sub>139-151</sub>) molecules to 20 kDa 4-arm PEG-azide. Both qualitative and quantitative analytical techniques were used to characterize

4-arm PLP<sub>139-151</sub> and its components. Peptide conjugation was determined through gradient RP-HPLC. Total hpPLP<sub>139-151</sub> in solution was determined by taking an aliquot from the reaction before NaAsc was added.

<sup>1</sup>H/<sup>13</sup>C Heteronuclear Single Quantum Coherence (HSQC) NMR spectroscopy was used to qualitatively confirm the absence of the unique resonance signal for the homopropargyl linker on hpPLP<sub>139-151</sub> ( $\delta(^1\text{H}) \approx 2.6$  ppm,  $\delta(^{13}\text{C}) \approx 70$  ppm) in the 4-arm PLP<sub>139-151</sub> spectrum (Figure 2C); thus, confirming the final products contained only the conjugated protein. Further, the incorporation of both components into the final product can be observed by comparing the individual resonances from 20 kDa 4-arm PEG-azide (Figure 2A) and hpPLP<sub>139-151</sub> (Figure 2B), to the HSQC spectrum of 4-arm PLP<sub>139-151</sub>.

### **3.2. Competitive ELISA Demonstrating PLP<sub>139-151</sub> Specificity**

Serum from EAE mice was pre-incubated with 4-arm PLP<sub>139-151</sub>, 20 kDa 4-arm PEG-azide, or free PLP<sub>139-151</sub> prior to addition to a PLP<sub>139-151</sub>-coated ELISA plate. The result of this pre-incubation is the loss of signal due to PLP<sub>139-151</sub>-specific antibodies binding during pre-incubation. As seen in Figure 3, pre-incubation with 4-arm PLP<sub>139-151</sub> greatly reduces the signal in the competitive ELISA assay compared to pre-incubation with PBS, indicating that PLP<sub>139-151</sub>-specific antibody binding sites are occupied following 4-arm PLP<sub>139-151</sub> pre-incubation. This result indicates that 4-arm PLP<sub>139-151</sub> is more effective at occupying the binding sites of PLP<sub>139-151</sub>-specific antibodies in EAE serum, compared to equimolar concentrations of free PLP<sub>139-151</sub>. Additionally, pre-incubation with 20 kDa 4-arm PEG-azide reduces ELISA signal, suggesting that free azides may introduce some degree of non-specific binding to serum antibodies (Figure S1).

### **3.3. *In Vivo* Efficacy of 4-arm PLP<sub>139-151</sub>**

*In vivo* screening of 4-arm PLP<sub>139-151</sub> in the EAE mouse model was studied through subcutaneous injection of treatments in 40 mg/mL mannitol at equimolar PLP<sub>139-151</sub> concentrations of 200 nmol. Treatments were administered on days 4, 7, and 10 with mice being observed for 25 days. Clinical scores are assigned based on disease severity, with higher scores representing more severe symptoms. Treatment with 4-arm PLP<sub>139-151</sub> proved to be most effective at eliminating EAE symptoms, as mice treated with 4-arm PLP<sub>139-151</sub> displayed no signs of paralysis (Figure 4). This result represents a drastic change from the control treatments which both developed symptoms of paralysis. Furthermore, the mouse weight data (Figure 5) parallels the clinical score data, with the 4-arm PLP<sub>139-151</sub> treated mice maintaining a healthy and stable weight throughout the study. This contrasts with the control groups, which displayed a rapid loss of weight beginning at approximately day 10.

### **3.4. Analysis of Key Immune Cell Populations**

*In vitro* treatment of EAE splenocytes harvested at peak of disease with 4-arm PLP<sub>139-151</sub> was assessed through flow cytometric analysis of key immune cell populations. These populations include CD11c<sup>+</sup> antigen-presenting cells, CD19<sup>+</sup> B cells, and CD3<sup>+</sup> T-cells. Additionally, the expression of two co-stimulatory markers, CD80 and CD86, was analyzed in these splenocytes. Treatment groups included media, 25 μM free PLP<sub>139-151</sub>, 4-arm PLP<sub>139-151</sub>, and a combination 4-arm PLP<sub>139-151</sub> + 25 μM free PLP<sub>139-151</sub>. This strategy provides insight into the ability of these treatment options to suppress PLP<sub>139-151</sub>-specific cell expansion in the presence of free, cognate antigen. Additionally, 20 kDa 4-arm PEG-azide and 20 kDa 4-arm PEG-azide + 25 μM free PLP<sub>139-151</sub> treatments were explored and these data are included in the supplement.

CD11c<sup>+</sup> cells represent the smallest population observed in this study, and with the inclusion of 25  $\mu$ M PLP<sub>139-151</sub> rechallenge, the presence of this population was further reduced through treatment with 4-arm PLP<sub>139-151</sub> (Figure 6). This reduction in CD11c<sup>+</sup> cells was not observed in the presence of 20 kDa 4-arm PEG-azide without conjugation of PLP<sub>139-151</sub>. T-cell populations remained relatively constant across all treatment options except for a small reduction in T-cells when treated with 4-arm PLP<sub>139-151</sub> alone, compared to media alone (Figure 6). Two populations of CD19<sup>+</sup> B cells were observed throughout this study. The first population, labeled CD19<sup>+lo</sup> represents a lower expression of CD19 on the cell surface (Figure S5). This population remained mostly constant across all treatment groups with the exception of a slight increase in CD19<sup>+lo</sup> cells in splenocytes treated with 4-arm PLP<sub>139-151</sub> + 25  $\mu$ M free PLP<sub>139-151</sub> (Figure 6). Most interestingly, the CD19<sup>+hi</sup> B cell population appears to be highly responsive to PLP<sub>139-151</sub>-rechallenge, as the inclusion of 25  $\mu$ M free PLP<sub>139-151</sub> results in marked expansion of this cell population (Figure 6). Furthermore, treatment with 4-arm PLP<sub>139-151</sub> nearly completely eliminates CD19<sup>+hi</sup> B cells from these splenocytes, both in the presence of 25  $\mu$ M free PLP<sub>139-151</sub> and without rechallenge (Figure 6).

Co-stimulatory markers CD80 and CD86 were observed broadly across all splenocytes, and treatment with 4-arm PLP<sub>139-151</sub> also had striking results on the expression of these co-stimulatory molecules. CD80 expression was broadly increased following treatment with 4-arm PLP<sub>139-151</sub>, a result that was maintained both with and without PLP<sub>139-151</sub> rechallenge (Figure 7A). In contrast, the expression of CD86 was significantly reduced in splenocytes treated with 4-arm PLP<sub>139-151</sub> (Figure 7B). The expression of CD86 was upregulated in the presence of 25  $\mu$ M free PLP<sub>139-151</sub> in the control treatment groups, but the inclusion of 4-arm PLP<sub>139-151</sub> prevented this upregulation despite the presence of PLP<sub>139-151</sub> rechallenge (Figure 7B).

### 3.5. Cytokine Expression

In addition to investigating changes in key immune cell population statistics, the treated samples were also tested for differences in cytokine expression. Cytokines investigated in this assay include: IFN- $\gamma$ , TNF- $\alpha$ , GM-CSF, IL-2, IL-6, IL-10, IL-12p70, IL-15, IL-17A, and IL-23. Samples were designed for analysis in triplicate, however, GM-CSF, IL-12p70, IL-15, and IL-23 each resulted in fewer than 3 samples within detectable range. Of the remaining cytokines, the effects of 4-arm PLP<sub>139-151</sub> are clear. General inflammatory cytokines such as IFN- $\gamma$  (Figure 8A) and TNF- $\alpha$  (Figure 8B) are highly expressed in the presence of 25  $\mu$ M free PLP<sub>139-151</sub> for control treatment groups. Despite this increase due to the presence of free PLP<sub>139-151</sub>, 4-arm PLP<sub>139-151</sub> treatment prevents the increased secretion of IFN- $\gamma$  (Figure 8A) and TNF- $\alpha$  (Figure 8B) in the presence of PLP<sub>139-151</sub> rechallenge. It should be noted that treatment with 20 kDa 4-arm PEG-azide in the presence of 25  $\mu$ M free PLP<sub>139-151</sub> significantly increases the secretion of TNF- $\alpha$ , possibly due to the presence of free azides (Figure S4B). The anti-inflammatory effects of 4-arm PLP<sub>139-151</sub> are also observed in expression of IL-2 (Figure 8C), as the cellular response to PLP<sub>139-151</sub> rechallenge is significantly reduced. IL-17A (Figure 8D) and IL-6 (Figure 8E) expression is also increased in the presence of free PLP<sub>139-151</sub>, but treatment with 4-arm PLP<sub>139-151</sub> significantly reduces the secretion of both cytokines in response to PLP<sub>139-151</sub> rechallenge. Lastly, expression of IL-10 (Figure 8F) appears to remain unchanged in response to the treatment groups explored in this study.

## 4. Discussion

Soluble multivalent antigen displays have the potential to selectively tolerize self-reactive B cells at various stages of B cell maturity due to their high affinity interactions with the BCR.<sup>11-12, 15</sup> Of note, early works in the development of multivalent arrays for tolerance induction

indicated that low molecular weight antigen arrays were most effective at eliminating circulating IgGs.<sup>16</sup> In studies reported here, low molecular weight tetravalent antigen arrays were explored. To implement this strategy for the treatment of autoimmunity in EAE, we aimed to develop an easily characterizable and soluble multivalent antigen array with high functional affinity for PLP<sub>139-151</sub>-specific BCRs.

As seen in Figure 3, pre-incubation with 4-arm PLP<sub>139-151</sub> resulted in the greatest reduction of absorbance in the competitive ELISA assay. In fact, the reduction in absorbance associated with 4-arm PLP<sub>139-151</sub> when pre-incubated at a 25  $\mu$ M PLP<sub>139-151</sub> basis is significantly larger than that of pre-incubation with equimolar concentrations of free PLP<sub>139-151</sub>. This result suggests that the multivalent nature of 4-arm PLP<sub>139-151</sub> is more effective at occupying the binding site of PLP<sub>139-151</sub>-specific antibodies in solution due to higher avidity; a feature likely resulting from the molecular design of 4-arm PLP<sub>139-151</sub>. Notably, the average length of the 5 kDa PEG arms in 20 kDa 4-arm PEG-azide is approximately 6 nm. As such, the greatest distance between two PLP<sub>139-151</sub> moieties in 4-arm PLP<sub>139-151</sub> would be approximately 12 nm, which is nearly identical to the average spacing between the two arms of an IgG class antibody.<sup>17</sup> Furthermore, high avidity interactions between antigen and respective BCRs in the absence of secondary co-stimulatory signals are often associated with induction of B cell anergy, a state of immunological unresponsiveness.<sup>18-20</sup> Prior work by the Cambier group demonstrated that B cell anergy was only maintained through constant antigen receptor occupancy.<sup>19</sup> We hypothesize that the molecular design of 4-arm PLP<sub>139-151</sub> exploits this B cell pathway in order to induce tolerance against autoantigens.

Indeed, *in vivo* treatment of EAE mice through subcutaneous injection of 4-arm PLP<sub>139-151</sub> prevented symptom onset in “at-risk” animals. As seen in Figure 4, subcutaneous

administration of 4-arm PLP<sub>139-151</sub> at a 200 nmol PLP<sub>139-151</sub> basis was capable of completely ameliorating EAE symptoms in mice, with none of the treated mice showing signs of paralysis throughout the 25-day study. This is in contrast to mice treated with mannitol and with free PLP<sub>139-151</sub>, both of which experienced symptoms of paralysis. Additionally, mice treated with 4-arm PLP<sub>139-151</sub> also maintained a healthy weight throughout the study (Figure 5), further supporting the efficacy associated with multivalent display of antigen. Investigations into the phenotypic changes associated with the amelioration of EAE symptoms at peak of disease further support the role of B cell interactions in the efficacy of 4-arm PLP<sub>139-151</sub> treatment. Most notably, 72-hour *in vitro* treatment with 4-arm PLP<sub>139-151</sub> resulted in nearly complete depletion of CD19<sup>hi</sup> cells (Figure 6), a B cell population which appears to be highly responsive to treatment with 25 μM free PLP<sub>139-151</sub>. We postulate that these CD19<sup>hi</sup> B cells are associated with EAE disease onset due to their rapid expansion when treated with 25 μM free PLP<sub>139-151</sub>. This is supported by literature indicating overexpression of CD19 in transgenic mice results in a breakdown of peripheral tolerance, allowing autoreactive B cells to overcome anergy.<sup>21</sup> Therefore, depletion of CD19<sup>hi</sup> B cells is likely a key mechanism by which 4-arm PLP<sub>139-151</sub> is capable of ameliorating EAE symptoms.

In addition to the depletion of seemingly autoreactive B cells, 4-arm PLP<sub>139-151</sub> treatment also alters the expression of co-stimulatory markers CD80 and CD86. CD80 expression significantly increased following treatment with 4-arm PLP<sub>139-151</sub> both with and without the addition of 25 μM free PLP<sub>139-151</sub> (Figure 7A). Conversely, the expression of CD86 was significantly reduced when treated with 4-arm PLP<sub>139-151</sub> + 25 μM free PLP<sub>139-151</sub>, in comparison to 25 μM free PLP<sub>139-151</sub> alone (Figure 7B). In order to interpret these results, it is important to first understand the role these co-stimulatory markers play in regard to T-cell activation. As

demonstrated by Manzotti et al., the functions of these two ligands are distinct and opposing.<sup>22</sup> Manzotti and colleagues found that ligation of cytotoxic T lymphocyte-associated antigen 4 (CTLA-4) with CD86 was associated with T-cell proliferation, whereas ligation of CTLA-4 with CD80 resulted primarily in inhibition of T-cell activation.<sup>22</sup> Therefore, treatment with 4-arm PLP<sub>139-151</sub> results in a shift toward T-cell inhibition, in addition to direct depletion of autoreactive B cells.

Despite the minor change in CD3<sup>+</sup> cell counts associated with 4-arm PLP<sub>139-151</sub> treatment (Figure 6), downstream T-cell activity appears to be greatly inhibited through multivalent antigen treatment. To assess the effects of 4-arm PLP<sub>139-151</sub> treatment on effector T-cells, cytokine levels in splenocytes were analyzed following treatment. Generally, only samples which included 25  $\mu$ M free PLP<sub>139-151</sub> resulted in significant changes in cytokines (Figure 8). EAE splenocytes treated with 25  $\mu$ M free PLP<sub>139-151</sub> alone resulted in increased secretion of inflammatory cytokines such as IFN- $\gamma$ , TNF- $\alpha$ , IL-2, IL-17A, and IL-6. Interestingly, splenocytes treated with 4-arm PLP<sub>139-151</sub> + 25  $\mu$ M free PLP<sub>139-151</sub> expressed significantly lower levels of each of these inflammatory cytokines despite the inclusion of free, cognate antigen. This result suggests that the depletion in CD19<sup>hi</sup> B cells as well as the increased expression of CD80 may be inhibiting effector T-cell activation.

## 5. Conclusions

In summary, we have outlined the synthesis and characterization of a low molecular weight, soluble tetravalent antigen display system for the induction of antigen-specific tolerance. The distinct molecular properties of 4-arm PLP<sub>139-151</sub> provide high avidity interactions with PLP<sub>139-151</sub>-specific antibodies, which imparts its therapeutic efficacy *in vivo*. *In vitro* culture of 4-arm PLP<sub>139-151</sub> with EAE mouse splenocytes demonstrates that the therapeutic efficacy

observed *in vivo* is likely the result of depletion of PLP<sub>139-151</sub>-responsive CD19<sup>hi</sup> B cells.

Furthermore, these effects are maintained in cultures containing equimolar, free PLP<sub>139-151</sub>, indicating that the presence of cognate antigen does not inhibit tolerance induction.

Additionally, the overall expression of CD80, associated with preferential inhibition of T-cells, is increased, while the expression of CD86, associated with T-cell proliferation, is decreased. This indicates a shift toward inhibition of PLP<sub>139-151</sub>-specific inflammatory responses and reduced activation of effector T-cells. A reduction in numerous inflammatory cytokines in response to free PLP<sub>139-151</sub> further corroborates this trend. Future investigations will focus on direct observations of interactions between 4-arm PLP<sub>139-151</sub> and B cells, as well as demonstrating the effects of tolerance induction during relapse *in vivo*.

## Figures and Schemes

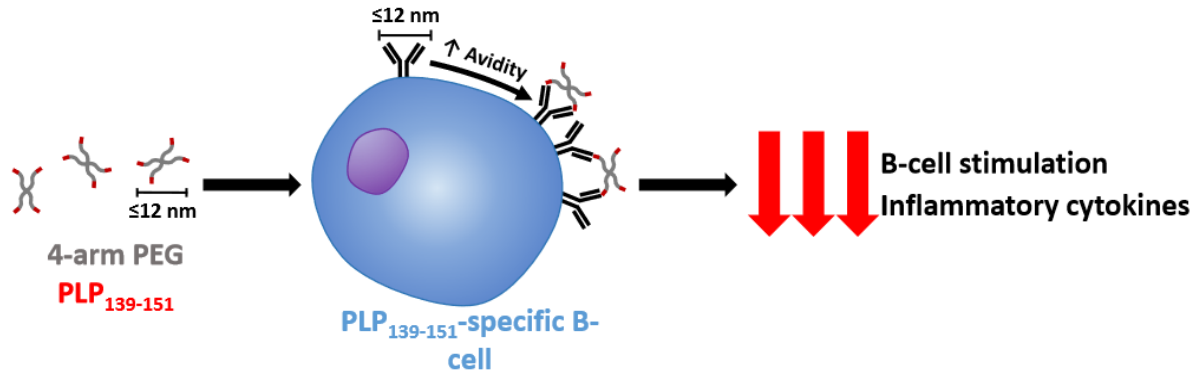
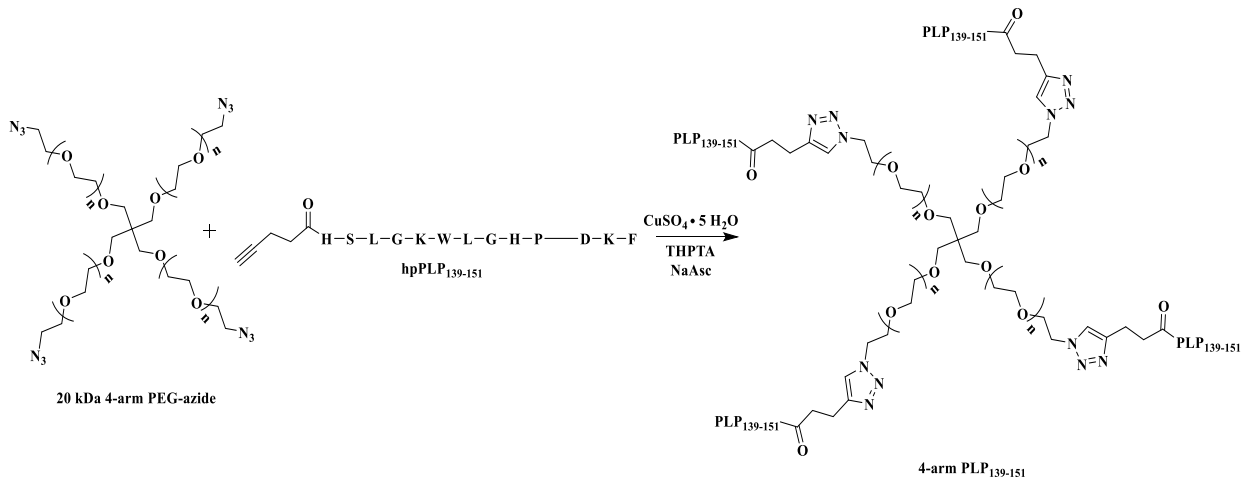


**Figure 1.** Schematic of how high avidity interactions between 4-arm PLP<sub>139-151</sub> and PLP<sub>139-151</sub>-specific B cell receptors may induce tolerance in autoreactive B cells.



**Scheme 1.** Reaction scheme for the synthesis of 4-arm PLP<sub>139-151</sub>.

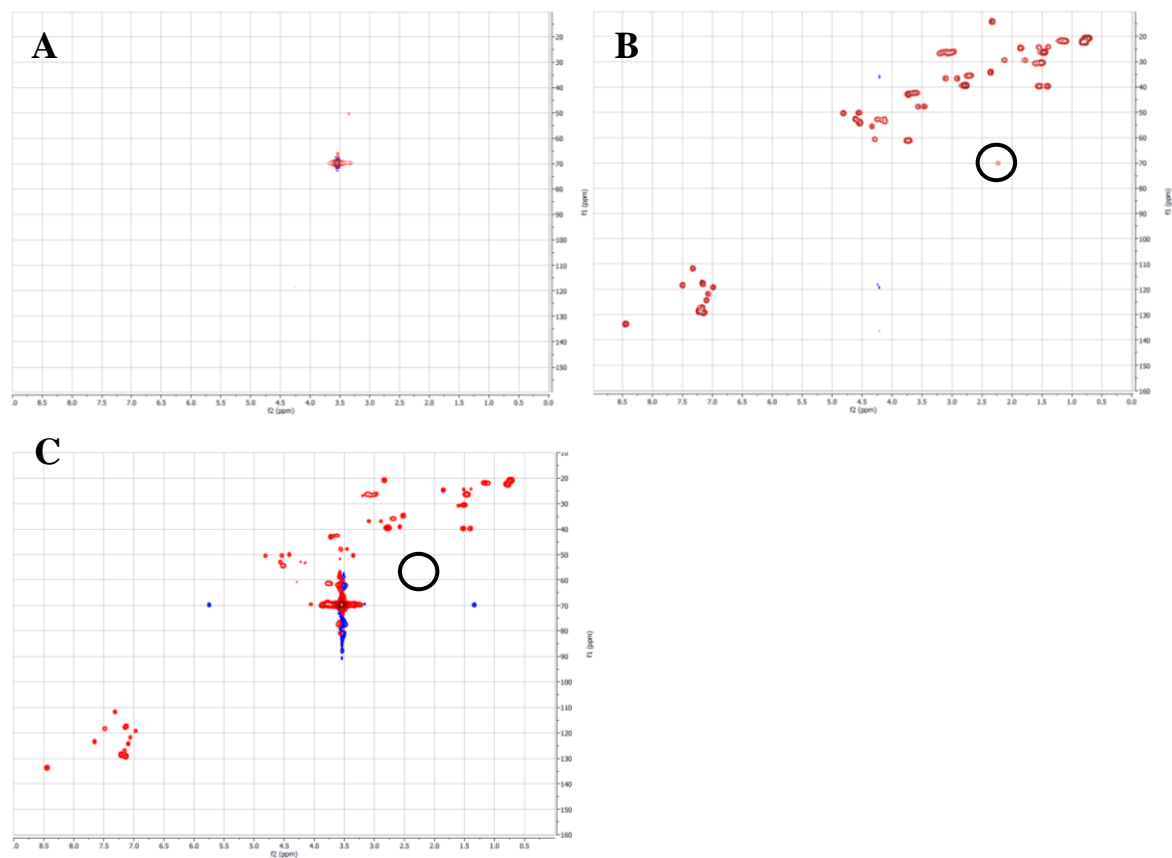


**Figure 2.** HSQC NMR spectra of 20 kDa 4-arm PEG-azide (A), hpPLP<sub>139-151</sub> (B), and 4-arm PLP<sub>139-151</sub> (C). hpPLP<sub>139-151</sub> (B) shows a unique resonance from the alkyne peak. 4-arm PLP<sub>139-151</sub> (C) does not show the resonance from the alkyne peak, indicating that no residual unconjugated PLP<sub>139-151</sub> is present in the final product.

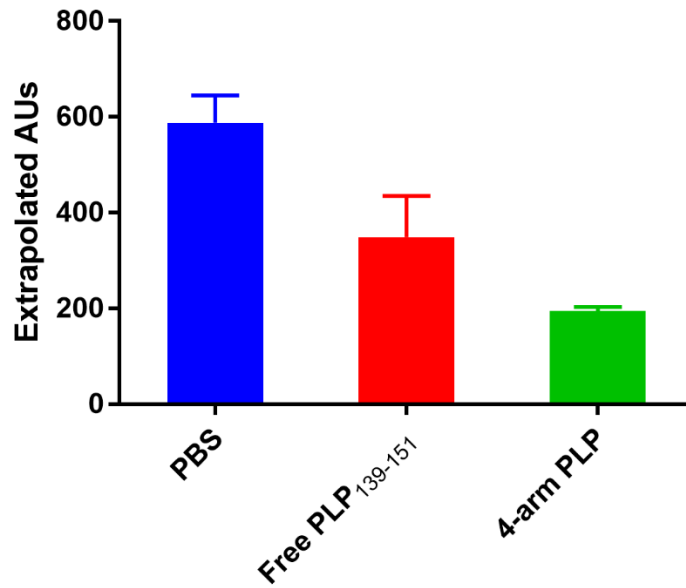


**Figure 3.** PLP<sub>139-151</sub>-specific IgG antibody titers in EAE mouse serum detected by ELISA following one-hour serum incubation with (A) PBS vehicle control (B) Free PLP<sub>139-151</sub> and (C) 4-arm PLP<sub>139-151</sub>.

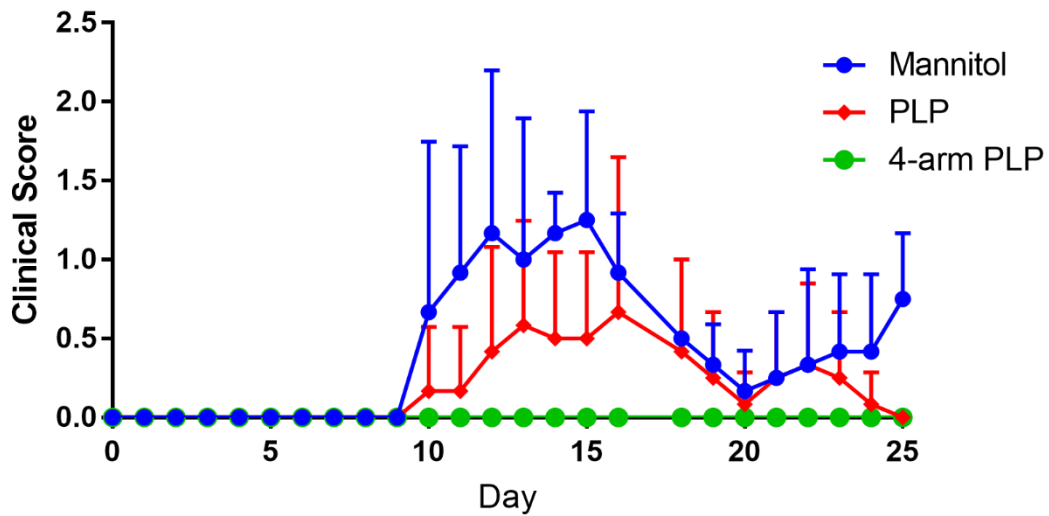


**Figure 4.** Clinical scores of EAE mice treated *in vivo* with (A) free PLP<sub>139-151</sub> and (B) 4-arm PLP<sub>139-151</sub>. Treatments were administered subcutaneously on days 4, 7, and 10 with 40 mg/mL mannitol as vehicle. All doses were based on 200 nmol PLP<sub>139-151</sub> basis. N=6 for all groups. Data is presented as mean ± SD.

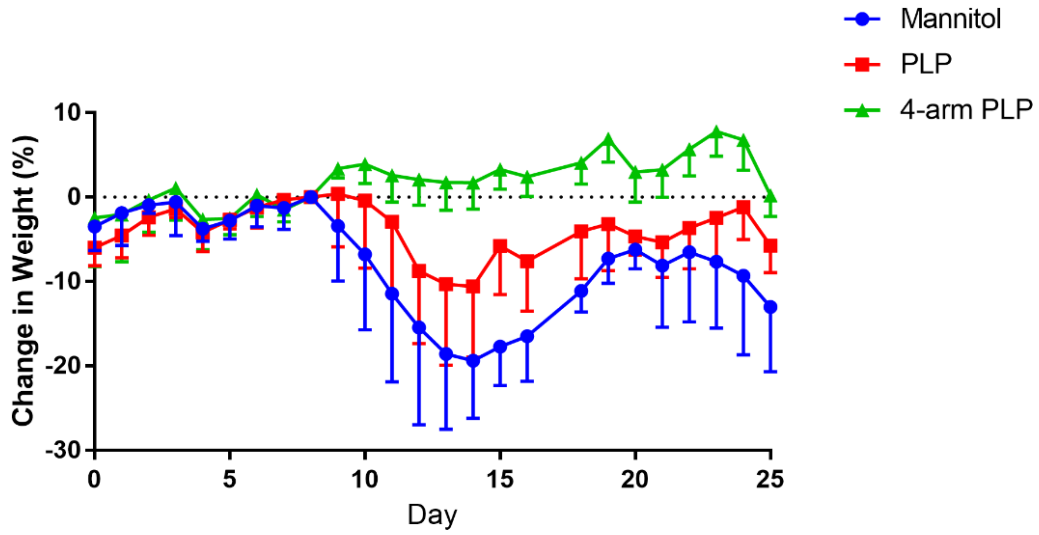


**Figure 5.** Animal weight data of EAE mice treated *in vivo* with (A) free PLP<sub>139-151</sub> and (B) 4-arm PLP<sub>139-151</sub>. Treatments were administered subcutaneously on days 4, 7, and 10 with 40 mg/mL mannitol as vehicle. All doses were based on 200 nmol PLP<sub>139-151</sub> basis. N=6 for all groups. Data is presented as mean  $\pm$  SD of % change in weight normalized to mouse weight at day 8.

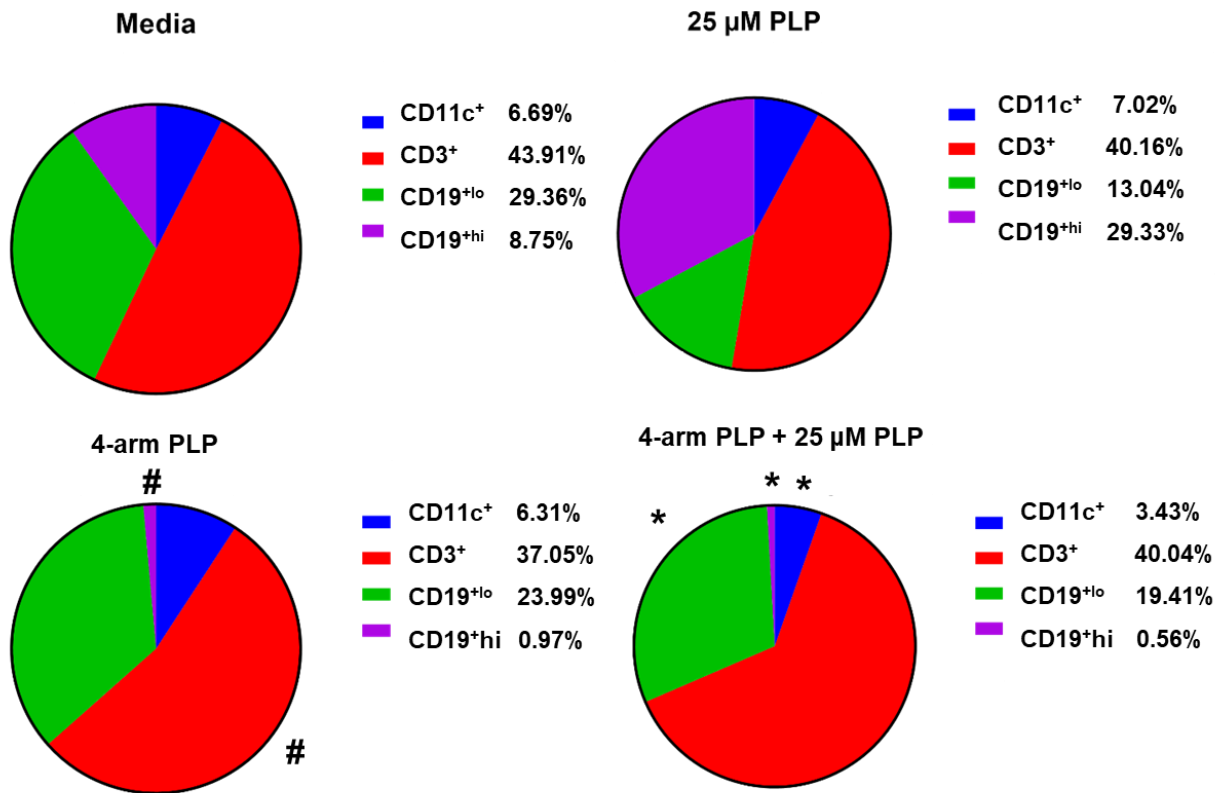


**Figure 6.** Percent of total singlet splenocytes expressing CD11c, CD3, CD19<sup>lo</sup>, and CD19<sup>hi</sup> following *in vitro* incubation for 72 hours with media, 25 μM free PLP<sub>139-151</sub>, 4-arm PLP<sub>139-151</sub>, and 4-arm PLP<sub>139-151</sub> + 25 μM free PLP<sub>139-151</sub>. Data is presented as mean ± SD. N=3, \* represents significance from 25 μM free PLP<sub>139-151</sub>. # represents significance from Media.

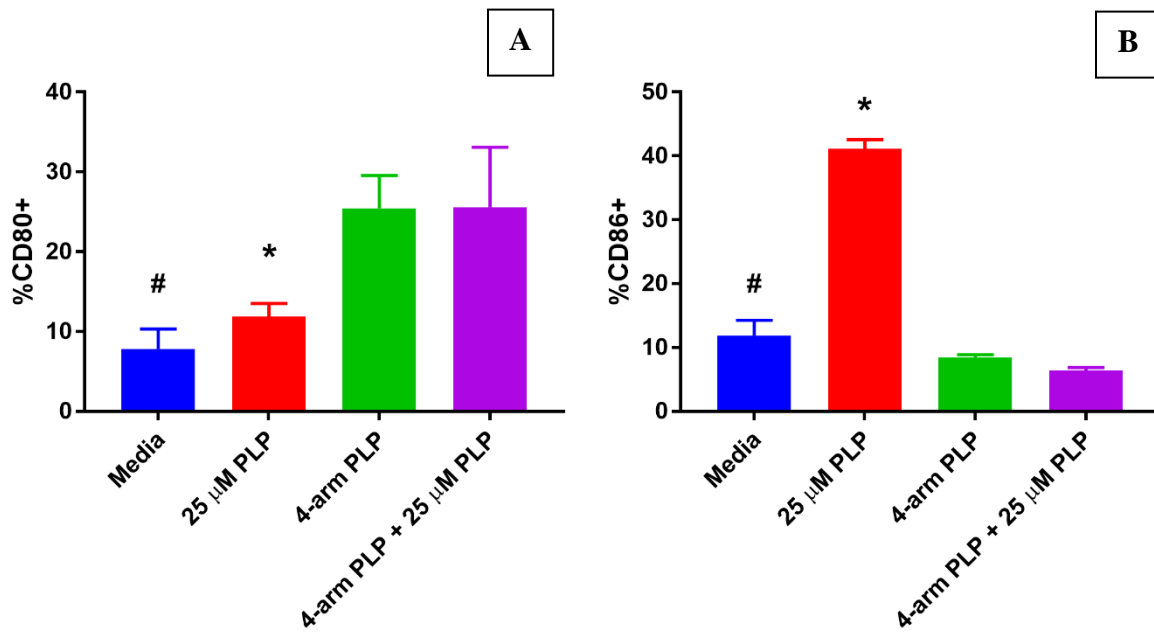


**Figure 7.** Percent of total singlet splenocytes expressing (A) CD80 and (B) CD86 following *in vitro* incubation for 72 hours with (I) media (II) 25 μM free PLP<sub>139-151</sub> (III) 4-arm PLP<sub>139-151</sub> and (IV) 4-arm PLP<sub>139-151</sub> + 25 μM free PLP<sub>139-151</sub>. Data is presented as mean ± SD. N=3, \* represents significance from 4-arm PLP<sub>139-151</sub> + 25 μM free PLP<sub>139-151</sub>. # represents significance from 4-arm PLP<sub>139-151</sub>.

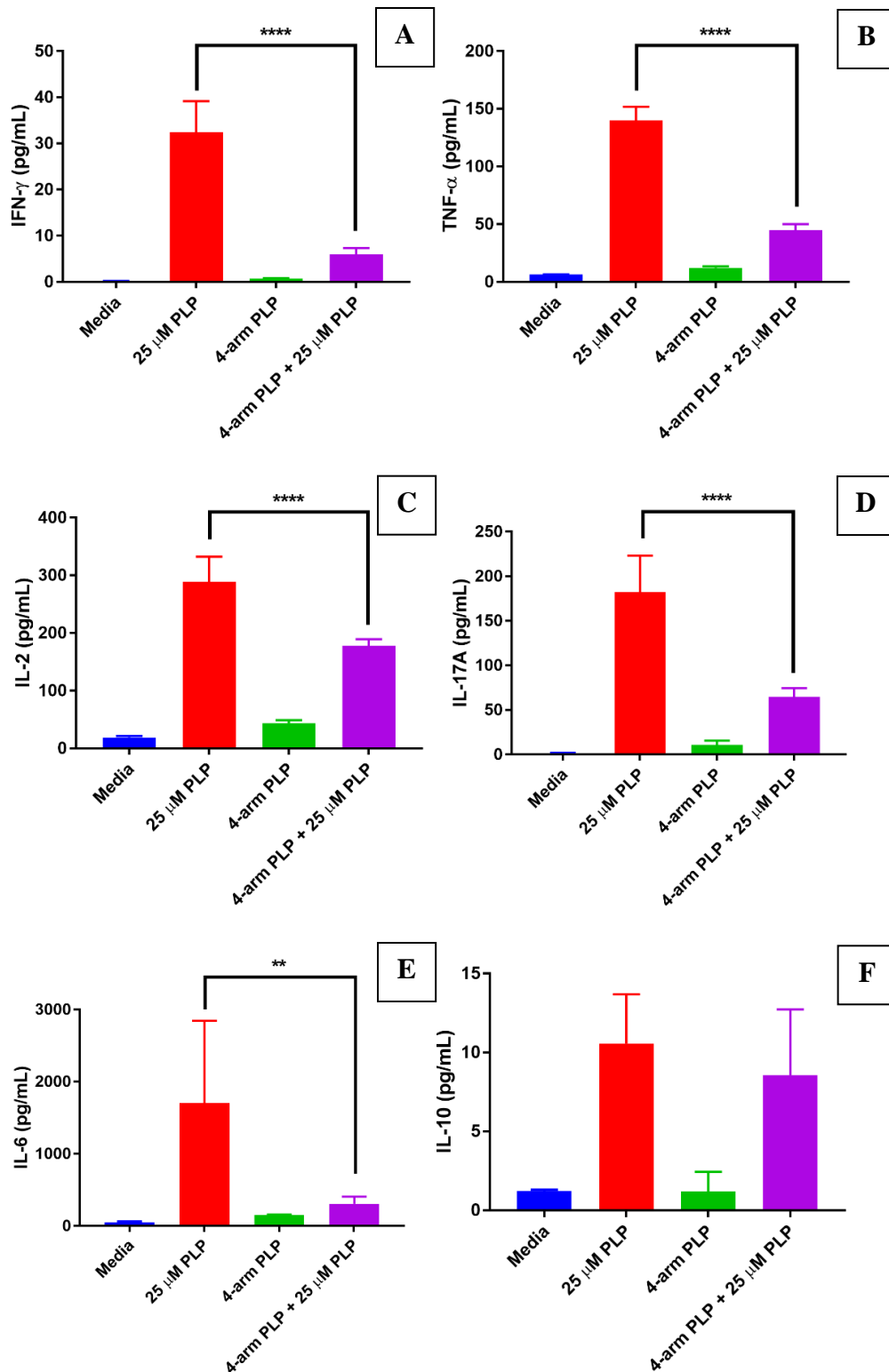


**Figure 8.** Concentrations of (A) IFN- $\gamma$  (B) TNF- $\alpha$  (C) IL-2 (D) IL-17A (E) IL-6 and (F) IL-10 following 72 hr *in vitro* incubation with (I) media (II) 25  $\mu\text{M}$  free PLP<sub>139-151</sub> (III) 4-arm PLP<sub>139-151</sub> and (IV) 4-arm PLP<sub>139-151</sub> + 25  $\mu\text{M}$  free PLP<sub>139-151</sub>. Data is presented as mean  $\pm$  SD. N=3, \* p<0.05, \*\* p<0.01, \*\*\* p<0.001, \*\*\*\* p<0.0001.

## Supplementary Figures

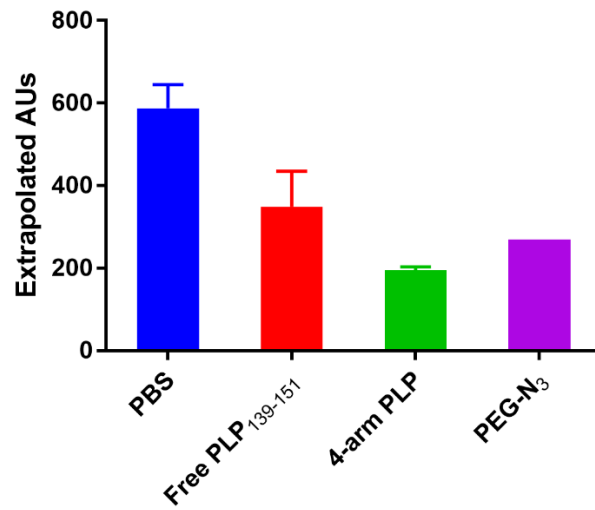


**Figure S1.** PLP<sub>139-151</sub>-specific IgG antibody titers in EAE mouse serum detected by ELISA following one-hour incubation with (A) PBS (B) Free PLP<sub>139-151</sub> (C) 4-arm PLP<sub>139-151</sub> and (D) 20 kDa 4-arm PEG-N<sub>3</sub>.

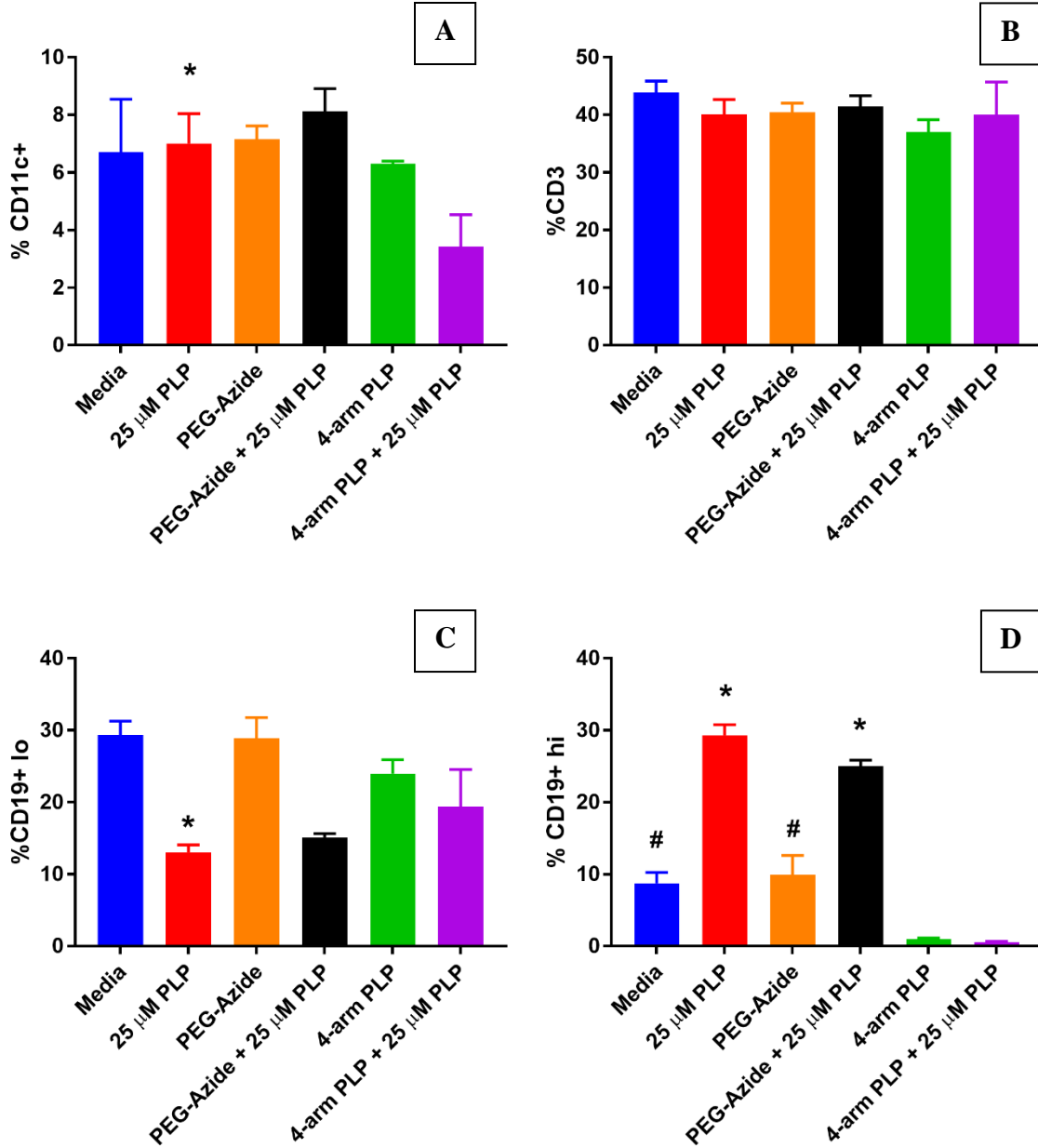


**Figure S2.** Percent of total singlet splenocytes expressing (A) CD11c (B) CD3 (C) CD19<sup>lo</sup> and (D) CD19<sup>hi</sup> following *in vitro* incubation for 72 hours with (I) media (II) 25  $\mu$ M free PLP<sub>139-151</sub> (III) 20 kDa 4-arm PEG-N<sub>3</sub> (IV) 20 kDa 4-arm PEG-N<sub>3</sub> + 25  $\mu$ M free PLP<sub>139-151</sub> (V) 4-arm PLP<sub>139-151</sub> and (VI) 4-arm PLP<sub>139-151</sub> + 25  $\mu$ M free PLP<sub>139-151</sub>. Data is presented as mean  $\pm$  SD. N=3, \* represents significance from 4-arm PLP<sub>139-151</sub> + 25  $\mu$ M free PLP<sub>139-151</sub>. # represents significance from 4-arm PLP<sub>139-151</sub>.

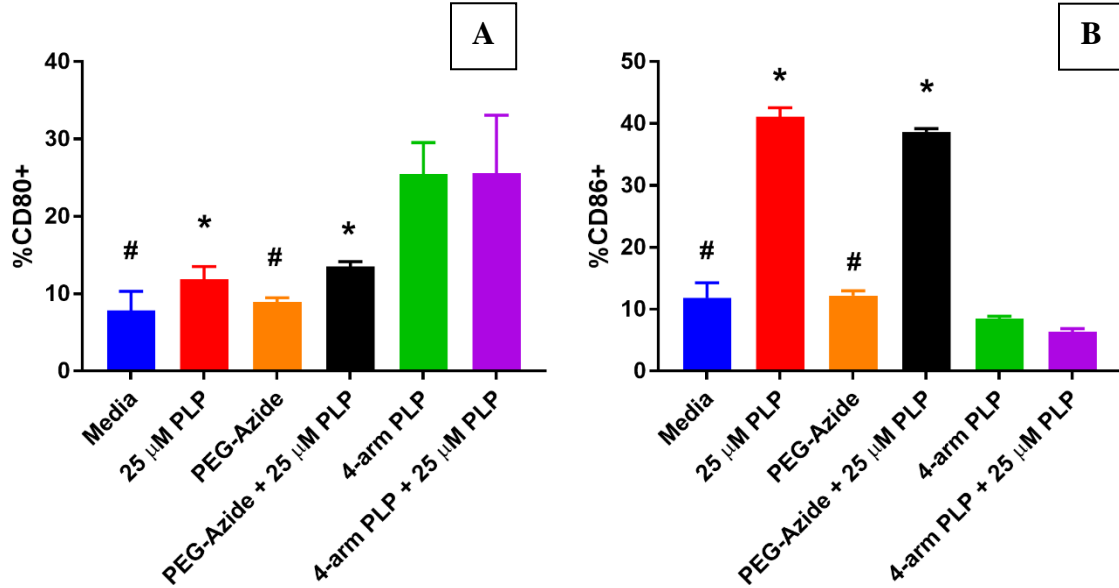


**Figure S3.** Percent of total singlet splenocytes expressing (A) CD80 and (B) CD86 following *in vitro* incubation for 72 hours with (I) media (II) 25  $\mu$ M free PLP<sub>139-151</sub> (III) 20 kDa 4-arm PEG-N<sub>3</sub> (IV) 20 kDa 4-arm PEG-N<sub>3</sub> + 25  $\mu$ M free PLP<sub>139-151</sub> (V) 4-arm PLP<sub>139-151</sub> and (VI) 4-arm PLP<sub>139-151</sub> + 25  $\mu$ M free PLP<sub>139-151</sub>. Data is presented as mean  $\pm$  SD. N=3, \* represents significance from 4-arm PLP<sub>139-151</sub> + 25  $\mu$ M free PLP<sub>139-151</sub>. # represents significance from 4-arm PLP<sub>139-151</sub>.

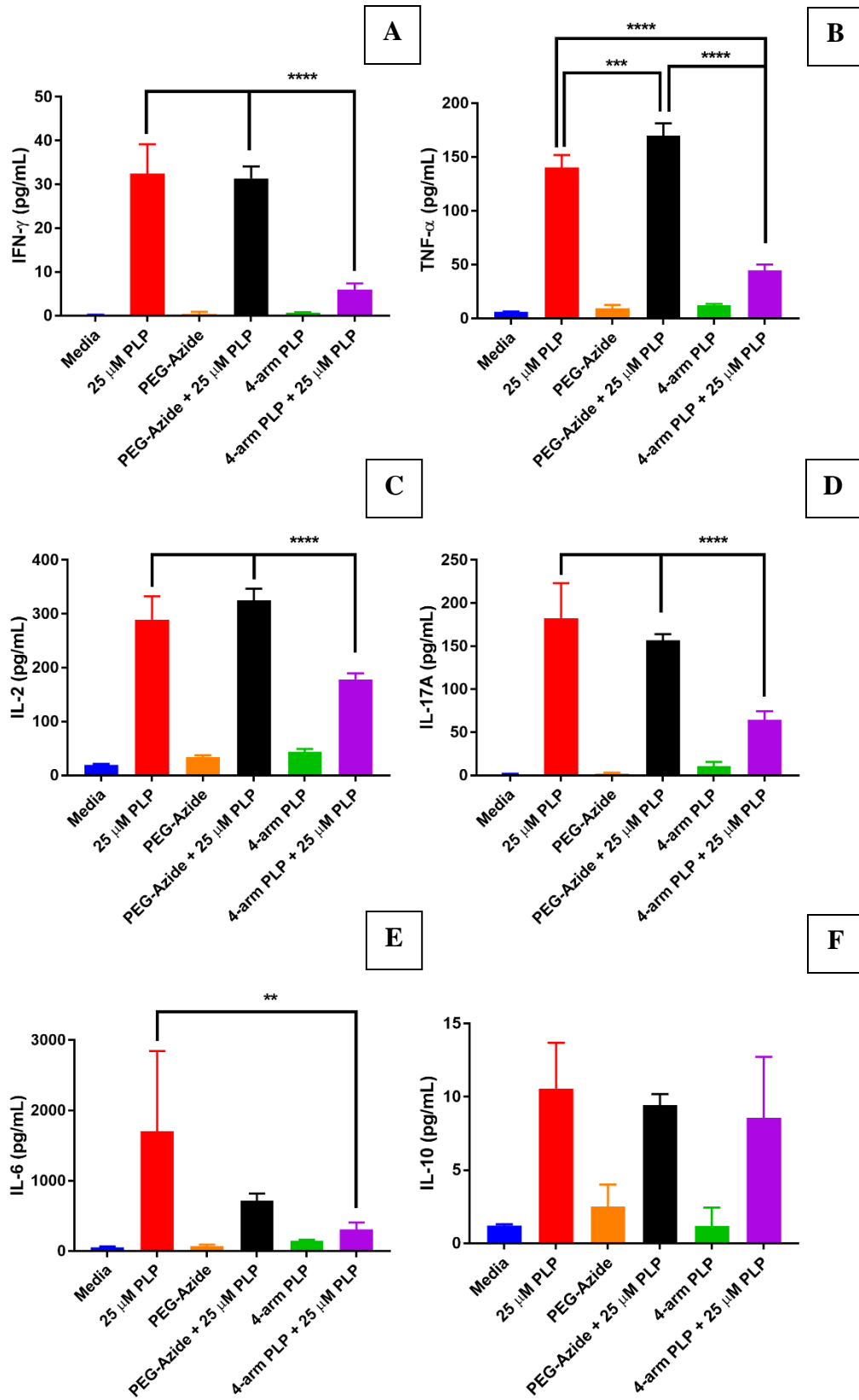


**Figure S4.** Concentrations of (A) IFN- $\gamma$  (B) TNF- $\alpha$  (C) IL-2 (D) IL-17A (E) IL-6 and (F) IL-10 following 72 hr *in vitro* incubation with (I) media (II) 25  $\mu$ M free PLP<sub>139-151</sub> (III) 20 kDa 4-arm PEG-N<sub>3</sub> (IV) 20 kDa 4-arm PEG-N<sub>3</sub> + 25  $\mu$ M free PLP<sub>139-151</sub> (V) 4-arm PLP<sub>139-151</sub> and (VI) 4-arm PLP<sub>139-151</sub> + 25  $\mu$ M free PLP<sub>139-151</sub>. Data is presented as mean  $\pm$  SD. N=3, \* p<0.05, \*\* p<0.01, \*\*\* p<0.001, \*\*\*\* p<0.0001.

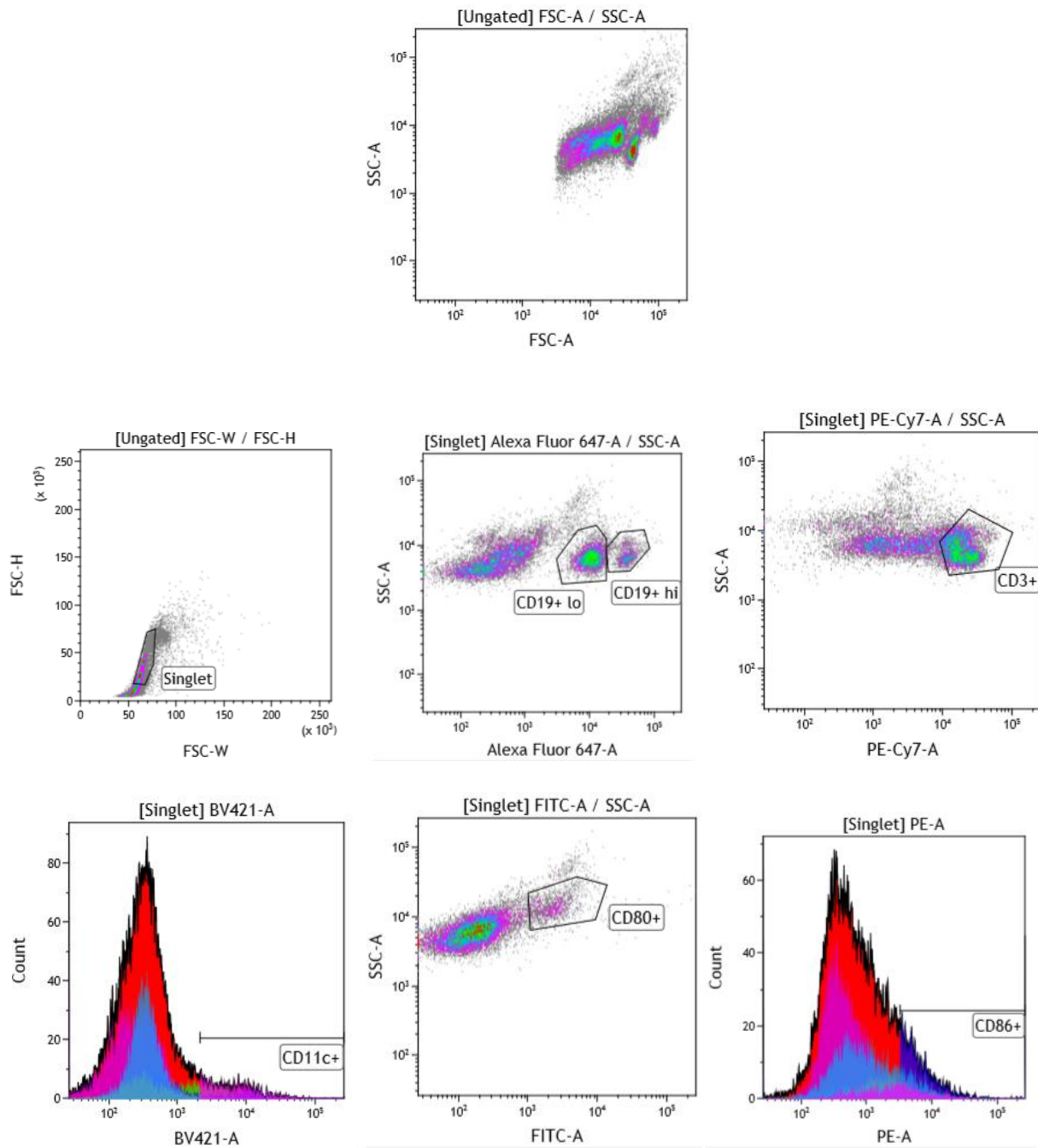


**Figure S5.** Representative flow cytometric analysis of a Media treated sample displaying the gating scheme for each fluorescent channel.

## References

1. Torkildsen, Ø.; Myhr, K.-M.; Bø, L., Disease-modifying treatments for multiple sclerosis – a review of approved medications. *European Journal of Neurology* **2016**, *23* (S1), 18-27.
2. Jones, J. L.; Coles, A. J., New treatment strategies in multiple sclerosis. *Experimental Neurology* **2010**, *225* (1), 34-39.
3. Boster, A.; Edan, G.; Frohman, E.; Javed, A.; Stuve, O.; Tselis, A.; Weiner, H.; Weinstock-Guttman, B.; Khan, O., Intense immunosuppression in patients with rapidly worsening multiple sclerosis: treatment guidelines for the clinician. *The Lancet Neurology* **2008**, *7* (2), 173-183.
4. Fletcher, J. M.; Lalor, S. J.; Sweeney, C. M.; Tubridy, N.; Mills, K. H. G., T-cells in multiple sclerosis and experimental autoimmune encephalomyelitis. *Clinical & Experimental Immunology* **2010**, *162* (1), 1-11.
5. Lehmann-Horn, K.; Kronsbein, H. C.; Weber, M. S., Targeting B cells in the treatment of multiple sclerosis: recent advances and remaining challenges. *Therapeutic advances in neurological disorders* **2013**, *6* (3), 161-173.
6. Amor, S.; Puentes, F.; Baker, D.; Van Der Valk, P., Inflammation in neurodegenerative diseases. *Immunology* **2010**, *129* (2), 154-169.
7. Bar-Or, A.; Calabresi, P. A.; Arnold, D.; Markowitz, C.; Shafer, S.; Kasper, L. H.; Waubant, E.; Gazda, S.; Fox, R. J.; Panzara, M.; Sarkar, N.; Agarwal, S.; Smith, C. H., Rituximab in relapsing-remitting multiple sclerosis: a 72-week, open-label, phase I trial. *Annals of neurology* **2008**, *63* (3), 395-400.
8. Hauser, S. L.; Waubant, E.; Arnold, D. L.; Vollmer, T.; Antel, J.; Fox, R. J.; Bar-Or, A.; Panzara, M.; Sarkar, N.; Agarwal, S.; Langer-Gould, A.; Smith, C. H., B-cell depletion with rituximab in relapsing-remitting multiple sclerosis. *The New England journal of medicine* **2008**, *358* (7), 676-88.
9. Kappos, L.; Li, D.; Calabresi, P. A.; O'Connor, P.; Bar-Or, A.; Barkhof, F.; Yin, M.; Leppert, D.; Glanzman, R.; Tinbergen, J.; Hauser, S. L., Ocrelizumab in relapsing-remitting multiple sclerosis: a phase 2, randomised, placebo-controlled, multicentre trial. *Lancet* **2011**, *378* (9805), 1779-87.
10. Sorensen, P. S.; Lisby, S.; Grove, R.; Derosier, F.; Shackelford, S.; Havrdova, E.; Drulovic, J.; Filippi, M., Safety and efficacy of ofatumumab in relapsing-remitting multiple sclerosis: a phase 2 study. *Neurology* **2014**, *82* (7), 573-81.
11. Reim, J. W.; Symer, D. E.; Watson, D. C.; Dintzis, R. Z.; Dintzis, H. M., Low molecular weight antigen arrays delete high affinity memory B cells without affecting specific T-cell help. *Molecular Immunology* **1996**, *33* (17), 1377-1388.
12. Johnson, J. G.; Jemmerson, R., Tolerance induction in resting memory B cells specific for a protein antigen. *The Journal of Immunology* **1992**, *148* (9), 2682-2689.
13. Sestak, J.; Mullins, M.; Northrup, L.; Thati, S.; Laird Forrest, M.; Siahaan, T. J.; Berkland, C., Single-step grafting of aminoxy-peptides to hyaluronan: A simple approach to multifunctional therapeutics for experimental autoimmune encephalomyelitis. *Journal of Controlled Release* **2013**, *168* (3), 334-340.
14. Hartwell, B. L.; Martinez-Becerra, F. J.; Chen, J.; Shinogle, H.; Sarnowski, M.; Moore, D. S.; Berkland, C., Antigen-Specific Binding of Multivalent Soluble Antigen Arrays Induces Receptor Clustering and Impedes B Cell Receptor Mediated Signaling. *Biomacromolecules* **2016**, *17* (3), 710-722.

15. Linton, P. J.; Rudie, A.; Klinman, N. R., Tolerance susceptibility of newly generating memory B cells. *The Journal of Immunology* **1991**, *146* (12), 4099-4104.
16. Symer, D. E.; Reim, J.; Dintzis, R. Z.; Voss, E. W.; Dintzis, H. M., Durable elimination of high affinity, T-cell-dependent antibodies by low molecular weight antigen arrays in vivo. *The Journal of Immunology* **1995**, *155* (12), 5608-5616.
17. Sosnick, T. R.; Benjamin, D. C.; Novotny, J.; Seeger, P. A.; Trewhella, J., Distances between the antigen-binding sites of three murine antibody subclasses measured using neutron and X-ray scattering. *Biochemistry* **1992**, *31* (6), 1779-86.
18. Parker, D. C., T-cell-Dependent B Cell Activation. *Annual Review of Immunology* **1993**, *11* (1), 331-360.
19. Gauld, S. B.; Benschop, R. J.; Merrell, K. T.; Cambier, J. C., Maintenance of B cell anergy requires constant antigen receptor occupancy and signaling. *Nature Immunology* **2005**, *6* (11), 1160-1167.
20. Hartwell, B. L.; Pickens, C. J.; Leon, M.; Berkland, C., Multivalent Soluble Antigen Arrays Exhibit High Avidity Binding and Modulation of B Cell Receptor-Mediated Signaling to Drive Efficacy against Experimental Autoimmune Encephalomyelitis. *Biomacromolecules* **2017**, *18* (6), 1893-1907.
21. Fujimoto, M.; Poe, J. C.; Inaoki, M.; Tedder, T. F., CD19 regulates B lymphocyte responses to transmembrane signals. *Seminars in Immunology* **1998**, *10* (4), 267-277.
22. Manzotti, C. N.; Tipping, H.; Perry, L. C. A.; Mead, K. I.; Blair, P. J.; Zheng, Y.; Sansom, D. M., Inhibition of human T-cell proliferation by CTLA-4 utilizes CD80 and requires CD25+ regulatory T-cells. *European journal of immunology* **2002**, *32* (10), 2888-2896.

## **Chapter 5: Conclusions and Future Directions**

## 1. Conclusions

Modulating the immune system through the use of antigen-specific immunotherapies (ASITs) has had a major impact on human health and quality of life. Vaccines represent the greatest breakthrough in our ability to direct human immune responses through administration of the antigen of interest alongside an adjuvant. Additionally, as described in chapter 1, ASIT has also proven effective in tolerizing the immune system against antigens of interest, namely in the form of hyposensitization therapies. Nevertheless, adaptation of ASIT strategies for the treatment of human autoimmunity has proven unsuccessful thus far, with numerous clinical trials of antigen-only therapies failing to demonstrate efficacy. Despite the limited success of antigen-only therapies, the promising pre-clinical results of ASIT for autoimmunity drive further development of therapies capable of modulating aberrant immune responses through disruption of the two-signal model of immune cell activation.

Dexamethasone, a potent corticosteroid used in the treatment of autoimmune diseases, has been shown to potentially induce long-term tolerization against an antigen through the development of regulatory T-cells. In chapter 2, a novel class of immunotherapeutic drugs was developed through direct conjugation of dexamethasone to an MS disease causing antigen PLP<sub>139-151</sub> utilizing click chemistry. This antigen-drug conjugate (AgDC) completely ameliorated clinical symptoms in EAE mice and significantly reduced effector helper T-cell responses. Simple co-administration of these components also displayed some promise in alleviating clinical symptoms, however efficacy was reduced in this delivery format. The enhanced specificity of AgDC in delivering potent immunosuppressants to disease-causing immune cell populations has the potential to greatly reduce off-target drug effects and enhance the safety and tolerability of otherwise globally immunosuppressive treatments. Due to their

efficacy and modular nature, AgDCs represent a promising class of immunotherapeutic drugs for the treatment of numerous autoimmune diseases.

In chapter 3, we explored the role of a major co-inhibitory pathway, programmed cell death 1 (PD-1), in the EAE model of autoimmunity. The PD-1 pathway is of great interest due to its role in downregulating immune responses, and numerous strategies to antagonize this pathway have been explored for applications such as cancer. Antagonizing the PD-1 pathway in adaptive immune responses alongside the antigen of interest, PLP<sub>139-151</sub>, resulted in severely impaired immune cell function rather than enhanced inflammation. This result indicates that long-term disruption of the PD-1 pathway may induce irreversible exhaustion in inflammatory cell populations, thereby limiting future immune responses against the antigen of interest.

Antigen-only immunotherapies represent perhaps the safest means of tolerizing the immune system against an antigen, however, such strategies have typically lacked efficacy in human clinical trials of autoimmunity. In chapter 4, we discuss the design of a multivalent display of PLP<sub>139-151</sub> capable of tolerizing PLP<sub>139-151</sub>-specific B cells. This low molecular weight antigen display is comprised of a tetravalent PEG backbone with PLP<sub>139-151</sub> conjugated to each terminus, imparting enhanced avidity for PLP<sub>139-151</sub>-specific B cells. 4-arm PLP<sub>139-151</sub> ameliorated clinical EAE symptoms through depletion of PLP-responsive CD19<sup>hi</sup> B cells, even in the presence of equimolar free PLP<sub>139-151</sub>. Expression of the key co-stimulatory markers CD80 and CD86 shifted toward a tolerogenic phenotype following treatment with 4-arm PLP<sub>139-151</sub>, thereby limiting the ability of PLP<sub>139-151</sub>-B cells to act as antigen-presenting cells. Furthermore, immune tolerizing effects were witnessed in downstream effector helper T-cell populations through a significant reduction in numerous inflammatory cytokines in the presence of free PLP.

## 2. Future Directions

This dissertation has outlined multiple approaches for ASIT development in a preclinical setting, however there is still more work to be done to understand the underlying mechanisms for tolerance induction. Chapter 2 focused on the molecular design of AgDCs to direct the action of an immunosuppressant corticosteroid to offending immune cell populations, but we have yet to demonstrate the longevity of the tolerance induced by this novel class of drugs. Future *in vivo* studies on the efficacy of AgDCs should observe symptom severity over a longer time-frame to assess relapses in these mice. This would indicate if administration of PLP<sub>139-151</sub>-DEX prior to disease onset results in protection from induction of EAE or simply enhanced, long-term symptom suppression. Indeed, the focus of our work with AgDCs thus far has been on demonstrating the efficacy associated with this immunomodulatory strategy, however, we have only scratched the surface with regards to the underlying immune mechanisms associated with this efficacy. Namely, these works should focus on identifying and observing any changes in PLP-specific B cells as well as investigating the development of regulatory T-cells associated with DEX treatment. Probing the cell phenotypic changes responsible for *in vivo* efficacy may also provide insight into the longevity of tolerance induction and may direct the screening of other immunosuppressive drug molecules, which may be adapted for use in AgDCs in place of dexamethasone.

The work contained in chapter 3 supports the importance of the PD-1 pathway in autoimmune regulation, but there is much more work to be done to understand the role of PD-1. We have demonstrated that peptide antagonists of PD-1 are capable of reducing inflammation in the presence of cognate antigen, but further demonstration of T-cell exhaustion is required. Future studies should focus on observing changes in both cytokines and receptor expression in T-

cells at various timepoints throughout treatment to characterize the exhausted phenotype and assess the durability of this exhaustion.

The development of a tetravalent antigen display system outlined in chapter 4 demonstrates the efficacy of multivalent antigen arrays in inducing tolerance in a specific manner. The 4-arm PLP<sub>139-151</sub> has shown great success in eliminating offending B cell populations in EAE, however, future work should focus on exploring the potential for bystander suppression following treatment. In our model, disease is induced and treated with the same peptide epitope, PLP<sub>139-151</sub>, but MS in humans is not usually confined to a single responsible epitope. In MS, epitope spreading following destruction of the myelin sheath results in the development of autoreactive lymphocytes directed against numerous epitopes. In order to develop effective immunotherapies for MS the immunotherapy must either encompass multiple CNS antigens or induce bystander suppression. Although we have demonstrated the depletion of PLP<sub>139-151</sub>-reactive B cells and suppression of effector helper T-cells, we have yet to investigate the induction of regulatory T-cells capable of bystander suppression. Identification of regulatory T-cells induced *in vivo* following 4-arm PLP<sub>139-151</sub> treatment would demonstrate the potential for bystander suppression and would further support the development of an already very promising class of immunomodulator.

Lastly, the strategies implemented in the development of AgDCs and tetravalent antigen displays are not unique to MS. These immunomodulatory therapies could be applied to a variety of autoimmune diseases with known autoantigens, such as T1D and RA, and may show even greater success in these indications. Adaptation of these therapeutic strategies for other autoimmune indications would deepen our understanding of immune modulation and tolerance induction and may eventually lead to a cure for debilitating autoimmune diseases.